A COMBINATORIAL PROOF OF THE INVARIANCE OF TANGLE FLOER HOMOLOGY

by

TIMOTHY HOMAN

LAWRENCE ROBERTS, COMMITTEE CHAIR
BULENT TOSUN
BRUCE TRACE
MARTIN EVANS
BENJAMIN C. HARMS

A DISSERTATION

Submitted in partial fulfillment of the requirements
for the degree of Doctor of Philosophy
in the Department of Mathematics
in the Graduate School of
The University of Alabama

TUSCALOOSA, ALABAMA

2019

ABSTRACT

The aim of this work is to take the combinatorial construction put forward by Petkova and Vértesi for tangle Floer homology and show that many of the arguments that apply to grid diagrams for knots can be applied to grid diagrams for tangles. In particular, we showed that the stabilization and commutation arguments used in combinatorial knot Floer homology can be applied mutatis mutandis to combinatorial tangle Floer homology, giving us an equivalence of chain complexes (either exactly in the case of commutations or up to the size of the grid in stabilizations). We then added a new move, the stretch move, and showed that the same arguments which work for commutations work for this move as well.

We then extended these arguments to the context of A_∞-structures. We developed for our stabilization arguments a new type of algebraic notation and used this notation to demonstrate and simplify useful algebraic results. These results were then applied to produce type D and type DA equivalences between grid complexes and their stabilized counterparts.

For commutation moves we proceeded more directly, constructing the needed type D homomorphisms and homotopies as needed and then showing that these give us a type D equivalence between tangle grid diagrams and their commuted counterparts. We also showed that these arguments can also be applied to our new stretch move.

Finally, we showed that these grid moves are sufficient to accomplish the planar tangle moves required to establish equivalence of the tangles themselves with the exception of one move.

ACKNOWLEDGMENTS

My sincere appreciation goes out to my advisor, Dr. Lawrence Roberts, for his support and willingness to always make time for me. I would also like to thank the members of my committee for being willing to be a part of this process, especially at such a busy time of the semester. I would like to thank my parents, my sister, Shannon Brunner, Olivia Brunner, and Isaac Brunner for all their love and support, the importance of which cannot be overstated. A special thanks goes out to Tish and Bill Lollar whose support and encouragement have helped me more than they know. I would like to thank Khanh Dinh for being my friend and for making me a better mathematician. Finally, I would like to thank Summer Atkins for her patience and support and for being a source of joy in my life.

CONTENTS

LIST OF FIGURES

CHAPTER 1

BACKGROUND

Knot Floer homology is a homological theory built on the ideas of Floer homology for manifolds in low-dimensional topology. It was developed by Peter Ozsváth and Zoltán Szabó and independently by J. Rasmussen in 2003 ([1] and [2]). It has several versions, but we will focus throughout this paper on what is called the tilde version. The whole theory can be constructed combinatorially. The basic idea behind combinatorial knot Floer homology is not hard to understand. We would like to work on classifying knots into knot types by assigning to each knot some algebraic structure. In the case of the tilde version of knot Floer homology, that algebraic structure is a bigraded vector space. We wish to show that these structures are invariants of the knot type. That is, if two knots K_1 and K_2 are equivalent as knots, then our assignment will yield the same algebraic structure. Thus, if we calculate the algebraic structure for K_1 and K_2, and those structures are not equivalent, then we know that the knots in question are not equivalent either.

In [3] and [4], the authors show that knot Floer homology can be constructed combinatorially in the following manner. First, you start with a knot diagram, that is a projection of the knot onto a plane. Any such diagram can be manipulated (without changing the knot type) to produce a diagram consisting of only vertical and horizontal lines (see figure 1.1). We can then replace the corners of the knot diagram with X's and O's (see figure 1.2) in such a way that the X's and O's alternate along the knot, the knot travels vertically from X to O and horizontally from O to X, and the vertical line segments go over the horizontal line segments. This is always possible.

Now, all of the information about the knot is captured in the information about the relative positions of these X's and O's. So, we can condense down this information by

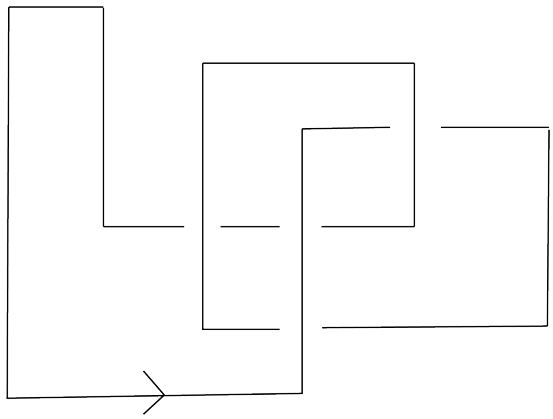

Figure 1.1: Every knot has a diagram consisting of only straight vertical and horizontal lines.

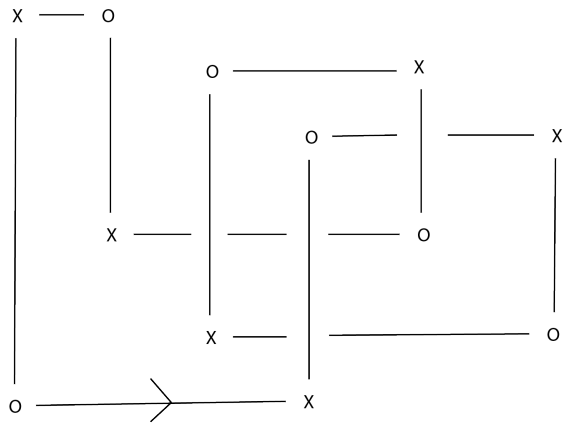

Figure 1.2: If we replace the corners in the knot diagram with X's and O's, they can capture the information of the knot simply in their layout. We require that the X's and O's alternate and that the knot travels vertically from X to O and horizontally from O to X. We further require that whenever they cross, vertical lines cross over horizontal lines.

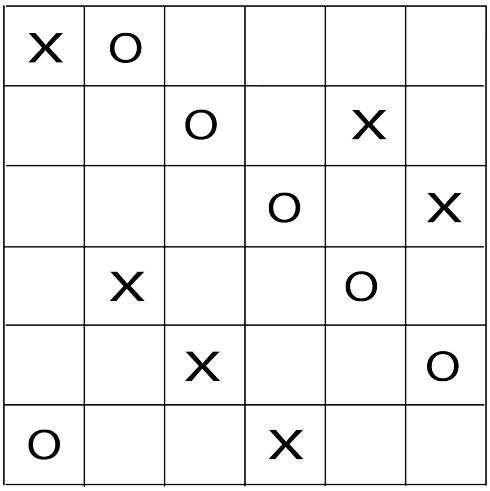

Figure 1.3: The grid diagram which corresponds to the knot diagram in 1.2. The vertical lines are referred to as β curves and the horizontal lines are referred to as α curves.

assigning to the diagram a grid structure. If the knot diagram in question has n vertical segments, then we draw a square grid diagram by arranging $n+1$ vertical lines, called the β curves, and $n+1$ horizontal lines, called the α curves, into a grid. We place the X's and O's from the planar diagram into the grid diagram so that every column has exactly one X and one O, every row has exactly one X and one O, and so that the relative positions of the X's and O's are maintained (see figure 1.3). There is only one way to do this. We will now define a chain complex using this grid diagram. The chain complex defined is in general a bigraded module over $\mathbb{Z}/2\mathbb{Z}$, although we will not worry about the gradings here.

We will start by imagining that our square diagram represents a torus instead of a square. This is accomplished by gluing the top and bottom together and then gluing the two sides together. This means that there are actually only n β curves and n α curves as the first and last of each are identified. The generators of the chain complex are bijections $x : \{1, 2, \ldots, n\} \to \{1, 2, \ldots, n\}$. We will represent these generators as dots on our diagram by a simple rule. If x takes 1 to 3, then we will place a dot on the intersection between β_1 and α_3. There is only one such intersection. This means that every generator has a dot representation where every α and β curve has exactly one dot on it, and every such grid state represents a generator. An example of a grid state is given in figure 1.4.

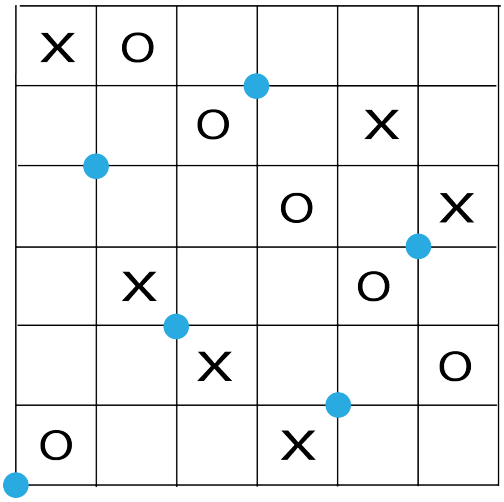

Figure 1.4: While technically bijections, we will always think of the generators of the chain complex as arrangements of dots on the grid diagram, called grid states.

The boundary map for the chain complex counts suitable rectangles on the grid diagram. To be suitable the rectangles must have a dot as their upper right and lower left corners (bearing in mind that we are still on a torus), and their interiors must be free of all other dots, X's, and O's. See figure 1.5 for an example of a suitable rectangle. Rectangles resolve by shifting the dots on their corners to the other corners of the rectangle while keeping all of the dots not on the rectangle the same. This yields a new generator (i.e. a new grid state). While a single grid state may contain many suitable rectangles, rectangles are resolved one at a time, and each one yields a single term in the output of the boundary map. If we think of our generators as permutations on the set of n letters, then the rectangles represent composition with a transposition. Figure 1.6 shows the resolution of a suitable rectangle for a grid state. While we will not worry about gradings, the boundary map is homogeneous of degree $(-1, 0)$, and the homology of this bigraded complex is an invariant of the underlying knot.

This material was laid out in its essence in [3] and [4]. See [5] for a textbook summary of all of the ideas.

The idea arises that if one could figure out a way to slice the diagram into pieces in such a way that one could analyze the whole from the pieces, then one could possibly build

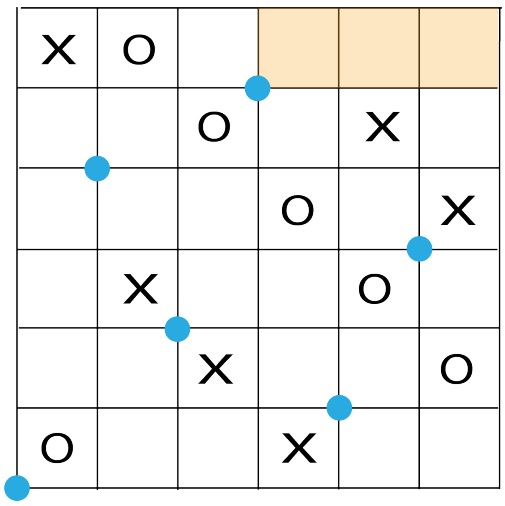

Figure 1.5: An example of a suitable rectangle in the boundary map used in combinatorial knot Floer homology.

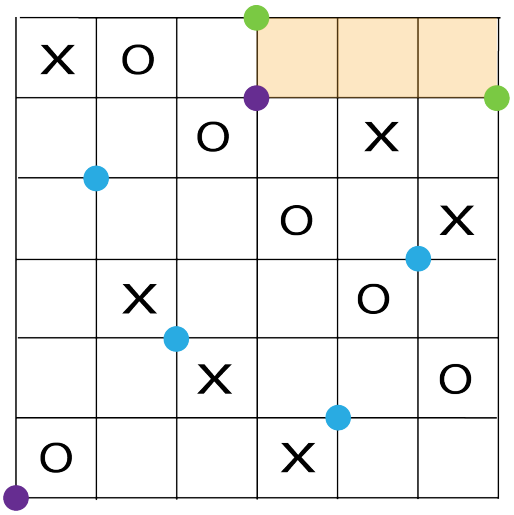

Figure 1.6: This figure shows the resolution of a rectangle on the corner. The original generator consisted of the blue dots combined with the purple dots, and the boundary map maps it to the blue dots combined with the green dots.

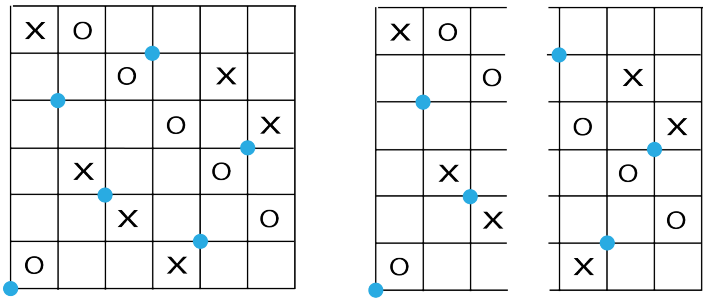

Figure 1.7: This figure shows the slicing of a grid diagram into two pieces. One then assigns to each piece an algebraic structure that preserves all of the information about the original chain complex.

up a theory for braids or tangles or at least be able to calculate the knot Floer homology (which is sometimes quite a task to do) from the individual pieces. In [6], Lipshitz, Ozsváth and Thurston make an attempt to do just that. In particular they lay out how you could slice a knot's grid diagram into two pieces (see figure 1.7). One would like to be able to preserve the information about the full diagram in some kind of algebraic structures associated to each piece.

Notice that the generator in figure 1.7 is also sliced when the grid diagram itself is sliced. The idea put forward was to assign a complex to each half of the diagram, say $\mathcal{H}^A$ to the left and $\mathcal{H}^D$ to the right, by allowing generators for each possible set of dots such that each β curve in this piece has exactly one dot in it. For an example see figure 1.8. Then, one could recombine the generators by taking some kind of product. The problem is that not every combination of generators in the pieces, when glued together, equals a generator in whole diagram. To solve the problem an algebra is introduced to store information about the edge of the diagrams. It then serves as an interface between the two pieces. We can think of this algebra as storing information about what kinds of generators with which the right generator would be compatible and then "asking" the left generator if it is that kind of generator or not.

Another problem that arises when slicing the diagram is that rectangles themselves may get sliced as well. In figure 1.9, the rectangle involving the purple dots can be

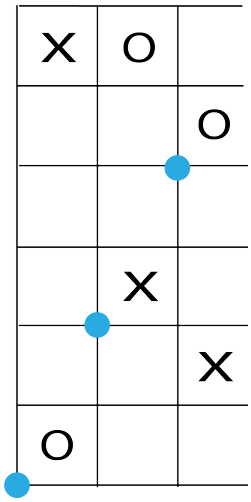

Figure 1.8: An example of a generator in the complex $\mathcal{H}^A$ assigned to the left half of a sliced grid diagram.

accounted for in the chain complex $\mathcal{H}^D$. However, the rectangle involving the green dots crosses the slicing line and would therefore change dots in both $\mathcal{H}^A$ and $\mathcal{H}^D$. The solution is to let the differential of $\mathcal{H}^D$ spit out both the generator with its dot moved and information in the form of an algebra element about how to move the dot in the other generator. If the rectangle was incompatible, then the algebra action on the generator in $\mathcal{H}^A$ will kill the element, and the tensor product will thus be zero as well. Actually, both of these tasks are accomplished using the same algebra. The algebra has an idempotent subalgebra whose sole purpose is to decide if grid states in $\mathcal{H}^A$ and grid states in $\mathcal{H}^D$ are compatible, and non-idempotent elements of the algebra which are used to communicate information about rectangles.

In total, we associate to the left hand piece $\mathcal{H}^A$, a type A structure which consists basically of a chain complex and an algebra action to interpret the algebra elements from $\mathcal{H}^D$. For the right side, $\mathcal{H}^D$, we do the opposite and let the boundary map spit out algebra elements. We call this type of structure a type D structure. The algebra involved, the type A structure, and the type D structure all belong to a class of objects called A_∞ structures. For a vast amount of information on these objects see [7]. For a more concise introduction involving just the algebras, see [8].

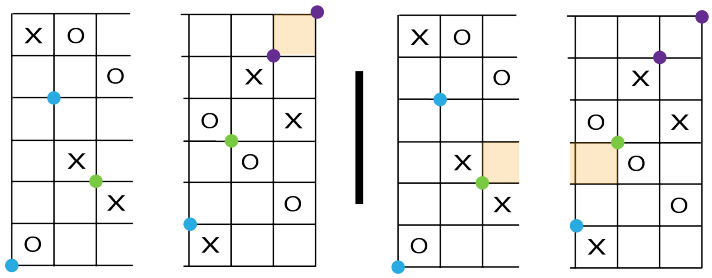

Figure 1.9: Rectangles too are bound to get caught up in the slicing process. The rectangle involving the purple dots is counted in the chain complex of $\mathcal{H}^D$. However, something must be done about the rectangle involving the green dots because that rectangle would shift one dot in $\mathcal{H}^D$ and one dot in $\mathcal{H}^A$.

Lipshitz, Ozsváth, and Thurston ran into trouble, however, and were never able to quite get the situation to work out properly (Note that since then Ozsváth and Szabó were able to slice knots using a different setup involving Kauffman states. See [9]). In 2014, though, inspired by the work of Lipshitz, Ozsváth, and Thurston, Ina Petkova and Vera Vértesi produced a manuscript, [10], which did solve the slicing problem for tangles. In it they discussed how one could assign to tangles the kinds of diagrams that one does for knots. However, instead of the diagram being on a torus, it is on an n-holed torus. This results in a kind of staircase diagram (see figure 3.15 for an example of this type of grid and some rectangles on it) which can be sliced into pieces which are assigned structures that combine the ability to interpret algebra pieces on the right with the ability to spit out algebra pieces on the left, fittingly called type DA structures.

1.1 Task at Hand

Tangles, which amount to slices of knots with end information preserved, are the perfect recipient of this type of structure. Petkova and Vértesi managed to define a version of knot Floer homology for tangles, called appropriately tangle Floer homology, and while they gave both a topological and a combinatorial description of the construction, the proof of invariance was strictly topological. Our goal in this paper is thus to provide a combinatorial proof for the invariance of tangle Floer homology.

In the knot theory setting, this was accomplished by noting that any planar

diagram for a knot can be transformed into any other knot diagram by a series of Reidemeister moves (a fact well known) and then showing that those moves can be realized in the grid diagram setting by a series of grid moves. It was then showed that each of these grid moves does not change the algebraic structure assigned to the knot diagram (up to some notion of equivalence). Since every diagram of a knot can be reached from any other diagram of the same knot, the algebraic structure is an invariant of the knot itself.

We seek to do the same thing with tangles and tangle Floer homology. While any planar diagram of a knot can be transformed into any other planar diagram of a knot via only three Reidemeister moves (see figure 1.10), the situation is more complicated with tangles. There is a similar set of moves, but the total number of moves comes to 10. See figure 1.11 for reference. Our goal is to show that these 10 moves can be realized by a small number of grid moves just as in the knot diagram case, and that each of the grid moves does not change the DA structure assigned to the diagram (again up to some notion of equivalence). This will show that the DA structure assigned to the grid diagram is an invariant of the tangle itself. We will begin by analyzing the algebra needed and then move on to the construction of the grid diagram complex. After that, we will discuss each grid move and then show that it does not affect the type DA structure assigned to the complex. Finally, we will show that each of the tangle moves in figure 1.11 can be realized by a sequence of grid moves, and thus the DA structure assigned to the grid diagram is actually an invariant of the tangle itself.

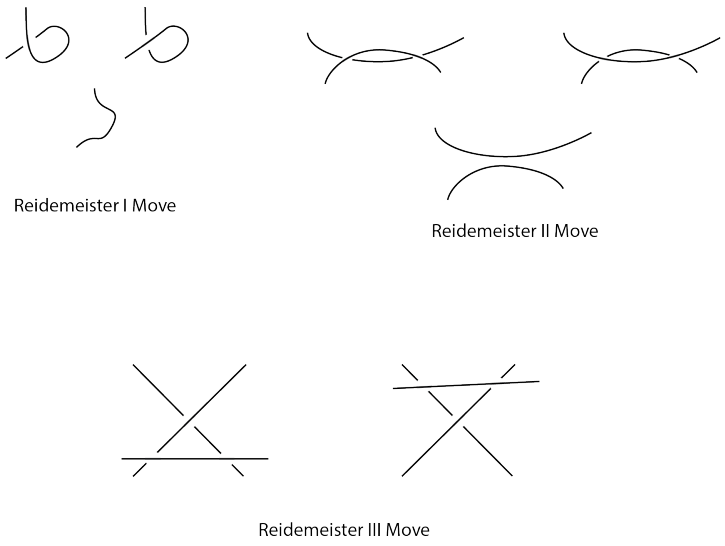

Figure 1.10: Using these moves (and their equivalent counterparts) one can transform any planar knot diagram into any other planar diagram of the same knot, and these moves never change the knot type. These moves are made locally and the rest of the diagram is left alone.

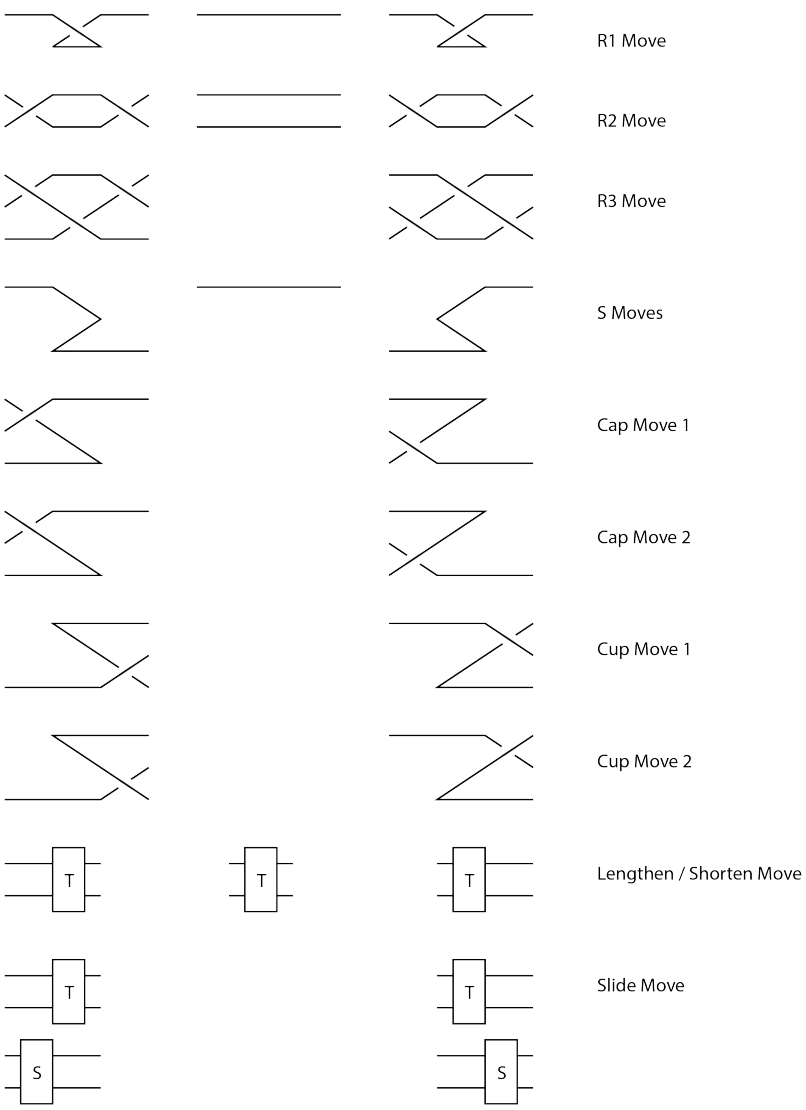

Figure 1.11: Using these moves (and their equivalent counterparts) one can transform any planar tangle diagram into any other planar diagram of the same tangle, and these moves never change the tangle type. These moves are made locally and the rest of the diagram is left alone. That is, there may be more straight strands above or below the parts shown, and other nontrivial movement may occur in the tangle to the left or right of what is shown.

CHAPTER 2

ALGEBRA

A dg-algebra $\mathcal{A}$ is an abelian group with a differential $\mu_1 : \mathcal{A} \to \mathcal{A}$ and a multiplication $\mu_2 : \mathcal{A} \otimes \mathcal{A} \to \mathcal{A}$ such that:

$$\mu_1^2 = 0,$$

$$\mu_2 \circ (\mu_1 \otimes \mathrm{Id} + \mathrm{Id} \otimes \mu_1) = \mu_1 \circ \mu_2,$$

and

$$\mu_2 \circ (\mu_2 \otimes \mathrm{Id}) = \mu_2 \circ (\mathrm{Id} \otimes \mu_2).$$

Our algebras will be thought of as being defined over a ground ring $\underline{\mathbf{k}}$, which will be a direct sum of finitely many copies of $\mathbb{Z}/2\mathbb{Z}$. For us, there will be a subalgebra, the idempotents, identified with $\underline{\mathbf{k}}$ and an element $1 = \sum e_i$, where each e_i is an idempotent, such that $\mu_1(1) = 0$.

2.1 Type A Structures

A right differential module M is a right $\underline{\mathbf{k}}$-module with maps $m_1 : M \to M$ and $m_2 : M \otimes \mathcal{A} \to M$ such that:

$$m_1^2 = 0,$$

$$m_2 \circ (m_1 \otimes \mathrm{Id} + \mathrm{Id} \otimes \mu_1) = m_1 \circ m_2,$$

and

$$m_2 \circ (m_2 \otimes \mathrm{Id}) = m_2 \circ (\mathrm{Id} \otimes \mu_2).$$

Our differential modules will be strictly unital, i.e. are such that $m_2(x, 1) = x, \forall x \in M$.

More generally, an $\mathcal{A}_\infty$-module is a $\underline{\mathbf{k}}$-module M with maps

$$m_i : M \otimes_{\underline{\mathbf{k}}} \mathcal{A} \otimes_{\underline{\mathbf{k}}} \cdots \otimes_{\underline{\mathbf{k}}} \mathcal{A} \to M$$

with i-1 $\mathcal{A}$ terms defined for all $i \geq 1$ satisfying:

$$\underline{m}(\underline{m}(x \otimes \underline{a})) + \underline{m}(x \otimes \underline{d}(\underline{a})) = 0,$$

where $\underline{a}$ represents some finite tensor product of algebra elements,

$$\underline{d}(a_1 \otimes \cdots a_n) = \sum_{j=1}^{n} a_1 \otimes \cdots \otimes \mu_1(a_j) \otimes \cdots \otimes a_n + \sum_{j=1}^{n-1} a_1 \otimes \cdots \otimes \mu_2(a_j, a_{j+1}) \otimes \cdots \otimes a_n,$$

and

$$\underline{m}(x \otimes a_1 \otimes \cdots \otimes a_n) = \sum_{j=0}^{n} m_{j+1}(x \otimes \cdots \otimes a_j) \otimes \cdots \otimes a_n.$$

The assumption here and throughout this paper is that our $\mathcal{A}_\infty$ structures are defined over dg-algebras rather than full $\mathcal{A}_\infty$-algebras. To be more precise, $\underline{a}$ is an element of the tensor algebra $T^*(\mathcal{A})$ defined by

$$T^*(\mathcal{A}) = \bigoplus_{i=0}^{\infty} \mathcal{A} \otimes_{\underline{\mathbf{k}}} \cdots \otimes_{\underline{\mathbf{k}}} \mathcal{A},$$

where there are i $\mathcal{A}$'s and the 0th entry is assumed to be $\underline{\mathbf{k}}$. $T^*(\mathcal{A})$ is a chain complex with differential $\underline{d}$. Furthermore, if we define $T^*(M) = M \otimes_{\underline{\mathbf{k}}} T^*(\mathcal{A})$, then the compatibility conditions for $M_\mathcal{A}$ being a type A structure amount to the map $\underline{d}_M$ on $T^*(M)$ defined by

$$\underline{d}_M(x \otimes \underline{a}) = \underline{m}(x \otimes \underline{a}) + (x \otimes \underline{d}(\underline{a}))$$

being a differential on $T^*(M)$.

A right differential module is a right $\mathcal{A}_\infty$-module where $m_i = 0$ for $i > 2$. We will think about our differential modules in the greater context of $\mathcal{A}_\infty$-structures. Our $\mathcal{A}_\infty$-modules will also satisfy the unitality conditions:

$$m_2(x \otimes 1) = x$$

for all $x \in M$, and

$$m_i(x \otimes a_1 \otimes \cdots \otimes a_{i-1}) = 0$$

if $i > 2$ and some $a_j = 1$. We will sometimes write our modules as $M_{\mathcal{A}}$ if we wish to indicate explicitly that they are right $\mathcal{A}_\infty$-modules. We will also say that M is or has a type A structure to mean that M is an $\mathcal{A}_\infty$-module.

A morphism from an $\mathcal{A}_\infty$-module $M_{\mathcal{A}}$ to another $\mathcal{A}_\infty$-module $N_{\mathcal{A}}$ is a sequence of $\underline{\mathbf{k}}$-module maps

$$\{\phi_i : M_{\mathcal{A}} \otimes_{\underline{\mathbf{k}}} \mathcal{A} \otimes_{\underline{\mathbf{k}}} \cdots \otimes_{\underline{\mathbf{k}}} \mathcal{A} \to N_{\mathcal{A}}\},$$

defined for $i \geq 1$, where there are $i - 1$ $\mathcal{A}$ terms. From this, we get an induced map $\underline{\phi} : M_{\mathcal{A}} \otimes T^*(\mathcal{A}) \to N_{\mathcal{A}} \otimes T^*(\mathcal{A})$ defined by

$$\underline{\phi}(x \otimes a_1 \otimes \cdots \otimes a_n) = \sum_{i=0}^{n} \phi_{1+i}(x \otimes a_1 \otimes \cdots \otimes a_i) \otimes \cdots \otimes a_n.$$

When $\underline{\phi}$ is a chain map, i.e. when $\underline{d}_N \circ \underline{\phi} + \underline{\phi} \circ \underline{d}_M = 0$, we say that ϕ is a homomorphism.

If M and N are both type A structures, then the set of morphisms from M to N,

$\mathrm{Mor}_{\mathcal{A}}(M,N)$ is also a chain complex with differential

$$\begin{aligned}(d\phi)_i(x\otimes a_1\otimes\cdots\otimes a_{i-1}) &= \sum_{j=1}^{i}\phi_{i-j+1}(m_j^M(x,a_1,\ldots,a_{j-1}),a_j,\ldots,a_{i-1})\\ &= \sum_{j=1}^{i} m_{i-j+1}^N(\phi_j(x,a_1,\ldots,a_{j-1}),a_j,\ldots,a_{i-1})\\ &= \sum_{j=1}^{i-1}\phi_i(x,a_1,\ldots,\mu_1(a_j),\ldots,a_{i-1})\\ &= \sum_{j=1}^{i-2}\phi_{i-1}(x,a_1,\ldots,\mu_2(a_j,a_{j+1}),\ldots,a_{i-1}).\end{aligned} \tag{2.1}$$

By happenstance, most of our focus on $\mathcal{A}_\infty$ structures, will be on two other types, type D and an amalgamation of type D and type A structures, type DA structures.

2.2 Type D Structures

A type D structure over a dg-algebra is a left $\underline{\mathbf{k}}$-module with a $\underline{\mathbf{k}}$-linear map $\delta^1 : X \to \mathcal{A}\otimes_{\underline{\mathbf{k}}} X$ satisfying:

$$(\mu_2\otimes \mathrm{Id})\circ(\mathrm{Id}\otimes\delta^1)\circ\delta^1 + (\mu_1\otimes\mathrm{Id})\circ\delta^1 = 0.$$

As is common, where more specificity is required we will denote type D structures with a superscript denoting their algebras, i.e. ${}^{\mathcal{A}}M$ instead of M. Given two type D structures ${}^{\mathcal{A}}P$ and ${}^{\mathcal{A}}Q$, their morphism set $\mathrm{Mor}({}^{\mathcal{A}}P,{}^{\mathcal{A}}Q)$ is a chain complex consisting of maps $h^1 : P \to \mathcal{A}\otimes_{\underline{\mathbf{k}}} Q$ with differential defined by

$$d(h^1) = (\mu_1\otimes\mathrm{Id}_Q)\circ h^1 + (\mu_2\otimes\mathrm{Id}_Q)\circ(\mathrm{Id}_{\mathcal{A}}\otimes h^1)\circ\delta_P^1 + (\mu_2\otimes\mathrm{Id}_Q)\circ(\mathrm{Id}_{\mathcal{A}}\otimes\delta_Q^1)\circ h^1.$$

When $d(h^1)=0$, we say that h^1 is a homomorphism. Given the proper domains and codomains, we can form a composition of type D maps. Specifically, if $f :{}^{\mathcal{A}} P \to {}^{\mathcal{A}} Q$ and

$g :^{\mathcal{A}} Q \to^{\mathcal{A}} R$ are type D morphisms then their composition, denoted $g * f$ is given by

$$(g * f) = (\mu_2 \otimes \mathrm{Id}_R) \circ (\mathrm{Id}_{\mathcal{A}} \otimes g^1) \circ f^1.$$

The identity morphism is the map $\mathbb{I} : P \to \mathcal{A} \otimes P$ given by $x \mapsto 1 \otimes x$.

Two type D morphisms $\psi : P \to \mathcal{A} \otimes Q$ and $\phi : P \to \mathcal{A} \otimes Q$ are homotopic if there is a map $H : P \to \mathcal{A} \otimes Q$ such that

$$\psi - \phi = (\mu_2 \otimes \mathrm{Id}_Q) \circ (\mathrm{Id}_{\mathcal{A}} \otimes H) \circ \delta^1_P + (\mu_2 \otimes \mathrm{Id}_Q) \circ (\mathrm{Id}_{\mathcal{A}} \otimes \delta^1_Q) \circ H + (\mu_1 \otimes \mathrm{Id}_Q) \circ H.$$

Two type D structures (P, δ^1_P) and (Q, δ^1_Q) are homotopy equivalent if there are type D structure homomorphisms $\psi : P \to \mathcal{A} \otimes Q$ and $\phi : Q \to \mathcal{A} \otimes P$ such that $\phi * \psi \cong \mathbb{I}_P$ and $\psi * \phi \cong \mathbb{I}_Q$. It can be easily checked that homotopy equivalence of type D structures is an equivalence relation.

2.3 Type DA Structures

A type DA structure over dg-algebras $\mathcal{A}$ and $\mathcal{B}$ is a $\underline{\mathbf{j}}$-$\underline{\mathbf{k}}$ bimodule equipped with maps for $i \geq 1$

$$\delta^1_i : X \otimes_{\underline{\mathbf{k}}} \mathcal{B} \otimes_{\underline{\mathbf{k}}} \cdots \otimes_{\underline{\mathbf{k}}} \mathcal{B} \to \mathcal{A} \otimes_{\underline{\mathbf{k}}} \otimes X$$

satisfying for $(x, b_1, \ldots, b_{i-1})$:

$$\begin{aligned} 0 = &(\mu_1 \otimes \mathrm{Id}) \circ \delta^1_i(x, b_1, \ldots, b_{i-1}) \\ &+ \sum_{j=1}^{i-1} \delta^1_i(x, b_1, \ldots, \mu_1(b_j), \ldots, b_{i-1}) \\ &+ \sum_{j=1}^{i-2} \delta^1_{i-1}(x, b_1, \ldots, \mu_2(b_j, b_{j+1}), \ldots, b_{i-1}) \\ &+ \sum_{j=1}^{i} (\mu_2 \otimes \mathrm{Id}) \circ (\mathrm{Id} \otimes \delta^1_{i-j+1}) \circ (\delta^1_j \otimes \mathrm{Id}^{\otimes(i-j)})(x, b_1, \ldots, b_{i-1}) \end{aligned} \tag{2.2}$$

A morphism between type DA structures $h^1 :^{\mathcal{A}} X_{\mathcal{B}} \to^{\mathcal{A}} Y_{\mathcal{B}}$ is a sequence of maps

$$\{h^1_j : X \otimes_{\underline{\mathbf{k}}} \mathcal{B} \otimes_{\underline{\mathbf{k}}} \cdots \otimes_{\underline{\mathbf{k}}} \mathcal{B} \to \mathcal{A} \otimes_{\underline{\mathbf{j}}} Y\}_{j=1}^{\infty}.$$

As with type D structures, the morphism sets form chain complexes where the differential is given by

$$\begin{aligned} d(h^1)_i(x, b_1, \ldots, b_{i-1}) &= (\mu_1 \otimes \mathrm{Id}) \circ h^1_i(x, b_1, \ldots, b_{i-1}) \\ &+ \sum_{j=1}^{i-1} h^1_i(x, b_1, \ldots, \mu_1(b_j), \ldots b_{i-1}) \\ &+ \sum_{j=1}^{i-2} h^1_{i-1}(x, b_1, \ldots, \mu_2(b_j, b_{j+1}), \ldots, b_{i-1}) \\ &+ \sum_{j=1}^{i} (\mu_2 \otimes \mathrm{Id}) \circ (\mathrm{Id} \otimes h^1_{i-j+1}) \circ (\delta^1_j \otimes \mathrm{Id}^{\otimes(i-j)})(x, b_1, \ldots, b_{i-1}) \\ &+ \sum_{j=1}^{i} (\mu_2 \otimes \mathrm{Id}) \circ (\mathrm{Id} \otimes \delta^1_{i-j+1}) \circ (h^1_j \otimes \mathrm{Id}^{\otimes(i-j)})(x, b_1, \ldots, b_{i-1}) \end{aligned} \tag{2.3}$$

A homomorphism is a morphism whose differential is zero. Two homomorphisms are homotopic if their difference is the differential of another morphism. The composition of two morphisms $f^1 :^{\mathcal{A}} X_{\mathcal{A}} \to^{\mathcal{A}} Y_{\mathcal{B}}$ and $g^1 :^{\mathcal{A}} Y_{\mathcal{B}} \to^{\mathcal{A}} Z_{\mathcal{B}}$, $g * f$, is defined to be the type DA morphism which maps $(x, b_1, \ldots, b_{i-1})$ to:

$$\sum_{j=1}^{i} (\mu_2 \otimes \mathrm{Id}) \circ (\mathrm{Id} \otimes g^1_{i-j+1}) \circ (f^1_j \otimes \mathrm{Id}^{\otimes(i-j)})(x, b_1, \ldots, b_{i-1}). \tag{2.4}$$

A type DA structure is called strictly unital if $\delta^1_2(x, 1) = 1 \otimes x$ for any $x \in M$ and $\delta^1_i(x, b_1, \ldots, b_{i-1}) = 0$ if $i > 2$ and some $b_j \in \underline{\mathbf{k}}$. Our type DA structures will all be strictly unital.

It is sometimes more convenient to use a tree notation to represent type DA maps. In such cases, algebra elements are represented by a solid arrow, elements of the module

are represented by dashed arrows, and elements of the tensor algebra are represented by a double solid arrow. For example, the differential of a type DA morphism may also be written as below, where $\underline{\mathrm{d}}$ is the sum of all the ways of doing μ_1 and all of the ways of doing μ_2, and Δ is the standard comultiplication map.

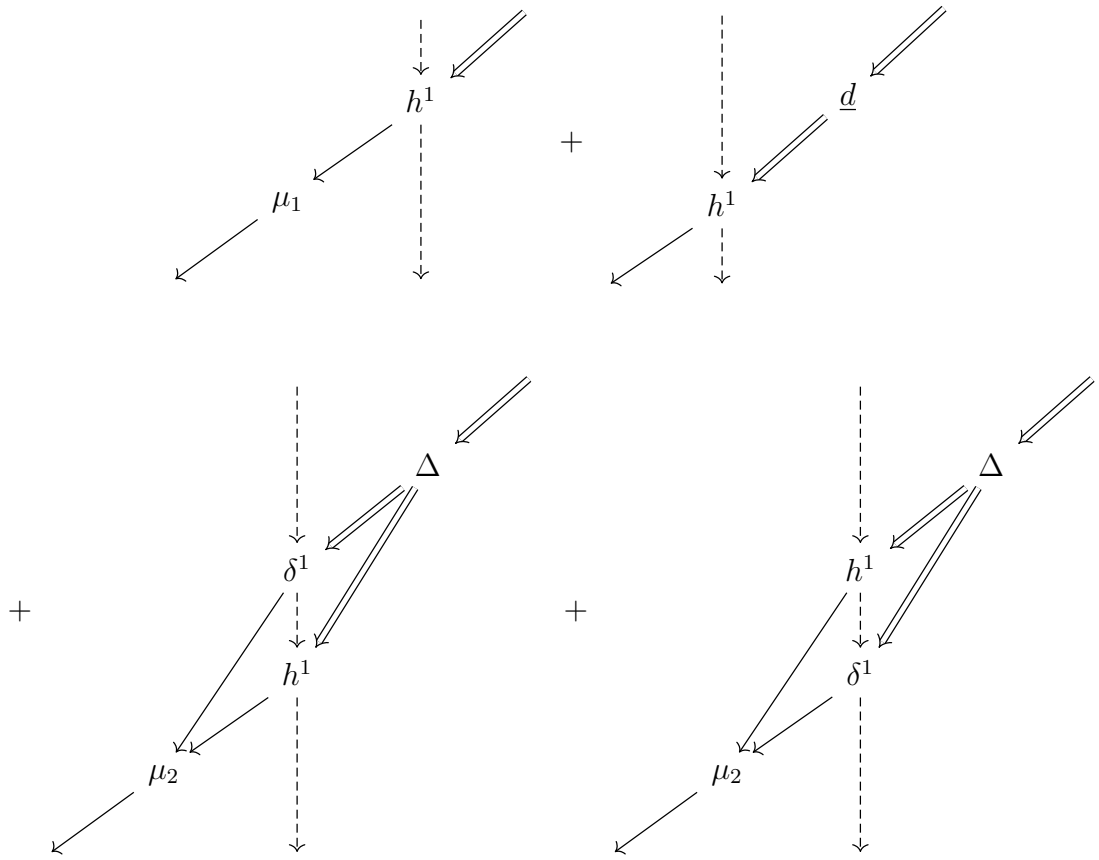

We will use a variant of this notation, called circle notation, which will be introduced later.

Our goal algebraically will be ultimately to show that two different type DA structures are equivalent. In this regard, we will take inspiration from [9], where we find the following lemma.

Lemma 1. *Let ${}^{\mathcal{A}}Y_{\mathcal{B}}$ be a strictly unital type DA bimodule, and let ${}^{\mathcal{A}}Z$ be a type D structure over $\mathcal{A}$. Suppose there are type D structure homomorphisms $f :^{\mathcal{A}} Z \to^{\mathcal{A}} Y$ and $g :^{\mathcal{A}} Y \to^{\mathcal{A}} Z$ and a type D structure morphism $T :^{\mathcal{A}} Y \to^{\mathcal{A}} Y$ such that $f * g = \mathbb{I}_Z$, $g * f = \mathbb{I}_Y + d(T)$, and $T \circ T = 0$. Then, ${}^{\mathcal{A}}Z$ can be converted to a type DA structure that*

is also strictly unital, denoted ${}^{\mathcal{A}}Z_{\mathcal{B}}$*, which is homotopy equivalent to* ${}^{A}Y_{\mathcal{B}}$ *via a homotopy equivalence* $\phi^1 :^{\mathcal{A}} Z_{\mathcal{B}} \to^{\mathcal{A}} Y_{\mathcal{B}}$ *such that* $\phi_1^1 = f$*.*

Before we continue the discussion further it will be fruitful for us to discuss the structures under consideration.

CHAPTER 3

CONSTRUCTIONS

The following construction is taken from [11] and [10]. An (m, n)-tangle $\mathcal{T}$ is a proper, smoothly embedded oriented 1-manifold in $I \times \mathbb{R}^2$, with boundary $\partial\mathcal{T} = \partial^L\mathcal{T} \sqcup \partial^R\mathcal{T}$, where $\partial^L\mathcal{T} = \{0\} \times \{1, \ldots, m\} \times \{0\}$ and $\partial^R\mathcal{T} = \{1\} \times \{1, \ldots, n\} \times \{0\}$. Either m or n or both may be zero in which case the boundary is the empty set. We will think of the boundaries as oriented sets of points and use them to build our algebras.

A planar diagram for a tangle is the projection of the tangle onto $I \times \mathbb{R} \times \{0\}$ with no triple intersections, self-tangencies, or cusps, along with information about whether a crossing is over or under. An example of a tangle diagram is shown in figure 3.1. We also wish to keep track of the direction that the components of a tangle are going. This is usually done by means of arrows along the strands of the tangle (see figure 3.2). The boundary of a tangle may be thought of as a sign sequence consisting of $+$'s and $-$'s depending on whether the strand runs left-to-right or right-to-left respectively. For instance, the tangle in figure 3.2 is a $(2, 2)$-tangle where $-\partial^L(\mathcal{T}) = (+, +)$ and $\partial^R(\mathcal{T}) = (+, +)$. The signs are given from bottom to top. Following [11], [10], and [12], we describe a way to assign an algebra to a sign sequence P, denoted $\mathcal{A}(P)$, and outline a certain subalgebra $I(P)$ which will serve as our ground ring $\underline{\mathbf{k}}$.

3.1 Our Algebra

Let P be a sign sequence and let $[n] = \{1, 2, \ldots, n + 1\}$. We wish to define a dg-algebra associated to the sign sequence representing the end of our tangle. We will

Figure 3.1: An example of a tangle diagram.

Figure 3.2: An example of a directed tangle diagram.

define the generators for this algebra as below:

Definition 1. *A generator associated to a sign sequence $P = \{\pm\}^n$ is defined to be a bijection between a subset $S \subset [n]$ to a subset $T \subset [n]$. If $S = T$, and x is the identity map between them, then we say that x is an idempotent generator. If $x : S \to S$ is an idempotent we will sometimes write x as e_S.*

We will represent the generators of our algebra in two different ways, strand diagrams and grid diagrams. They are equivalent. While almost all of our work will be done using grid diagrams, we include the strand diagram construction for the sake of completeness and because certain notions are easier to define and visualize in terms of strand diagrams.

3.1.1 Algebra Strand Diagrams

Let $x : [n] \to [n]$ be a generator and let $P = \{\pm\}^n$ be a sign sequence associated to the end of a tangle. Draw strands from $(0, 1/2 + k)$ to $(1, 1/2 + k)$ for $k = 1, 2, \ldots n$. Draw the k^{th} strand green if the k^{th} entry in the sign sequence is a $+$, and draw the strand orange if the entry is a $-$. Next, draw red dots at $(1, k)$ for $k = 1, 2, \ldots, n + 1$, and draw blue dots at $(0, k)$ for $k = 1, 2, \ldots n + 1$. When needed we will label the red dots as $a_1, a_2, \ldots, a_n$ from bottom to top and the blue dots as $b_1, b_2, \ldots, b_n$ again from bottom to top. Finally, draw a black strand from $(0, j)$ to $(1, x(j))$ for each $j \in S$. We will allow some leeway in how the strands are drawn, but we will require that they have no critical points with respect to the horizontal coordinate, that there are no triple intersections between any of the strands in the diagram (including the orange and green ones), and that the intersection number between strands is minimized. These conditions make the diagrams unique up to ambient isotopy and Reidemeister III moves. See figure 3.3 for two examples of possible generators

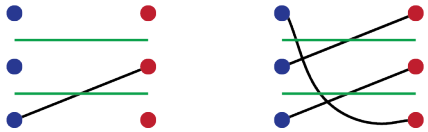

Figure 3.3: Two examples of generators for the algebra associated to the right edge of the tangle in figure 3.2. We can think of the green strands as flowing left to right, orange strands (if there were any) as flowing right to left, and the black strands as flowing left to right.

in the algebra corresponding to the right side of the tangle in figure 3.2. Our algebras will simply be the span of our generators over $\mathbb{Z}/2\mathbb{Z}$, and we will denote it by $A(P)$. We will also distinguish the subspace of the idempotent generators (i.e. the ones where the black strands are horizontal) as this will be our ground ring. We will denote it as $I(P)$.

Next, we need to define a multiplication and a differential on our algebras. We will define multiplication on generators by concatenation subject to certain conditions. If x and y are two generators, then $x \cdot y$, which we will also denote as $\mu_2(x, y)$, is obtained by deleting the red dots from the right side of x, deleting the blue dots from the left side of y and connecting all of the strands by gluing $\{1\} \times [1, n+1]$ of x's diagram to $\{0\} \times [1, n+1]$ of y's diagram. If each strand of both diagrams does not have a corresponding strand to glue to in the other diagram (without moving the ends of the strands), then the result of the multiplication is 0. Furthermore, if the resulting concatenated diagram does not have minimal crossing numbers for each combination of orange, green, and black strands (i.e. if any strands crosses any other strand more than once), then the result of the multiplication is also deemed to be 0. If neither of these situations happens, then the concatenated diagram is shrunk down to fit into a unit interval while respecting the relative heights of the ends and crossings of the strands. An example of each case is given in figure 3.4. To complete the multiplication map, just extend it linearly.

Next, we will define the differential on our algebra. We will again start by defining the map on the generators and then extend it linearly. The differential will operate by "smoothing" crossings between black strands, that is by resolving a crossing in the way shown in figure 3.5. The crossing is resolved locally while leaving the rest of the diagram

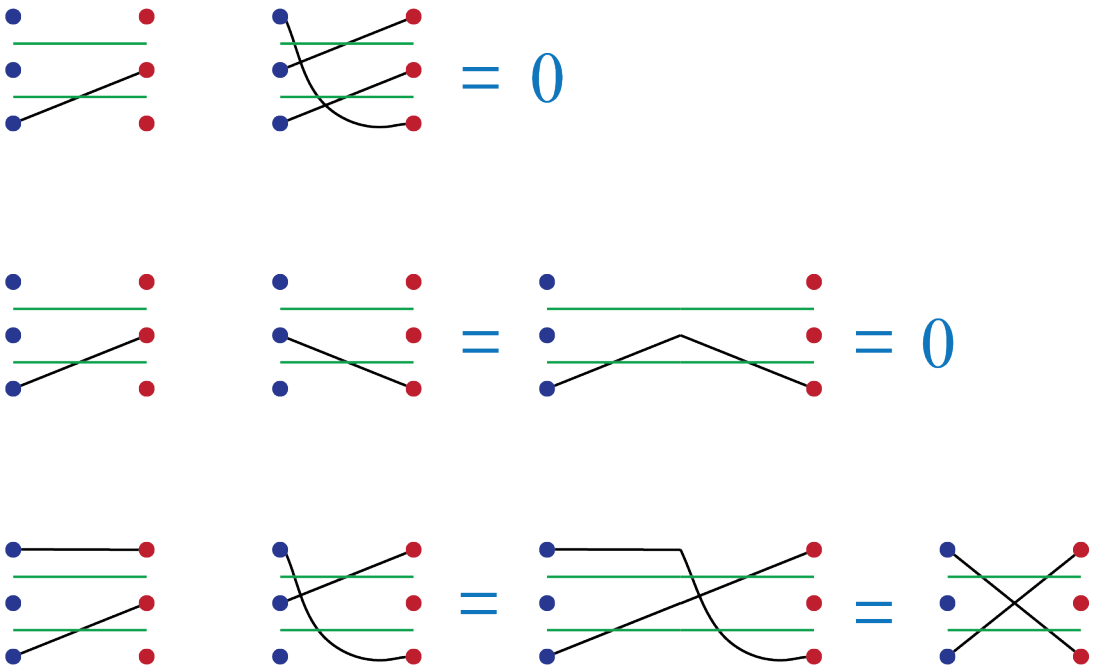

Figure 3.4: Three examples of multiplication in our algebras. In the top example, the result is 0 because the strands do not line up. In the middle example, the result is 0 because there is a double crossing between the black strand and the bottom green strand. In the bottom example, the strands line up and there are no double crossings, so the result is simply the concatenation of the two pieces.

Figure 3.5: The "smoothing" of a crossing. The crossing is changed locally while whatever is happening outside of the dotted circle remains unchanged.

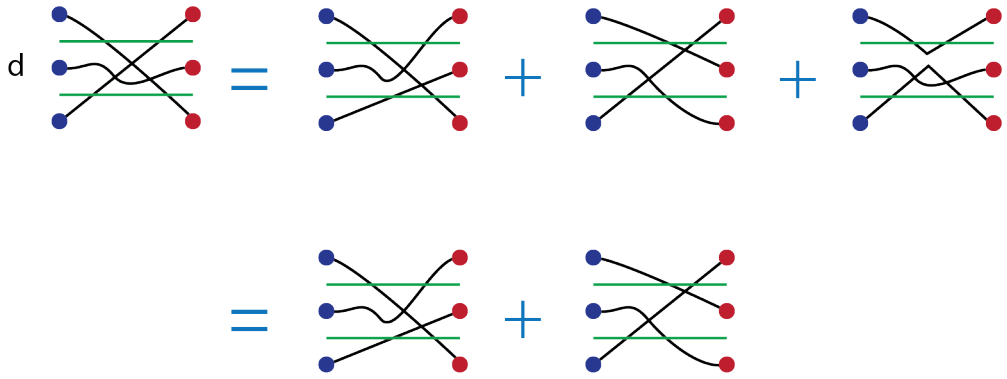

Figure 3.6: An example of the differential on a generator of one of our algebras. The differential works by trying to smooth out any crossings between black strands found in the generator diagram. In our example, the resolution of the bottom left and bottom right crossings result in terms of the differential; however, the smoothing of the top crossing is not allowed because it results in a double crossing (in fact multiple double crossings).

(including the rest of the strands involved) unchanged. Only one crossing is changed in each term of the resultant algebra element. A crossing is allowed to be smoothed if the resulting diagram does not result in a double crossing anywhere in the diagram. We will refer to the differential as d or μ_1. Refer to figure 3.6 for an example of the differential in action.

3.1.2 Algebra Grid Diagrams

We can also construct our algebra using a grid diagram consisting of α and β curves (which correspond to the a and b dots in the strand diagrams), X's and O's placed in the diagram (which correspond to the orange and green strands of our strand diagrams), and dots along the intersection points of the α and β curves (which correspond to the black strands of the strand diagrams).

Form a grid diagram for an algebra by letting the α curves be horizontal line

segments numbered sequentially $(\alpha_1, \alpha_2, \ldots, \alpha_n)$ and let the β curves be vertical line segments also numbered sequentially $(\beta_1, \beta_2, \ldots, \beta_n)$so that each α curve intersects each β curve exactly once and so that there is no intersection between any two α curves or any two β curves. We can label the α curves starting from either the top or the bottom, and we can label the β curves starting from either the left or the right. We will say that a sequence of β curves is labeled conventionally if the labeling starts on the left, and we will say that a sequence of α curves is labeled conventionally if the labeling starts at the bottom and increases upward.

We will call a grid diagram a shadow diagram if one of either the α or β curves is labeled conventionally and the other is not. We will call a grid diagram a mirror shadow diagram or simply a mirror diagram if both the α and β curves are labeled conventionally or if they are both not labeled conventionally. For grid diagrams associated to our algebras, we will always use shadow diagrams. Which labeling we use for our algebra will be determined by the context in which we use them, but they are both equivalent.

The orange and green strands of our tangle are indicated in the grid diagram by X's and O's respectively. If a green strand travels from $(0, i + 1/2)$ to $(1, j + 1/2)$ in the strand diagram, then this is indicated by putting an O in square formed by the lines β_i, β_{i+1}, α_j, and α_{j+1} (remember that green strands travel from the b side to the a side). Similarly, if an orange strand travels from $(1, j + 1/2)$ to $(0, i + 1/2)$ in the strand diagram, then this is indicated on the grid diagram by placing an X in the square created by the β_i, β_{i+1}, α_j, and α_{j+1} lines. An example of a strand diagram and its corresponding grid diagrams is shown in figure 3.7.

Finally, the black strands from a strand diagram are indicated on the grid diagram by placing a dot (usually black, light blue, or purple, although colors do not matter on a grid diagram) in a manner similar to the placement of X's and O's. If a black strand travels from $(0, i)$ to $(1, j)$ in a strand diagram, then that is indicated by placing a dot on the grid diagram at the intersection of β_i and α_j. Figure 3.8 shows an example of a strand

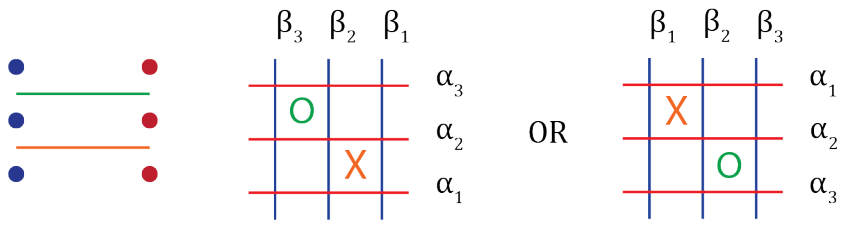

Figure 3.7: The two grid diagrams on the right both correspond to the strand diagram on the left.

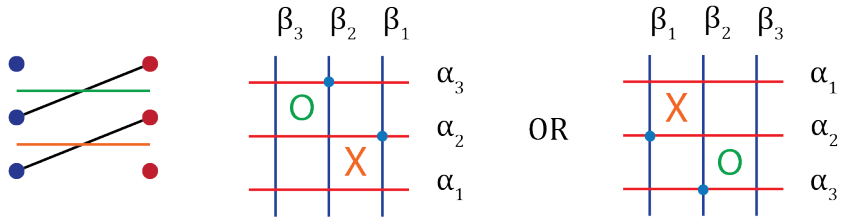

Figure 3.8: The grid diagrams on the right correspond to the strand diagram on the left. The dots correspond to the black strands in the strand diagram.

diagram generator and its corresponding grid diagram generator.

The algebra for each grid diagram is generated by grid diagrams where each α curve and each β curve can have a maximum of one dot. Notice that either way we draw the grid diagram the X's and O's form a diagonal line from the top left to the bottom right of the diagram. The idempotents are precisely the grid diagrams where all of the dots fall only on this diagonal. Whether or not they are idempotents, we will sometimes refer to generators in the grid diagram context as grid states, and we will denote the set of all such generators by $S(A)$ or $S(G)$, etc.

The differential in the grid diagram consists of counting rectangles where one dot forms the lower left corner of the rectangle and one dot forms the upper right corner of the rectangle. If the rectangle is allowable, the rectangle resolves by swapping the dots on the corners to the upper left and lower right corners. A rectangle is allowable if the interior of the rectangle is completely free of dots, X's, and O's. Two dots being in a position to form a rectangle correspond precisely to two black strands crossing in a strand diagram, and the

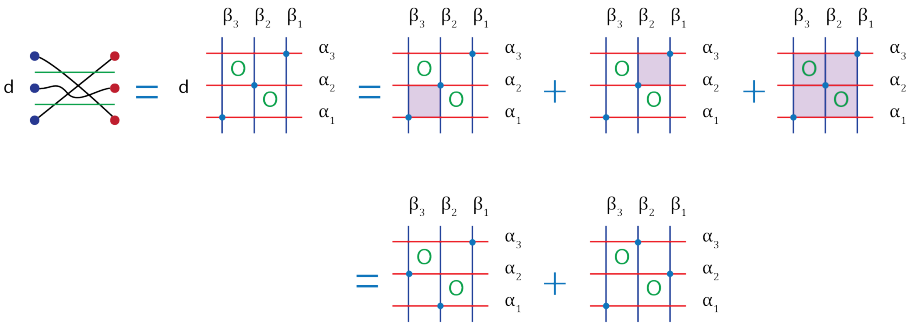

Figure 3.9: The differential in the grid diagram context for our algebra counts suitable rectangles in the diagram. This figure shows the same diagram from figure 3.6. The first two rectangles correspond to the first two crossing smoothings in the figure. The third rectangle is not allowable because of the dot and the two O's in its interior. These correspond to the double crossings from the strand diagram picture.

conditions on a rectangle being allowable correspond precisely to the conditions of whether or not a crossing is smoothable in the strand diagram. Note: these rectangles cannot wrap around the grid.

We will denote the set of all allowable rectangles which take a grid state x to a grid state y (by swapping the corners the dots are on) by $R(x, y)$. We can then define the differential on generators to be:

$$d(x) = \sum_{y \in S(A)} \sum_{r \in R(x,y)} y,$$

and then extend the map linearly. See figure 3.9 for an example of the differential in action.

Multiplication in the grid diagram picture is more complicated. It is sometimes easier to convert the grid diagram into a strand diagram and analyze the multiplication there. Multiplication in the grid diagram picture is determined by resolving suitable sets of partial rectangles which go off the edge of the diagram (either to the left or the right). The sets of partial rectangles should be thought to exist on the left grid diagram and are determined by the right grid diagram. First, there should be a dot on every α of the left diagram for every dot on a β curve in the right diagram, and there should be a dot on

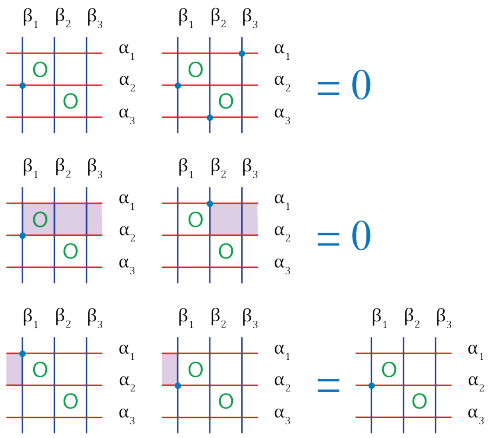

Figure 3.10: Three examples of the multiplication of grid states in an algebra. The top example is zero because there is not an α dot on the left diagram for each β dot in the right diagram. The middle example is zero because the rectangle determined by the dot on the right has an O in it when transferred to the left diagram. The last example works because the rectangle determined by the dot on the right is empty when moved to the left.

every β curve in the right diagram for each dot on an α curve in the left diagram. If this is not the case, then the multiplication is automatically 0. This corresponds to the black strands of each diagram needing to match up when gluing the strand diagrams together.

To determine the partial rectangles, look at each dot not on the idempotent diagonal. We will refer to the lattice point of the grid diagram with the same β as a certain dot and whose α would place it in the idempotent diagonal line as that dot's corresponding diagonal point. The dot and its corresponding diagonal point will form the corners of the partial rectangle. Now, simply extend the rectangle to the left or the right in whichever way avoids intersecting the idempotent diagonal. The rectangle then continues off the edge of the diagram.

We then move the rectangle from the right diagram to the left diagram by maintaining the same α curves as edges and moving it over until the corner point corresponding to the idempotent diagonal matches the dot on the same α in the left diagram. This is the rectangle corresponding to the original dot in the right diagram. The question now is whether or not the rectangle is valid. If it is, then it is resolved.

If there is more than one dot off of the diagonal on the right, then simply determine

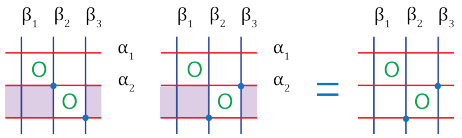

Figure 3.11: An example of multiplication in the grid diagram context where the right diagram has more than one dot off of the diagonal. In this case, the multiplication is nonzero because each rectangle determined by a dot in the right diagram is valid in the left diagram and the set of rectangles is compatible. The output of the multiplication is, thus, to simply resolve each rectangle at one time.

if each rectangle works individually. If they do, then determine if the set of rectangles itself is compatible. The set of rectangles is compatible if no partial rectangle is completely contained in another and no pair of rectangles whose edges go off different sides of the diagram have overlapping interiors.

The following theorem comes from [10]. We leave the discussion of the proof to the authors.

Theorem 1. *Both the strand construction of the algebra of a sign sequence and the grid construction of the algebra of a sign sequence yield differential graded algebras. Furthermore, the two constructions are isomorphic.*

3.2 Tangle Diagrams

Now we would like to extend this notion of diagrams to the entire tangle. We will all but abandon the notion of strand diagrams except as a transitional construction from our planar diagram to our grid diagrams. To obtain the strand diagram for a tangle, start with a planar diagram for the tangle such as the one in figure 3.2. Divide the diagram into an even number of pieces by cutting vertically such that no cup is in the first piece, no cap is in the last piece, and such that no crossing occurs on the vertical cut lines. Starting from the left, we will label the pieces $1, 2, \ldots$. Additionally, we require that each cup and cap have a cut line along its vertical tangency. Furthermore, we require that each crossing where the bigger slope is on top occurs in an even piece, and each crossing where the smaller slope is on top occurs in an odd piece. This setup is always achievable, although a

little ambient isotopy may be necessary.

From here, we start with the right edge and place a red dot below the first strand, then in between each strand up the edge, and finally above the last strand. We label the dots $a_1, a_2, \ldots, a_{n+1}$ starting at the bottom and working upwards. Moving to the first cut line, we place one blue dot blue dot below the first strand, then in between in each strand, and then, finally, above the last strand. We label the dots from the bottom to the top b_1, b_2, etc. We work our way down the tangle alternating between red and blue dots and ending on the boundary of the tangle.

Next, we color every strand going from b's to a's green and every strand going from a's to b's orange. This process is demonstrated in the left part of figure 3.12. Notice that each even piece of the strand complex corresponds to a shadow grid diagram just as with algebras. Similarly, we will let each odd piece of the strand complex correspond to a mirror shadow piece of the grid complex (i.e. one in which the labelings for the α and β curves are either both conventional or both not conventional).

From these shadow and mirror shadow pieces, we will create a grid complex by gluing together each mirror shadow and shadow sequentially to form a stair case. Each gluing of a mirror shadow to a shadow diagram where the mirror shadow is on the left in the strand diagram and the shadow piece is on the right in the strand diagram we will call a DA piece. In order to accomplish this gluing, we need to choose the labelings appropriately. We want the shared α and β curves to line up when glued, and we want the labelings to alternate between each two-piece. See the right side of figure 3.12 to see a finished example. We will call the first piece of a grid complex a type 1 piece, the second piece a type 2 piece, the next to last piece a type 3 piece, the last piece a type 4 piece, and any other piece a type 5 piece. If the grid complex only has two pieces, then the first is a type 1 and the second is a type 4. A finished grid complex will have a single X and O in every row and column created by the α and β curves except in the first and last piece (since we do not allow cups in type 1 pieces or caps in type 4 pieces). The α rows in the

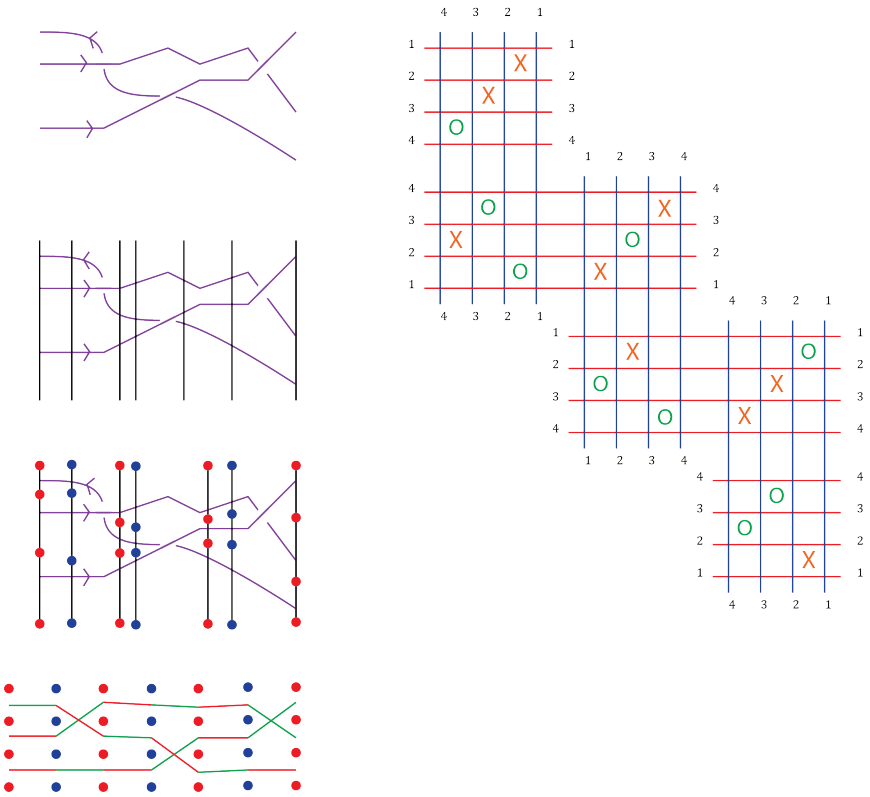

Figure 3.12: An example of building a strand diagram and then a grid diagram to represent a tangle. First you divide the tangle into pieces according to the conditions outlined in section 3.2, then you replace the cut lines with red and blue dots, placing one under the strands, one above the strands, and one in between each pair of strands on the cut line. Then, you color each strand of the diagram according to its orientation. From left to right, each segment of the strand diagram alternatively corresponds to a mirror grid diagram and a shadow grid diagram. These are then glued together to create a grid complex.

first and last piece will contain an X or an O, but not both.

Now we would like to provide a chain complex structure (as well as a type D and type DA structure) to a grid complex. We will let our chain complex be generated by sets of dots on the intersection points between the α and β curves. We will allow any such set of dots so long as:

- Every β curve has exactly one dot.
- Every α curve except those in the first and last piece has exactly one dot.
- Every α curve in the first and last piece has no more than one dot.

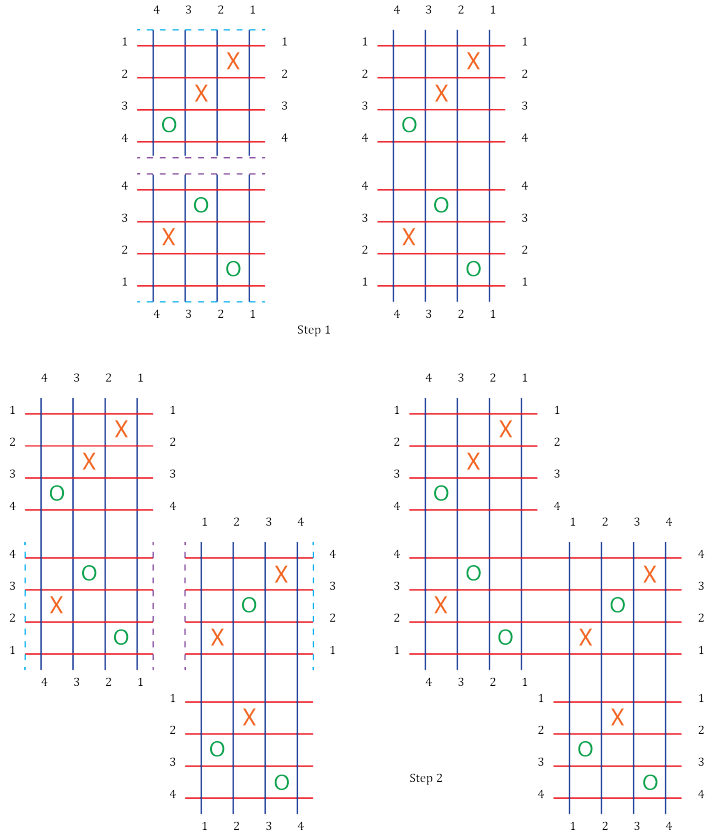

Figure 3.13: This figure shows the process of building a grid complex out of alternating mirror shadow grid diagrams and shadow grid diagrams. In step one, you glue piece 1 to 2, 3 to 4, etc. in such a way that the β curves line up. The diagram shows how each pair is glued (the purple dotted lines are glued together and the blue dotted lines are glued together). The combination of a mirror shadow and shadow glued together is called a DA piece. In step two, the DA pieces from step one are glued together, again blue to blue and purple to purple, forming a staircase pattern. See figure 3.12 for a finished example. Pay careful attention to how the β and α labelings alternate down the staircase.

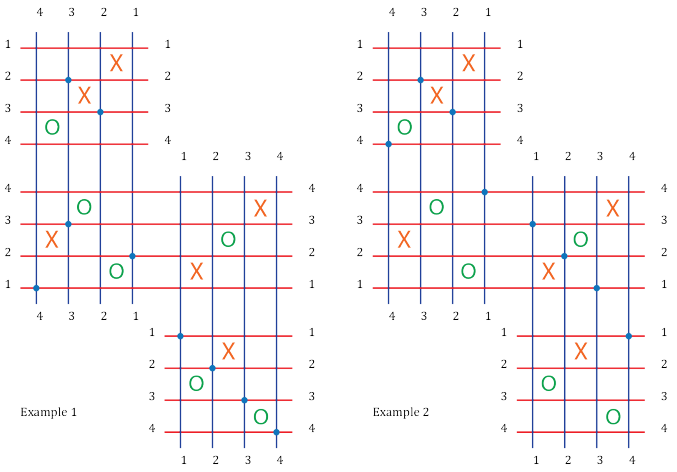

Figure 3.14: The "generator" on the left is not allowed for two reasons. First, there is a β curve that has more than one dot on it. Second, there is a long α curve which does not have any dots on it. Both of these things are not allowed. The generator on the right is fine. Note that it does not matter if some of the short α curves don't have dots.

The idea here is that we are gluing together the generators from our shadows and mirror shadows and throwing out the combinations that are incompatible.

We define $CT(G)$ to be the span of the set of generators, denoted $S(G)$, over $\mathbb{Z}/2\mathbb{Z}$. Next, we will define a boundary map, $\partial : CT(G) \to CT(G)$. This boundary map will count suitable rectangles between dots in the same way that μ_1 counted suitable rectangles between dots in our algebra. The only difference now is that the rectangles are allowed to go around the glued regions. However, rectangles are not allowed to go around corners. A rectangle between a grid state x and grid state y is called suitable if x and y differ only by the placement of two dots, those two dots are the upper right and lower left corners of the rectangle in x and the upper left and lower right corners in y, and the interior of the rectangle is free of X's, O's, and other dots. We will denote the set of all suitable rectangles between x and y $R(x, y)$. Then, we can define the boundary map on a grid state x by:

$$\partial(x) = \sum_{y \in S(G)} \sum_{r \in R(x,y)} y.$$

We then extend the map linearly.

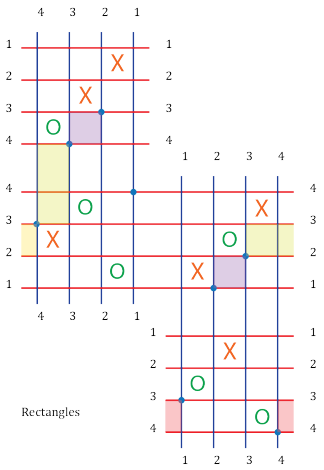

Figure 3.15: Rectangles in the boundary map of the grid complex. The purple rectangles are allowed because they are simply rectangles in the shadow or mirror shadow piece. The yellow rectangles are also allowed because the edges they go across have been glued together. The red rectangle, however, is not allowed because the α edges of the type 1 piece and type 4 piece have not been glued together.

The following theorem, along with its proof, can be found in [10]. See also [5] for a good discussion of how these types of proofs work.

Theorem 2. *The map $\partial^2 = 0$, and, thus, the complex $(CT(G), \partial)$ forms a chain complex.*

Next, we will define a map δ^L which will help us define our type D map. The map δ^L will count partial rectangles which go off of the edge in the type 1 piece. It will then store information about this rectangle in an algebra element. The map δ^L, thus, is a map from $CT(G)$ to $A(-\partial^L(\mathcal{T})) \otimes CT(G)$. Here, the tensor product is taken over the idempotent subring. You should think of this algebra diagram as the type of shadow piece that can be glued to the type 1 piece in the grid complex, except this piece specifically has all of its X's and O's along the idempotent diagonal.

To calculate the δ^L map on a generator, simply form the algebra shadow diagram and temporarily glue it to the grid complex. Provide the algebra piece with a dot on the idempotent diagonal for every α that is missing one in the type 1 piece of the grid complex. Then, form all of the rectangles that may be made by having one dot in the algebra piece and one dot in the original grid complex. The rectangles must be empty of

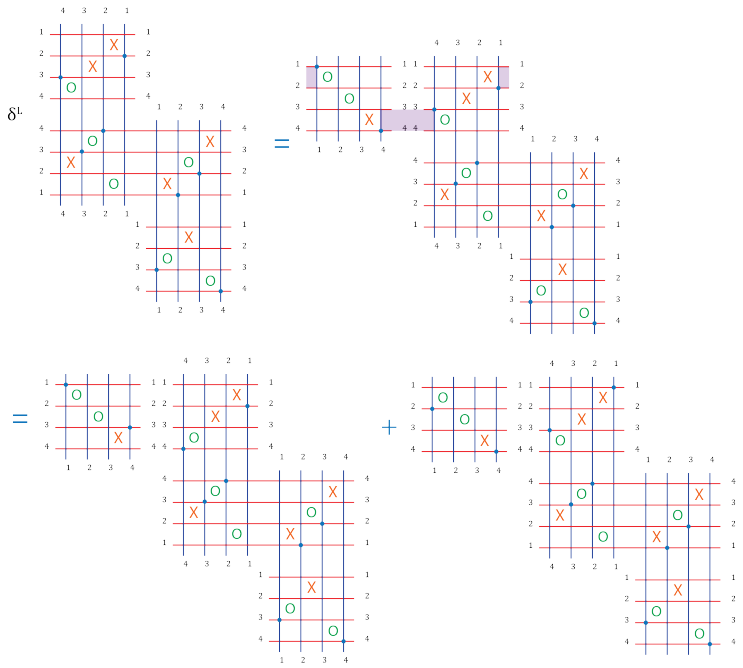

Figure 3.16: This figure shows an example of the δ_L map acting on a generator. First, form the idempotent algebra shadow grid which could be glued to the grid complex. Next, form suitable rectangles where one dot is in the original grid complex and one dot is in the algebra piece. Finally, resolve each rectangle independently and count each resolution as a term in the image.

all X's, O's, and other dots. Resolve each rectangle separately as an independent term of the output of the map.

Now, δ^L by itself would not be a type D map. Instead, we will combine the map δ^L with our boundary map ∂ to get the map $\delta_G : CT(G) \to A(-\partial^L(\mathcal{T})) \otimes CT(G)$ defined by:

$$\delta_G(x) = (1 \otimes \partial) + \delta^L,$$

where the map $(1 \otimes \partial)$ is defined by

$$(1 \otimes \partial)(x) = 1 \otimes \partial(x).$$

Theorem 3. *The map δ_G is a type D boundary map.*

Again, see [10] for a discussion of why this is true.

Finally, we will give the grid complex a type DA map, δ_i^G. Proceed first by declaring that $\delta_1^G = \delta_G$. Then, set $\delta_i^G = 0$ for all $i \geq 3$. So, we only need a δ_2^G. We will define this to essentially be our multiplication map from before. Recall that the map μ_2 provides a way to multiply two grid states in compatible shadow grid diagrams. The map δ_2^G maps elements in $CT(G) \otimes A(\partial^R(\mathcal{T}))$ to $CT(G)$. The grid diagram used in $A(\partial^R(\mathcal{T}))$ is precisely designed to be compatible with the type 4 shadow piece on the grid complex. The map δ_2^G is calculated by detaching the type 4 piece from the grid complex, performing the multiplication with the algebra piece as shadows in the algebra, and reattaching the result to the grid complex.

Theorem 4. *The sequence of maps δ_i^G is a type DA boundary map.*

CHAPTER 4

GRID MOVES

What follows is a description of the types of moves which may be executed on a grid diagram without changing the algebraic structure associated with the diagram (up to appropriate equivalence) along with the arguments that show that equivalence is maintained.

We will focus mainly on grid diagrams in making our later tangle move arguments. Thus, for the most part we will outline these moves in the grid diagram picture only. However, all of them may be executed and understood in the strand diagram picture as well. Whenever we have a need to use the strand diagram version of one of these moves, we will outline its consequences directly in the argument under consideration. The first move is outlined in both cases to help the reader get a feel for moving between the two systems.

4.1 Additions and Subtractions

The first grid "move" we will consider is actually not a move at all. Given a strand diagram, we will find it useful to add or remove an alpha or beta dot to the diagram (see figure 4.1). We will refer to these moves as addition or subtraction moves respectively. We will generally perform these moves in preparation for some other move.

When we have a sequence of dots with no X strands or O strands beginning or ending inside them, we will simply ignore all but one of them (the choice is somewhat arbitrary but if the possibility of leaving one of the outside α or β curves undotted is open to us, then we will always choose that), i.e. we will not allow any generator strands to start or end on these dots. Thus this move is actually just a relabeling of the original strand diagram and results in isomorphic chain complexes and DA structures.

We will also allow ourselves to move the transition point of a tangle strand (the

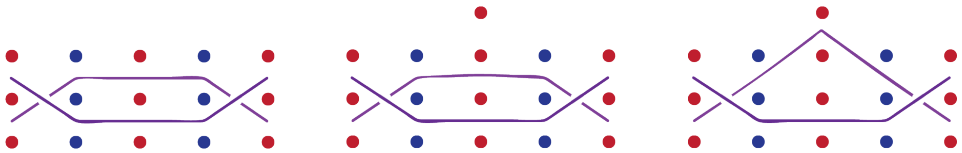

Figure 4.1: An example of an addition "move" on a strand diagram. Going from the left diagram to the right figure is an addition move, going from the middle diagram to the left diagram is a subtraction move, and going from the middle diagram to the right diagram is an example of reorganization.

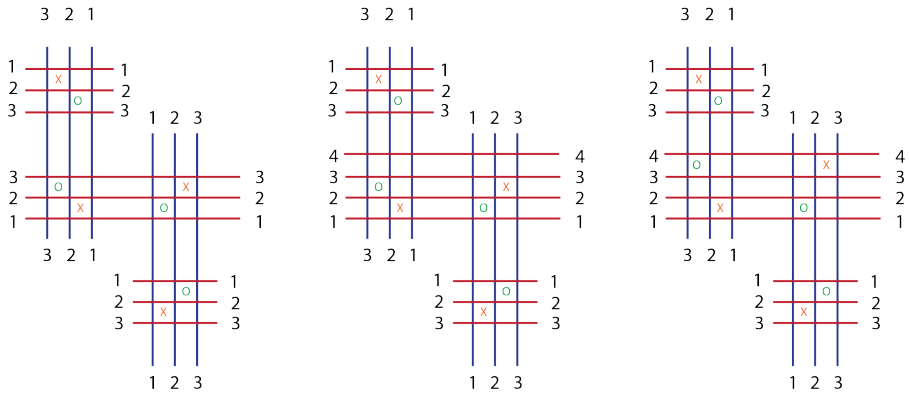

Figure 4.2: An example of an addition "move" on a grid diagram. Going from the left diagram to the middle diagram is an addition move, going from the middle diagram to the left diagram is a subtraction move, and going from the middle diagram to the right diagram is an example of reorganization.

place where it changes from an X strand to an O strand or vice versa) up or down if the spot is empty (see the right diagram of figure 4.1 for an example). This again simply results in a relabeling and therefore does not change the chain complex or DA structure.

Addition and subtraction moves and reorganization may all occur in the grid diagram picture as well (since they are in effect the same picture). For an addition move, one would add an alpha or beta curve instead of an alpha or beta dot, and alpha and beta curves forming empty rows and columns will simply be ignored save for one. Thus, they will play no role in either the generator dots or the maps we will discuss and ultimately result in a relabeling of the system. We will also allow ourselves to reorganize the picture by moving an X-O pair in the same row or column to an adjacent row or column if it is empty. See figure 4.2 to see examples of additions, subtractions, and reorganization in the grid diagram picture.

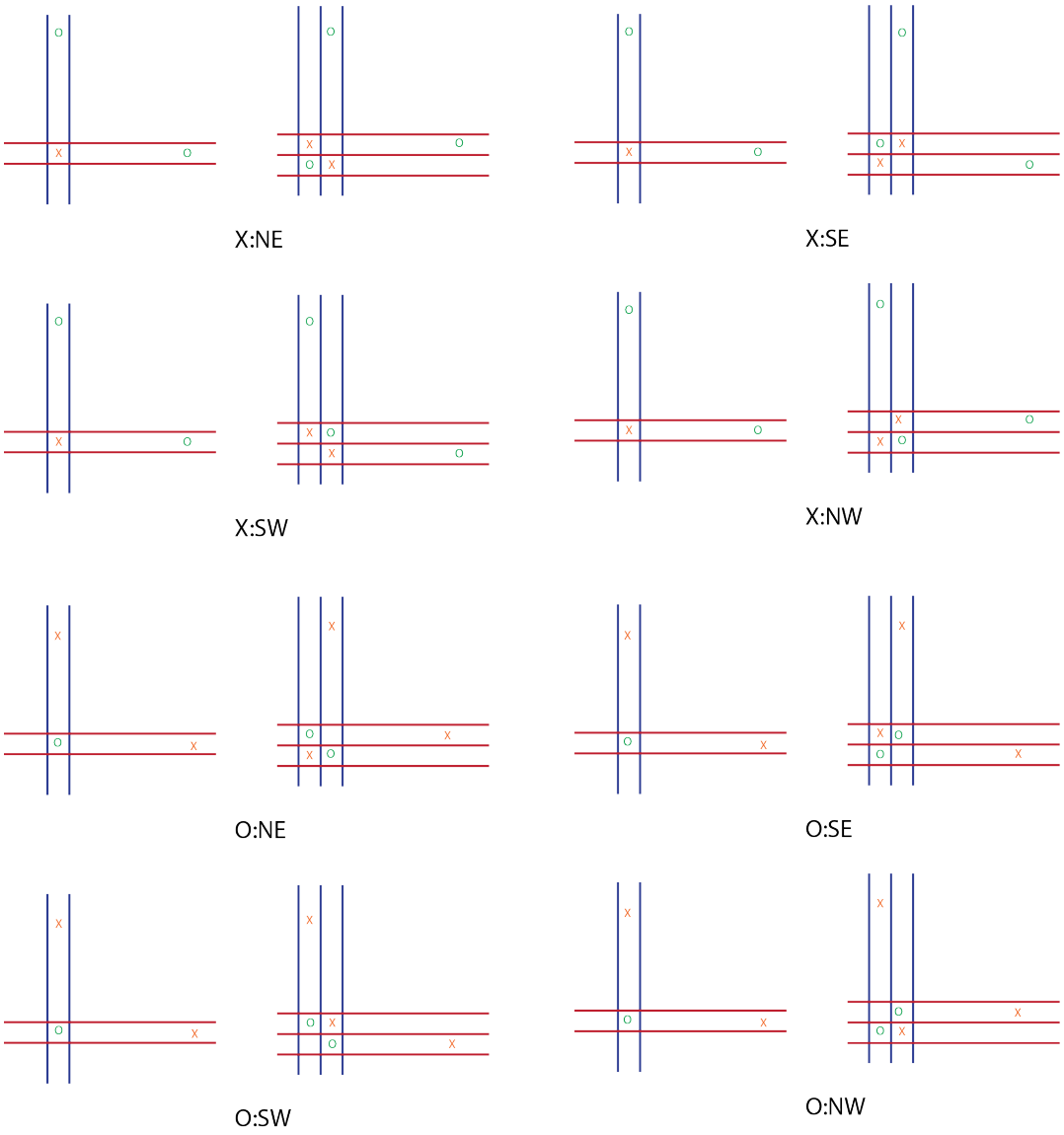

Figure 4.3: The eight types of stabilization grid moves.

4.2 Stabilizations

The first type of serious grid move that we will consider is called a stabilization move. There are eight different kinds, but our arguments will focus only on one. A stabilization move is attained when we add an extra alpha and extra beta curve and replace either a 1 by 1 grid with an X with a 2 by 2 grid with two X's and an O or replace a 1 by 1 grid with an O with a 2 by 2 grid with two O's and an X in the way shown in figure 4.3. The eight types are X:NW, X:NE, X:SE, X:SW, O:NW, O:NE, O:SE, and

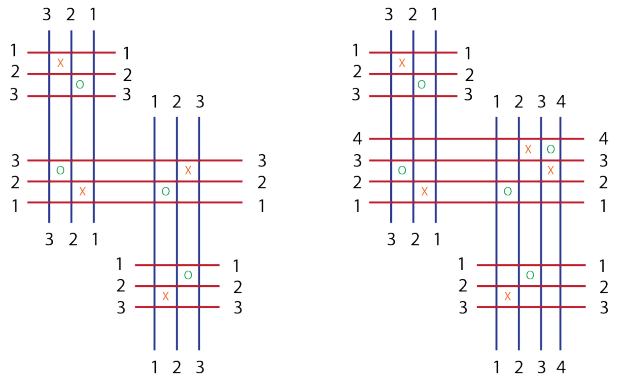

Figure 4.4: An example of an X:SW stabilization move wherein a single X is replace with two X's and an O by adding an additional row and column to the grid.

O:SW. The letter on the left of the colon indicates whether you are stabilizing on an X or an O, and the direction on the right of the colon indicates whether the blank square in the 2 by 2 grid will be in the northwest, northeast, southeast, or southwest corners. An example of an X:SW stabilization is shown in figure 4.4. The original X's and O's that were connecting to the stabilized letter will appear in the column or row containing the blank space of the 2 by 2 grid, i.e. in the only logical way allowable so as not to have two X's or O's in a single column or row. Note that the directions shown are relative to the way we see the grid and not the way it is labeled.

We may go the other way replacing a 2 by 2 grid in one of the ways shown in figure 4.3 with its 1 by 1 equivalent. In this case, we will call the move a destabilization. We will proceed by showing that a stabilization move results in equivalence of the chain complex up to direct sum of homology and equivalence of the type DA structure up to direct sum. This is the only move which will give us a lack of complete equivalence and is a consequence of using the "tilde" construction. A discussion of the implications of this and how we might extend the equivalence to the minus version of combinatorial tangle Floer homology is given in section 7. At present, we will concern ourselves only with an X:SW stabilization, but we will see that this is all we need.

Theorem 5. *If G' and G are tangle diagrams, and G' is obtained from G by a stabilization move of type X:SW, then $HT[G'] \cong HT[G] \oplus HT[G]$.*

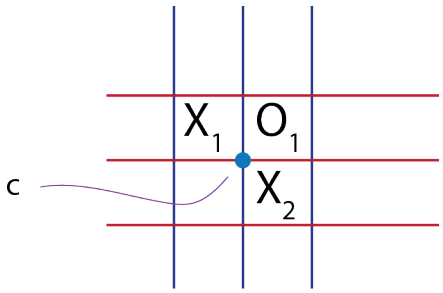

Figure 4.5: The labeling of the 2 by 2 grid created by an X:SW grid stabilization move.

The proof of theorem 5 will come after we establish a few definitions, some notation, and a few lemmas. The following work along with the preceding theorem was adapted from the work in [5]. First, we will distinguish a special alpha-beta crossing in the grid diagram of G'. The 2 by 2 grid created during an X:SW stabilization generates a central alpha-beta crossing in the middle of the grid. If there is a dot at this crossing, then we will refer to it as c. The upper left X in the grid we will call X_1 and the lower right X in the grid we will call X_2. The O in the upper right corner will be called O_1. See figure 4.5 for reference.

We may distinguish generators in $CT(G')$ by whether or not they contain the distinguished dot c. We will call the set of all generators which contain c I, and we will call the set of all generators which do not include c N. The span of I, we will call $\tilde{I}$, and the span of N we will call $\tilde{N}$. Now, $S(G') = I \cup N$, and $\tilde{I} \cup \tilde{N} = CT(G')$. Clearly, both $\tilde{I}$ and $\tilde{N}$ are subspaces of $CT(G')$, but we can say something more of $\tilde{N}$.

Lemma 2. *$\tilde{N}$ is a subcomplex of $CT(G')$.*

Proof. Any rectangle which takes an element of N into $\tilde{I}$ must have c as a top-left or bottom-right dot. However, any such rectangle must contain either X_1 or X_2 and, thus, is not valid. □

This means that it is possible to split up the boundary map into a matrix

$$\partial = \begin{pmatrix} \partial_I^I & 0 \\ \partial_I^N & \partial_N^N \end{pmatrix},$$

where ∂_I^N takes elements of I into elements of N, etc. The map ∂_I^N counts rectangles which are empty and have c as their top-right dot.

Lemma 3. *∂_I^N is a chain map between the complexes $(\tilde{I}, \partial_I^I)$ and $(\tilde{N}, \partial_N^N)$.*

Proof. We want to show that

$$\partial_I^N \circ \partial_I^I + \partial_N^N \circ \partial_I^N = 0.$$

The left hand side counts compatible pairs of rectangles, one of which has c as its top-right dot. There are three cases. See figure 4.6 for pictures. Case 1 is where the two rectangles do not have any dots in common. In that case, it doesn't matter which rectangle is resolved first, and the rectangle which does not have the point c at its corner is counted in both ∂_I^I and ∂_N^N. Resolving one first will yield an element in the image of $\partial_I^N \circ \partial_I^I$ and resolving the other first will yield an element in the image of $\partial_N^N \circ \partial_I^N$. Since we are working over $\mathbb{Z}/2\mathbb{Z}$, these elements cancel each other out.

The second case involves pairs of compatible rectangles which share one side of one of the rectangles and have a 90 degree turn in their combined shape. All such combined shapes are dividable into two different pairs of rectangles, each of which is a legitimate combination of rectangles. Since their ending dots are the same no matter which rectangle is resolved first, they again cancel each other out in the image.

The last case involves pairs of rectangles which share two sides by looping around the grid diagram. Such a pair would be problematic, but no such problematic pair can exist because they must either contain X_1 or X_2.

No other combination of rectangles forms an eligible pair. □

Now, we will define a map $\tilde{e} : \tilde{I} \to CT(G)$ by $x \cup \{c\} \mapsto x$.

Lemma 4. *The map $\tilde{e}$ forms an isomorphism between the chain complexes $(\tilde{I}, \partial_I^I)$ and $CT(G)$.*

Proof. The map $\tilde{e}$ is clearly an isomorphism of vector spaces. Furthermore, eligible

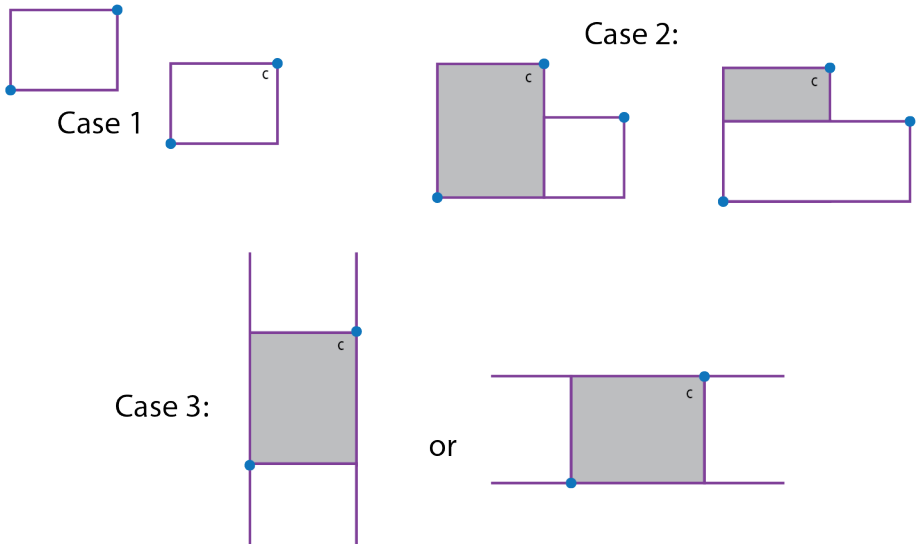

Figure 4.6: The three cases possible in showing that ∂_I^N is a chain map. The shaded rectangles are resolved first.

rectangles disjoint from X's and O's in G correspond to rectangles disjoint from X's and O's in G' which do not contain the point c as their top-right dot. □

Next we will define three more maps. First, define the map $H^I_{X_2} : \tilde{N} \to \tilde{I}$ by

$$H^I_{X_2} = \sum_{y \in I} \#\{r \in \text{Rect}^\circ(x,y) | \text{r contains only } X_2\} \cdot y.$$

Next, define $H^N_{O_1} : \tilde{I} \to \tilde{N}$ by

$$H^N_{O_1}(x) = \sum_{y \in N} \#\{r \in \text{Rect}^\circ(x,y) | \text{r contains only } O_1\} \cdot y.$$

Finally, define $H_{O_1,X_2} : \tilde{N} \to \tilde{N}$ by

$$H_{O_1,X_2}(x) = \sum_{y \in N} \#\{r \in \text{Rect}^\circ(x,y) | \text{r contains only} X_2 \text{ and } O_1\} \cdot y.$$

Thus, $H^I_{X_2}$ counts rectangles whose top-left corner is where c will be, $H^N_{O_1}$ counts rectangles whose bottom-left corner is at c, and H_{O_1,X_2} counts rectangles whose left edge lies on the

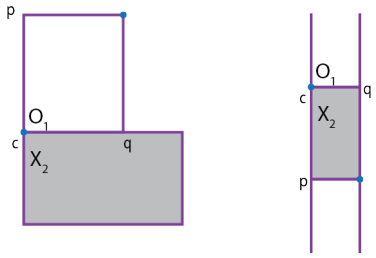

Figure 4.7: $H^I_{X_2} \circ H^N_{O_1}$ counts rectangles of the type on the left of this figure. However, only annuli will work as shown on the right. Furthermore, only a thin annulus will work, resulting in the identity.

beta curve which contains c and which contain X_2 and O_1.

Lemma 5. *Both $H^I_{X_2}$ and $H^N_{O_1}$ are chain maps.*

Proof. The proof of this follows exactly along the lines of the proof that ∂^N_I is a chain map. See lemma 3. □

Lemma 6. *The composition map $H^I_{X_2} \circ H^N_{O_1} = Id_{\tilde{I}}$.*

Proof. The map $H^I_{X_2} \circ H^N_{O_1}$ counts juxtapositions of rectangles of the type shown on the left hand side of figure 4.7. However, the X_2 rectangle must have the corners p and q as its bottom-left and top-right corners respectively. Thus, only annuli will work. However, any annulus which is more than one column wide will automatically pick up an X or an O. Thus, only a "thin" annulus is allowed, and this composition of rectangles results in the identity map. □

Lemma 7.

$$H^N_{O_1} \circ H^I_{X_2} + \partial^N_N \circ H_{O_1,X_2} + H_{O_1,X_2} \circ \partial^N_N = Id_N.$$

Proof. The left hand side of the equation counts eligible combinations of rectangles which together contain X_2 and O_1. All of the allowable combinations which do not form annuli are dividable into two different combinations and, therefore, cancel in pairs (see figure 4.8). The only allowable annulus has to again be thin lest it pick up an unwanted X or O. The thin annulus results in the identity. □

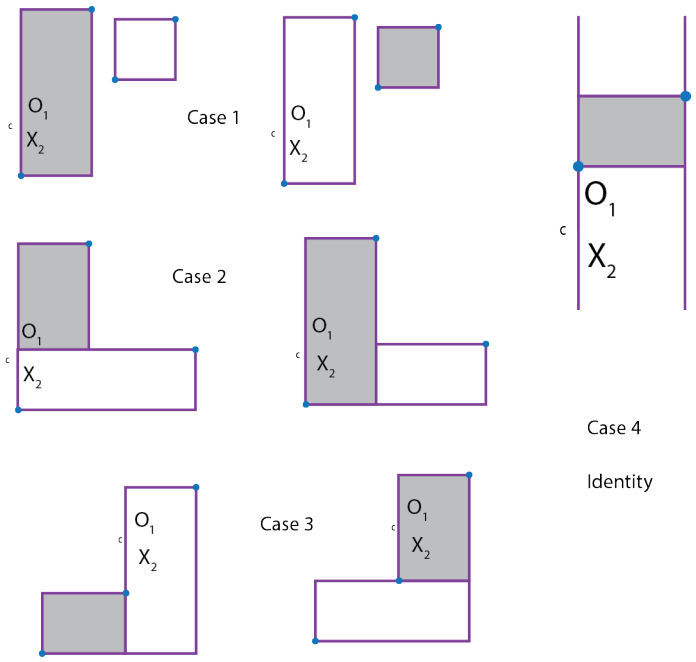

Figure 4.8: The possible cases involved in showing that $H^I_{X_2}$ and $H^N_{O_1}$ are homotopy equivalences.

Lemmas 6, 7, and 5 together show that $H^I_{X_2}$ and $H^N_{O_1}$ are chain homotopy equivalences between $(\tilde{I}, \partial^I_I)$ and $(\tilde{N}, \partial^N_N)$. In particular, they are quasi-isomorphisms. The maps $H^I_{X_2}$, $H^N_{O_1}$, and H_{O_1,X_2} have some additional properties that will prove useful to us.

Proposition 1.

$$H_{O_1,X_2} \circ H^N_{O_1} = 0,$$

$$H^I_{X_2} \circ H_{O_1,X_2} = 0,$$

and

$$H_{O_1,X_2} \circ H_{O_1,X_2} = 0.$$

Proof. For a pair of rectangles to work for the first equation, the top-left corner of the O_1 rectangle must be the bottom-left corner of the O_1, X_2 rectangle. Thus, there are two cases (shown in figure 4.9). In case 1, the dot r is in the way of the first rectangle. In case 2, the dot q is in the way of the second rectangle. Showing that the second equation holds is almost exactly analogous to showing that the first equation holds.

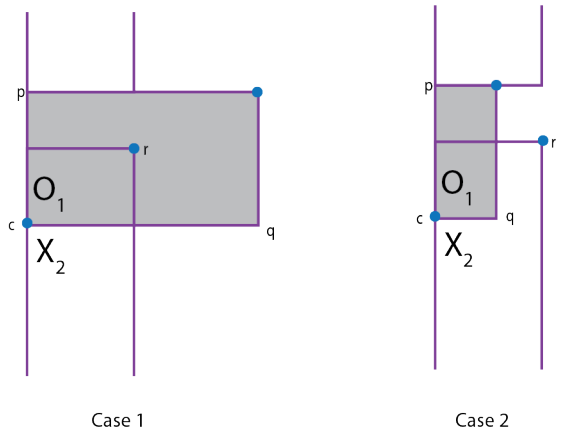

Figure 4.9: The two cases involved in showing that $H_{O_1,X_2} \circ H^N_{O_1} = 0$. On the left, the dot r is in the way. On the right, the dot q is in the way.

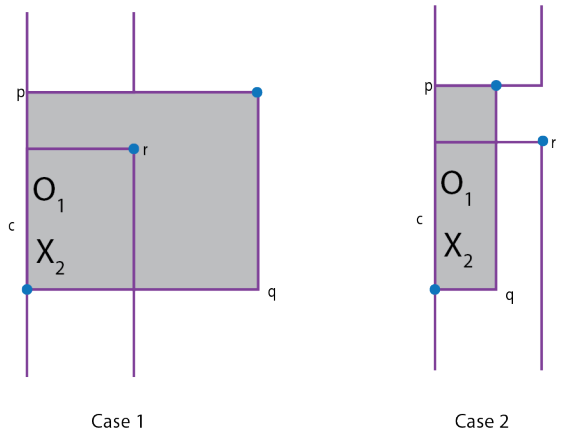

Figure 4.10: The two cases involved in showing that $H_{O_1,X_2} \circ H_{O_1,X_2} = 0$. On the left, the dot r is in the way. On the right, the dot q is in the way.

The third equation equation is also similar. See figure 4.10. Again, the point p must serve as the top-left and bottom-left corners of the first and second rectangles respectively. In case 1, r is in the way, and in case 2, q is in the way. □

Lemma 8. *The chain map ∂^N_I induces the zero map on homology.*

Proof. We will begin by showing that $H^I_{X_2} \circ \partial^N_I = 0$. We are looking for juxtapositions of rectangles of the type shown on the left in figure 4.11. However, the point p must be the top-right corner of the second rectangle and the point q must be the bottom-left. This only leaves an annulus. However, any such annulus must contain the O connected to X_2.

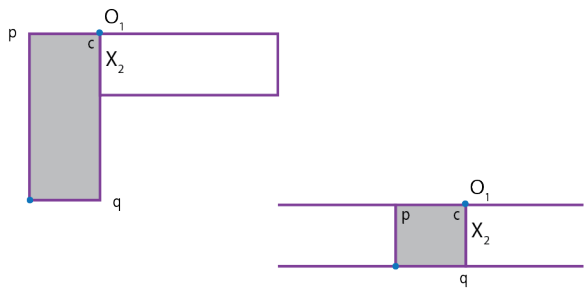

Figure 4.11: The situation for $H^I_{X_2} \circ \partial^N_I$ is shown on the left. The only possible case is shown on the right. That case must contain an O and, thus, is also not possible.

Now, $H^I_{X_2} \circ \partial^N_I = 0$ implies that $H(H^I_{X_2}) \circ H(\partial^N_I) = 0$. However, we showed before that $H(H^I_{X_2})$ is an isomorphism, so $H(\partial^N_I) = 0$. □

Now, we return to prove the big theorem (theorem 5).

Proof of theorem 5. Given what we know,

$$0 \to \tilde{N} \to CT(G') \to \tilde{I} \to 0$$

is a short exact sequence with corresponding connecting homomorphism $\eta = H(\partial^N_I) = 0$. Thus, the long exact sequence induced by this short exact sequence,

$$\cdots \to H(\tilde{N}) \to HT(G') \to H(\tilde{I}) \to^{\eta=0} H(\tilde{N}) \to CT(G') \to \cdots,$$

results in the short exact sequence

$$0 \to H(\tilde{N}) \to HT(G') \to H(\tilde{I}) \to 0.$$

So,

$$0 \to HT(G) \to HT(G') \to HT(G) \to 0$$

is exact and, over a vector space, splits. So, $HT(G') \cong HT(G) \bigoplus HT(G)$. □

Since, X's and O's are treated the same in the tilde variety of combinatorial tangle

Floer homology, this same argument works, mutatis mutandis, for an O:SW stabilization as well.

4.2.1 Stabilizations and type DA structures

We have now shown that $(CT(G), \partial)$ is isomorphic $(\tilde{I}, \partial^I_I)$ as chain complexes and that $(CT(G'), \partial')$ is homotopy equivalent to $(\tilde{I} \bigoplus \tilde{I}, \partial^I_I \bigoplus \partial^I_I)$. We have also shown that $(\tilde{N}, \partial^N_N)$ is chain homotopy equivalent to $(\tilde{I}, \partial^I_I)$ via a strong deformation retraction, that is via a chain homotopy equivalence and homotopy which meet the conditions in proposition 1. We would like to extend this picture to the type DA case. That is, we would like to find a structure $(\tilde{I}, \overline{\delta_i})$ that is homotopy equivalent to $(CT(G), \delta_i)$ as a type DA structure and a structure $(\tilde{I} \bigoplus \tilde{I}, \overline{\delta'_i})$ that is equivalent to $(CT(G'), \delta'_i)$ as a type DA structure such that $(\tilde{I} \bigoplus \tilde{I}, \overline{\delta'_i})$ is equivalent to $(\tilde{I} \bigoplus \tilde{I}, \overline{\delta_i} \bigoplus \overline{\delta_i})$.

The first part is not too difficult. Let's call the δ^L map for G δ^L_G. Let $\pi : CT(G) \to \tilde{I}$ be defined by $\pi(x) = x \cup \{c\}$, i.e. let π be the inverse of $\tilde{e}$ from earlier. Let i be $\tilde{e}$ from earlier. Furthermore, let $H = 0$. Define $\overline{\delta^L_I} = (\mathrm{Id} \otimes \pi) \circ \delta^L_G \circ i$. It is not hard to see that $\overline{\delta_1} = (1 \otimes \partial^I_I) + \overline{\delta^L_I}$ gives $\tilde{I}$ a type D structure and that it is actually equal to $(1 \otimes \partial^I_I) + \delta^L_I$. Thus, we simply define $\overline{\delta_i} = 0$ if $i \geq 3$ and H provides the needed homotopy. Furthermore, one can easily check $\overline{\delta_2} = (\mathrm{Id} \otimes \pi) \circ \delta^G_2 \circ i$ is actually equal to δ^I_2 and thus $H = 0$ serves as the homotopy for the DA equivalence.

Now, on to harder things. We would like to find some DA structure $\overline{\delta'_i}$ on $\tilde{I} \oplus \tilde{I}$ such that $(\tilde{I} \oplus \tilde{I}, \overline{\delta'_i})$ is homotopy equivalent to $(CT(G'), \delta'_i)$ as a type DA structure. We will start by looking at the more general case.

4.2.2 Transferring Type DA Structures via Strong Deformation Retractions

The work in this section was highly inspired by [13], [14] and [9]. Let M and N be modules such that (M, ∂^M) and (N, ∂^O) are chain complexes, $(M, (1 \otimes \partial^M) + \delta^L_M)$ and $(N, (1 \otimes \partial^O) + \delta^L_O)$ are type D structures, and (M, δ^M_i) and (N, δ^O_i) are type DA structures. Assume that $\delta_M := (1 \otimes \partial^M) + \delta^L_M = \delta^M_1$ and $\delta_O := (1 \otimes \partial^O) + \delta^L_O = \delta^O_1$. Furthermore,

assume that (M, ∂^M) and (N, ∂^O) are chain homotopy equivalent via a strong deformation retraction. That is, assume there are maps $\pi : M \to N$, $i : N \to M$, and $H : M \to M$ such that

$$\pi \circ \partial^M = \partial^O \circ \pi, \tag{4.1}$$

$$i \circ \partial^O = \partial^M \circ i, \tag{4.2}$$

$$\pi \circ i = \mathrm{Id}_N, \tag{4.3}$$

$$i \circ \pi = \mathrm{Id}_M + \partial^M \circ H + H \circ \partial^M, \tag{4.4}$$

$$\pi \circ H = 0, \tag{4.5}$$

$$H \circ i = 0, \tag{4.6}$$

and

$$H \circ H = 0. \tag{4.7}$$

We will see that this is exactly the situation we are in. Think N for new structure on N and O for the old structure on N. We would like to explore when it is possible to transfer the type D and type DA structure of M to N. That is, when can we provide N with a type D and type DA structure that is based on M and automatically equivalent to the type D and type DA structure on M. This will provide N with two type DA structures, one of which is equivalent to the type DA structure on M. If it then turns out that both of the type DA structures on N are equal, then we will know that the (N, δ_i^O) and (M, δ_i^M) were originally equivalent as type DA structures. This is our game plan. We will work step by step, first extending the type D structure and then extending the type DA structure to the type D structure.

Now, to accomplish this we will introduce some new notation. See figures 4.12 and 4.13 for a key to the new notation. Essentially we will represent maps on our modules by circles and maps on our algebras by triangles. We will let the maps flow downward

connecting circles in order to show composition. For instance, a green circle on top of an orange circle is simply the map $\partial^M \circ H$. Since we are working over a dg algebra, our μ_2 maps are truly associative and we will in general suppress their notation unless it becomes important.

We will also use rectangles to indicate infinite sums of maps which have certain repeating patterns. Those are defined in figure 4.13. Rectangles are either provided with an integer or an integer with a dot. The integer indicates which term to start with. If a dot is included along with the integer, then this indicates that were are picking out a certain term as opposed to the whole sum. We will also suppress additive notation since it takes up a lot of space and is in general superfluous; adjacent columns of circles are simply taken to be added together.

It will take a bit of investment to get used to this notation, but its benefit will become apparent when we get to type DA structures where our definitions will involve infinite sums of infinite sums of maps in various combinations.

To aid the reader in getting used to the new notation figure 4.14 rewrites our assumptions in circle notation. The beauty of this notation is that figure 4.14 tells us in the top right equation that π is a chain map, but it also tells us that we may simply replace a pink circle over a brown circle with an orange circle over a pink circle or vice versa. This is how we will make our arguments.

Figure 4.15 shows the definition of δ_M in circle notation and writes in two different ways the type D conditions on δ_M. We will often use the bottom right equation to replace two blue circles with the other three terms.

All right, now to our first use of our new tool. Define

$$\delta_N = (1 \otimes \partial_N) + (\mathrm{Id} \otimes \pi) \circ \delta_M^L \circ i + (\mathrm{Id} \otimes \pi) \circ (\mu_2 \otimes \mathrm{Id}) \circ (\mathrm{Id} \otimes \delta_M^L) \circ (\mathrm{Id} \otimes H) \circ \delta_M^L \circ i + \cdots$$

where each consecutive term adds one more H and δ_M^L map. We will now show that δ_N is a

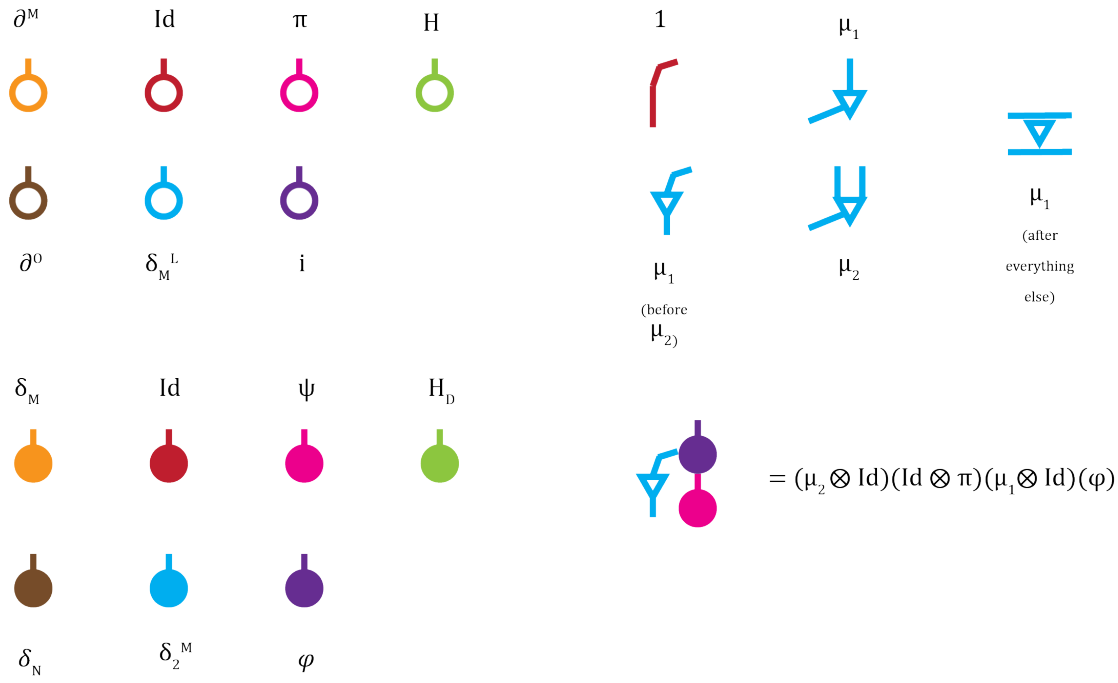

Figure 4.12: This figure provides a key for our circle notation. The open circles are in general maps on the chain complex with the exception of the blue circle which is the δ_M^L map. The filled circles are in general type D maps again with the exception of the blue circle which is the δ_2^M map. μ_2 is in general suppressed from the notation since it plays little role in the calculations and is associative. An example of a map in this notation is given in the bottom right of the diagram.

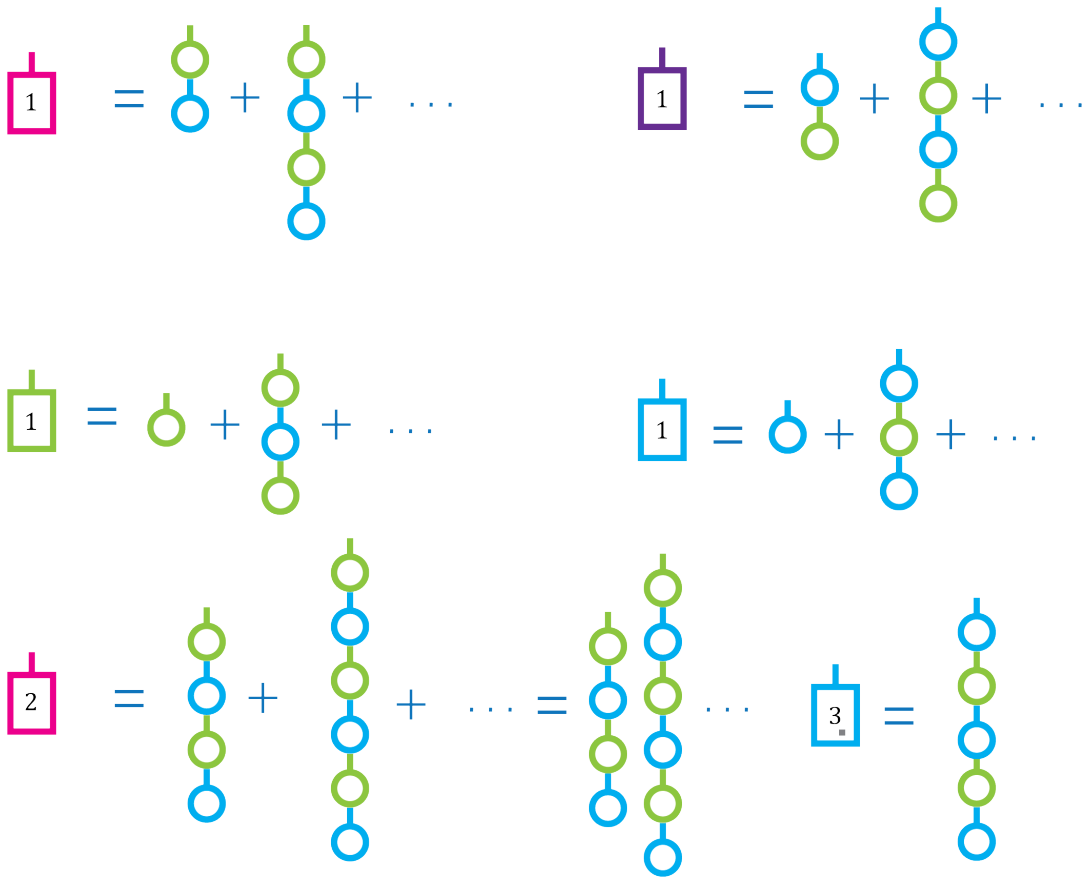

Figure 4.13: This figure provides a key for our rectangle notation. The number inside the rectange tells you where to start the sum. The numbers inside the pink, purple, and blue rectangles indicates how many blue circles there are in the first term. The number inside the green rectangle indicates how many green circles are in the first term. The rest of the terms simply increment based on the pattern. Rectangles always imply infinite sums of terms unless there is a dot inside the rectangle, which indicates that we are picking out a specific term (see bottom right). We will often omit the plus signs as they are superfluous.

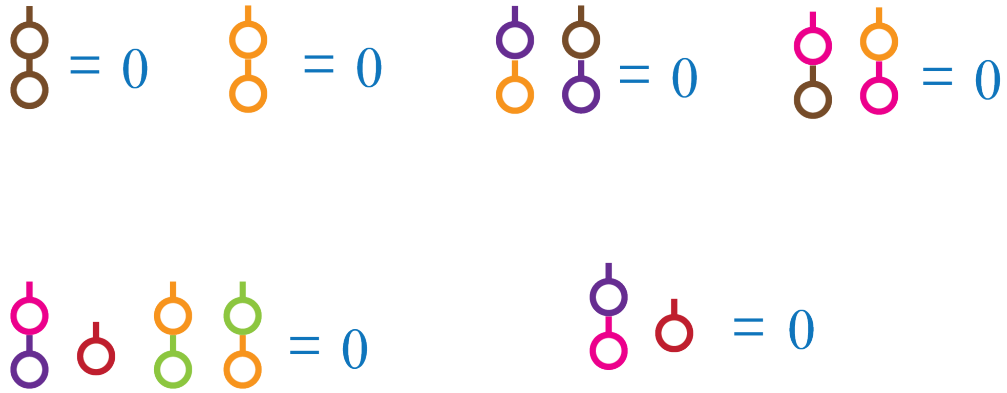

Figure 4.14: This figure rewrites our assumptions about our chain complexes in circle notation. TOP LEFT: ∂^O is a boundary map TOP MIDDLE: ∂^M is a boundary map TOP RIGHT (both): π and i are chain maps BOTTOM LEFT: $i \circ \pi + \mathrm{Id} + H \circ \partial^M + \partial^M \circ H = 0$ BOTTOM RIGHT: $\pi \circ i = \mathrm{Id}$

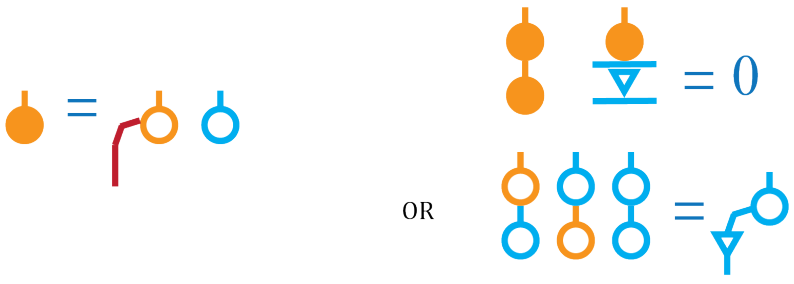

Figure 4.15: LEFT: The definition of δ_M in circle notation TOP RIGHT: The type D condition for δ_M BOTTOM RIGHT: Rewriting the type D condition in terms of open circles after taking into account the fact that $\partial^M \circ \partial^M = 0$ and $\mu_1(1) = 0$.

type D map boundary map.

Proposition 2. *Define δ_N as in the top of figure* 4.16. *If δ_N is finite, then δ_N is a type D boundary map on N.*

Proof. The proof is also given in figure 4.16. □

Note that we have included the condition that δ_N be finite as defined. There are ways of guaranteeing that the transferred structure is finite. However, we will opt to show that our maps are finite directly. The point here is that if δ_N is finite, then it cancels with itself in precisely the right way to be a type D boundary map.

Now, we will define our homomorphisms between the type D structure (M, δ_M) and the type D structure (N, δ_N) and show that they are type D homomorphisms. Define $\phi : (N, \delta_N) \to (M, \delta_M)$ and $\psi : (M, \delta_M) \to (N, \delta_N)$ as shown in figure 4.17.

Proposition 3. *The type D maps ϕ and ψ as defined above are type D homomorphisms.*

Proof. The proof that ϕ is a type D homomorphism is given in figure 4.18, and the proof that ψ is a type D homomorphism is given (more compactly) in figure 4.19. Note in figure 4.18 that the last equation is true because of the Leibnitz rule in our dg algebra and because $\mu_1(1) = 0$. The same is true for the first equals sign in the bottom row of figure 4.19. □

Now, define H_D as shown in figure 4.20. We will now show that the maps ϕ, ψ, and H_D have properties which mimic our starting conditions. Remember that we are assumming the assumptions in equations 4.1 through 4.7.

Theorem 6. *Let (M, ∂^M) and (N, ∂^O) be chain complexes which satisfy the assumptions of equations* 4.1 *through* 4.7. *Furthermore, assume that $\delta_M = (1 \otimes \partial^M) + \delta_M^L$ is a type D boundary map on M. Then ψ, ϕ, and H_D as defined above, when finite, form a strong deformation of type D structures between (M, δ_M) and (N, δ_N), i.e.*

$$\psi * \phi = \mathbb{I}_N, \tag{4.8}$$

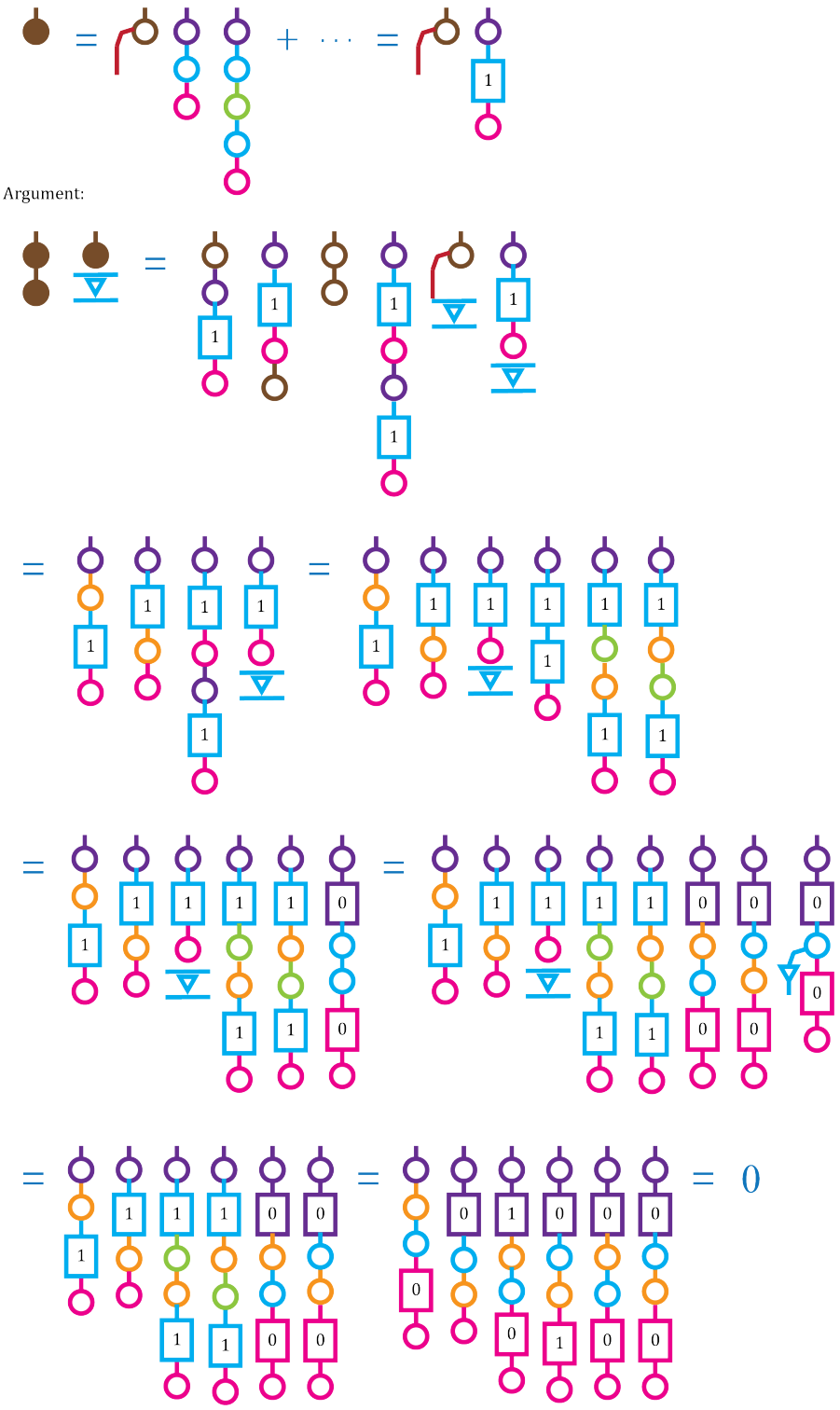

Figure 4.16: TOP: The definition of δ_N in circle notation. BELOW: The argument that δ_N is indeed a type D boundary map given in circle notation.

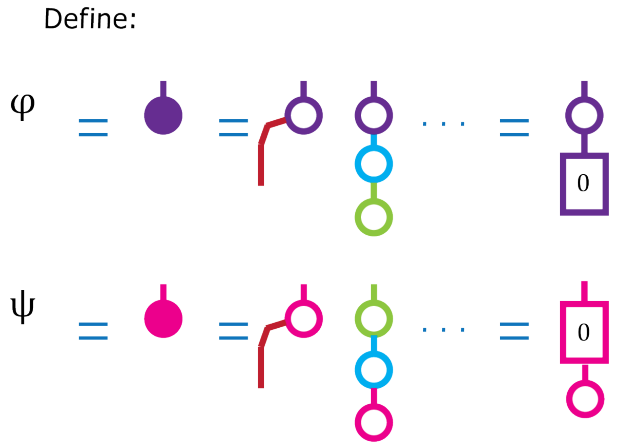

Figure 4.17: TOP: The definition of $\phi : (N, \delta_N) \to (M, \delta_M)$ in circle notation. BOTTOM: The definition of $\psi : (M, \delta_M) \to (N, \delta_N)$ in circle notation. The first terms in each are $(1 \otimes \phi)$ and $(1 \otimes \psi)$ respectively

$$\phi * \psi = \mathbb{I}_M + \delta_M * H_D + H_D * \delta_M + (\mu_1 \otimes Id) \circ H_D, \tag{4.9}$$

$$\psi * H_D = 0, \tag{4.10}$$

$$H_D * \phi = 0, \tag{4.11}$$

and

$$H_D * H_D = 0. \tag{4.12}$$

Proof. The proof of equation 4.8 is given in figure 4.21. The proof of equation 4.9 is given in figure 4.22. The proof of equation 4.10 is given in figure 4.23. In that figure, the second equals sign holds because $H^2 = 0$, and the third one holds because $\pi \circ H = 0$. The proof of equation 4.11 is analogous to that of equation 4.10, and equation 4.12 holds because $H^2 = 0$. □

Thus, we have shown that, under these conditions, we can extend the type D structure from M to N. We will now define a type DA boundary map δ_N^1, type DA homomorphisms ϕ^1 and ψ^1 and a type DA morphism H^1 so that $\phi_1^1 = \phi$, $\psi_1^1 = \psi$, and $H_1^1 = H$ and such that

$$\psi^1 * \phi^1 = \mathbb{I}_N^1, \tag{4.13}$$

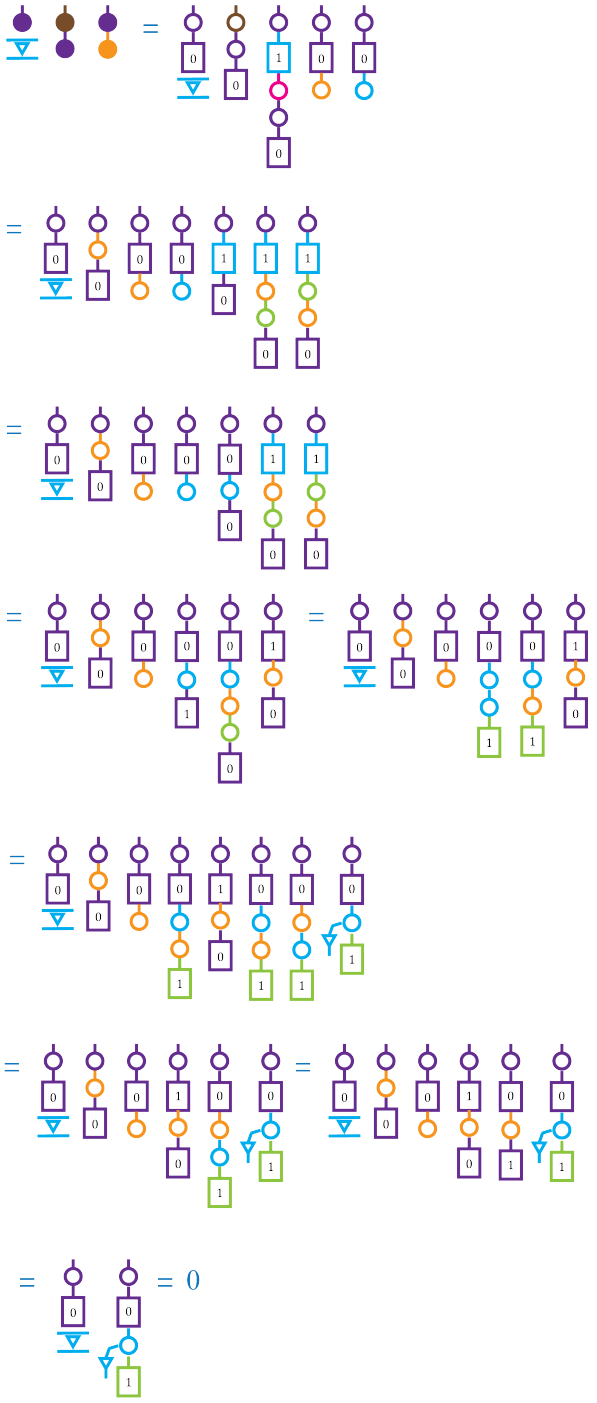

Figure 4.18: The proof in circle notation that ϕ is a type D homomorphism.

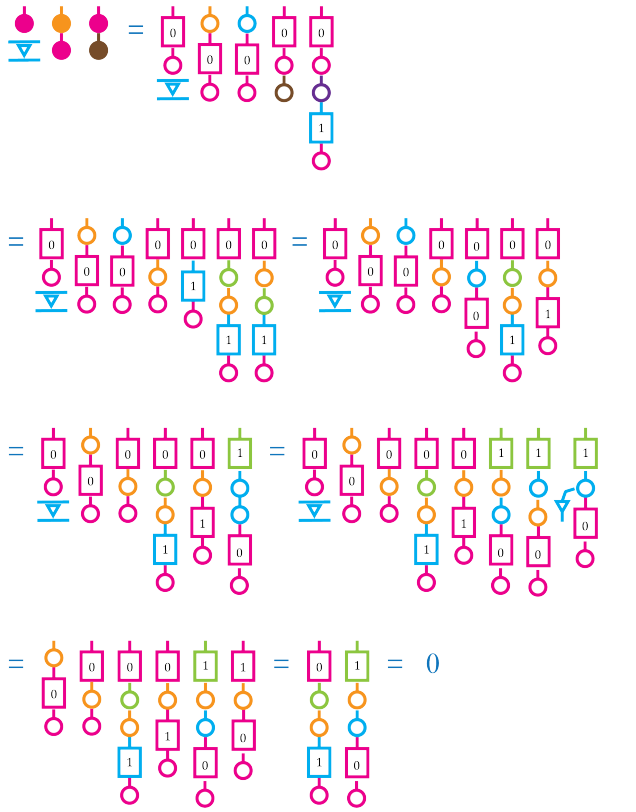

Figure 4.19: The proof in circle notation that ψ is a type D homomorphism.

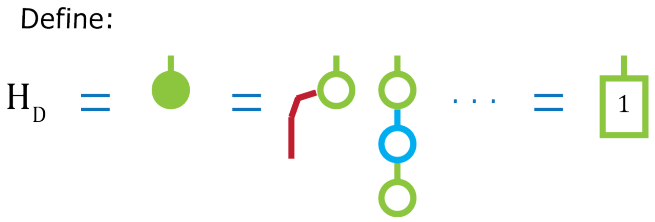

Figure 4.20: The definition of H_D, which will serve as our type D homotopy map.

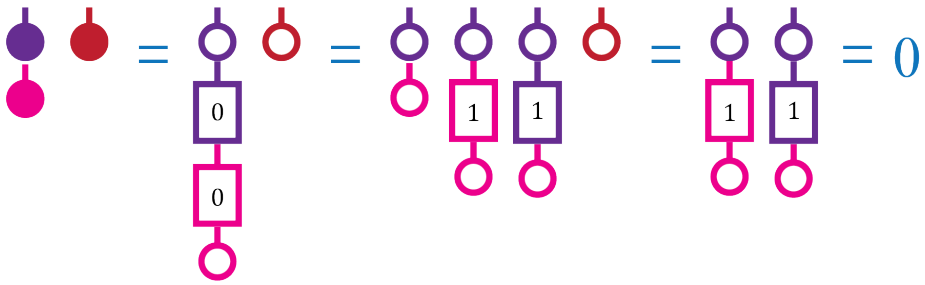

Figure 4.21: The argument for why $\psi * \phi = \mathbb{I}_N$. The argument follows from the definitions and the assumptions that N is a strong deformation retraction of M as a chain complex.

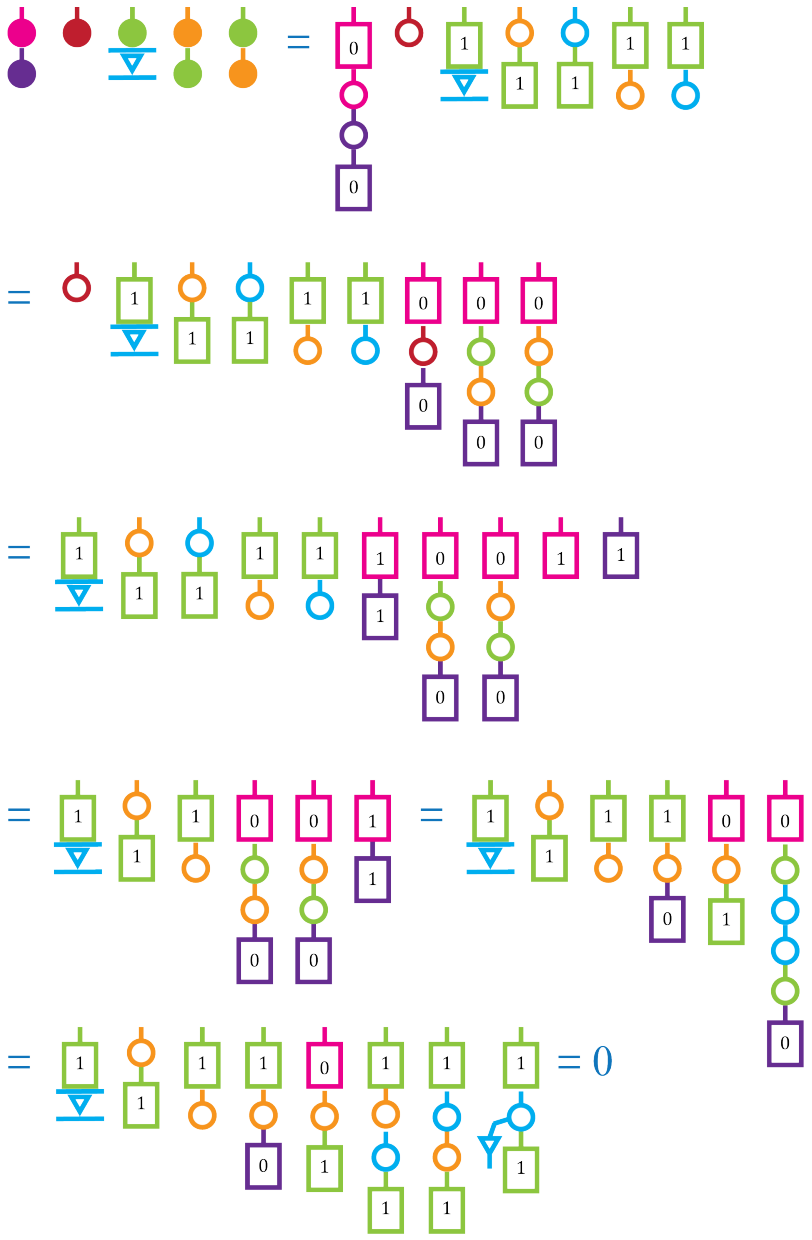

Figure 4.22: The rest of the argument for why ϕ is a type D homotopy equivalence.

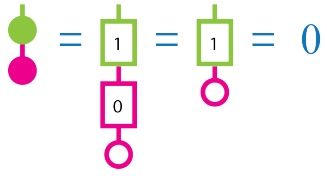

Figure 4.23: The argument for why $\psi * H_D = 0$. The second equals sign holds because $H^2 = 0$, and the third equals sign holds because $\pi \circ H = 0$.

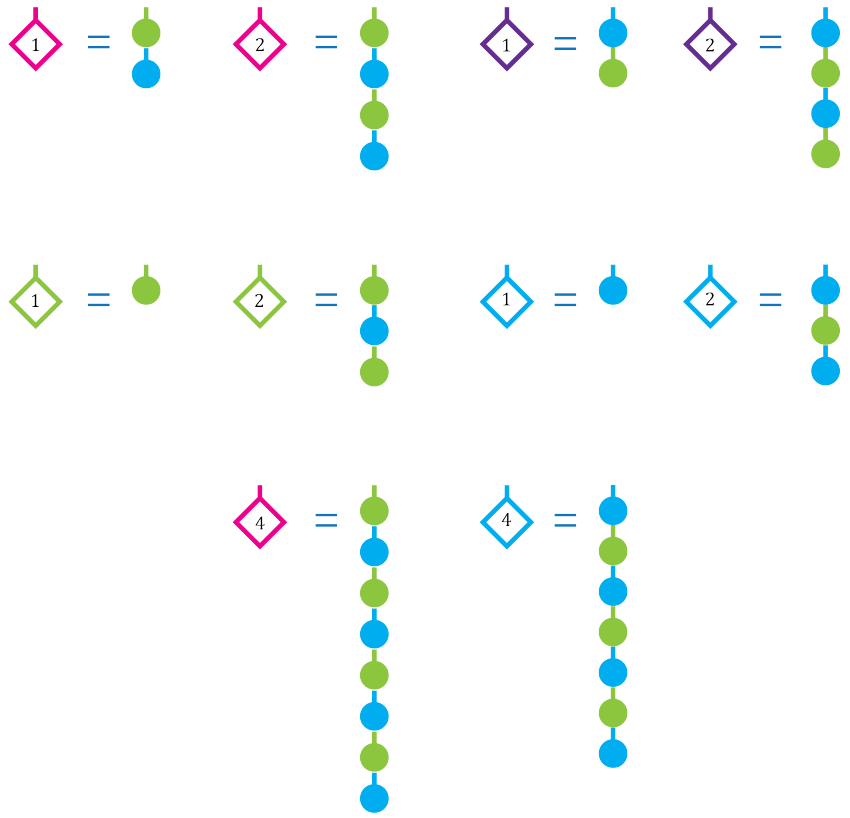

Figure 4.24: The diamond notation mimics the rectangle notation except that each diamond consists of compositions of filled circles instead of just circles. Furthermore, each diamond respresents a single term rather than an infinite sum, working like a rectangle with a dot in it.

$$\phi^1 * \psi^1 = \mathbb{I}^1_M + d(H^1), \tag{4.14}$$

$$\psi^1 * H^1 = 0, \tag{4.15}$$

$$H^1 * \phi^1 = 0, \tag{4.16}$$

and

$$H^1 * H^1 = 0. \tag{4.17}$$

First, we will extend our notation to include type DA maps. For this, we will use a diamond notation. Each diamond will serve the same purpose as the rectangles before, except that the diamonds represent single terms of filled circles rather than infinite sums and work like a rectangle with a dot in it (see figure 4.24). Now we will define our maps.

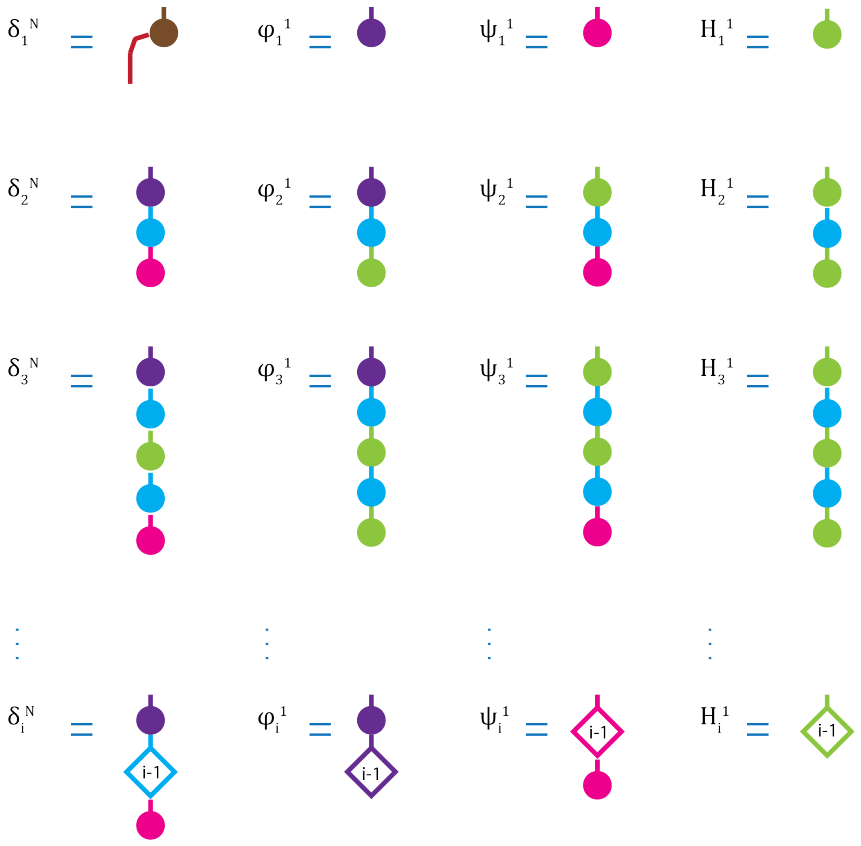

Figure 4.25: This figure shows the definitions of the maps δ^N, ϕ^1, ψ^1, and H^1.

Let the maps δ^N, ϕ^1, ψ^1, and H^1 be defined as in figure 4.25. We now need to show that δ_i^N is a type DA boundary map and that ϕ^1 and ψ^1 are type DA homomorphisms.

Lemma 9. *The map δ^N defined above, when finite, is a type DA boundary map.*

Proof. Recall that to be a type DA boundary map the map δ^N must satisfy for $(x, a_1, \ldots, a_{i-1})$:

$$(\mu_1 \otimes \mathrm{Id}) \circ \delta_i^N + \sum_{j=1}^{i-1} \delta_i^N \circ \mu_1(a_j) + \sum_{j=1}^{i-2} \delta_{i-1}^N \circ \mu_2(a_j, a_{j+1}) + \sum_{j=1}^{i} (\mu_2 \otimes \mathrm{Id}) \circ (\mathrm{Id} \otimes \delta_{i-j+1}^N) \circ (\delta_j^N \otimes \mathrm{Id}^{\otimes(i-j)}) = 0.$$

The proofs for DA structures will be slightly different than the proofs for type D structures. Essentially, we will fix an i, and then show that all of the pieces cancel in pairs. For each proof there will be a "quintessential piece" and all of the canceling pairs will be variations on this quintessential piece.

The four parts of the sum above result in six types of terms, labeled A through F in figure 4.26. The quintessential piece for this proof is a solid purple circle followed by an (i-1) blue diamond followed by a solid pink circle. There are three variations of the quintessential piece. First, an O_k piece is where there is a solid orange circle after the k^{th} circle in the quintessential piece. Second, a D_k piece is where the d^{th} green circle is deleted from the quintessential piece. Finally, an M_k piece results by attaching a μ_1 to the left side of the k^{th} circle in the quintessential piece. Examples of these are shown in figure 4.26 for $i = 3$.

Since δ^M is a type DA boundary map and $\delta_i^M = 0$ for $i \geq 3$, we have

$$\mu_1 \circ \delta_2^M + \delta_2^M \circ (\text{Id} \otimes \mu_1) + \delta_2^M \circ \delta_1^M + \delta_1^M \circ \delta_2^M = 0 \tag{4.18}$$

and

$$\delta_2^M \circ (\text{Id} \otimes \mu_2) + \delta_2^M \circ (\delta_2^M \otimes \text{Id}) = 0. \tag{4.19}$$

Thus, we have that for a fixed i, the type A piece yields $\sum_{k=1}^{2i-1} M_i$, the type B pieces yield $\sum_{k=1}^{i-1} S_{2k} + \sum_{k=1}^{2i-2} O_k$, the type C pieces yield $\sum_{k=1}^{i-1} D_k$, the type D piece yields $S_1 + O_1$, the type E pieces yield $\sum_{k=1}^{i-1} D_k + \sum_{k=1}^{i-2} S_{2k+1} + \sum_{k=2}^{2i-3} O_k$, and, finally, the type F piece yields $S_{2i-1} + O_{2i-2}$. Thus, they all cancel in pairs. This proof works when $i \geq 3$. it can be easily checked that everything cancels when i is 1 or 2 as well. □

Next, we will show that ϕ^1 and ψ^1 are homomorphisms.

Lemma 10. *The type DA maps ϕ^1 and ψ^1, defined above, when finite, are type DA homomorphisms.*

Proof. We will only show that ϕ^1 is a homomorphism. The proof that ψ^1 is a homomorphism is analogous. The proof that ϕ^1 is a homomorphism follows along the same lines as the proof that δ^N is a type DA boundary map. The terms and labeling are slightly different and the quintessential piece is different. See figure 4.27 for reference. The type A

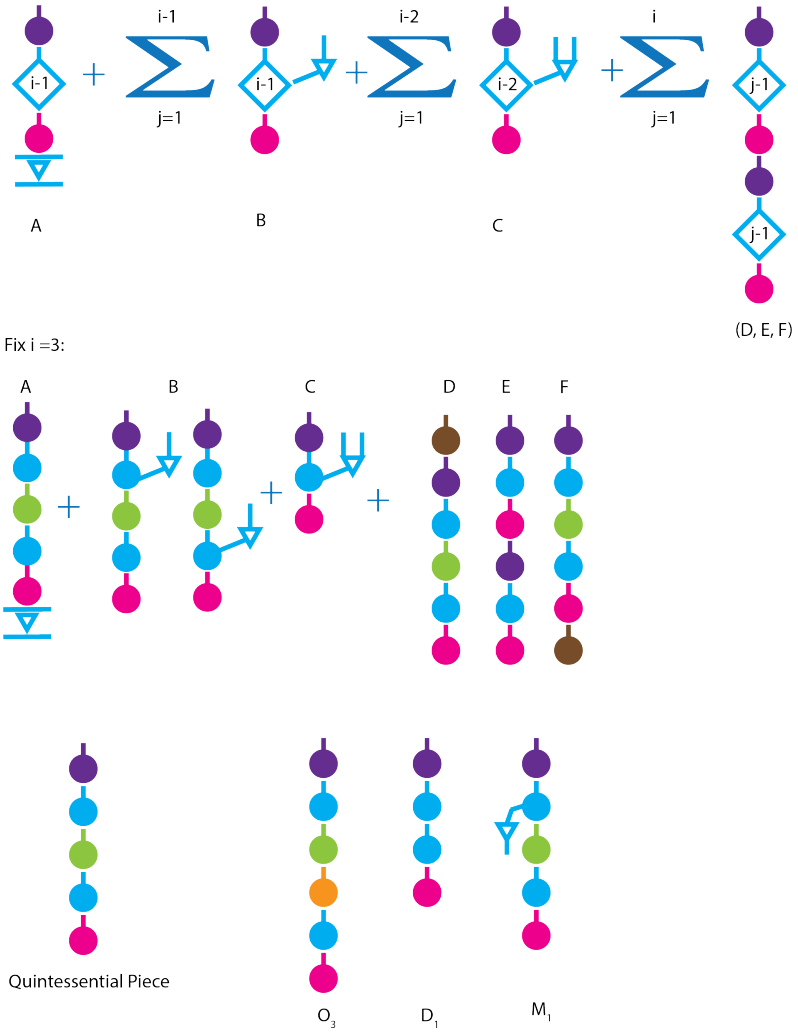

Figure 4.26: The labels used in the proof that δ^N is a type DA boundary map. We need to show that the top sum is equal to zero. The specific pieces for $i = 3$ are shown in the middle, and an example of each variation of the quintessential piece is shown at the bottom.

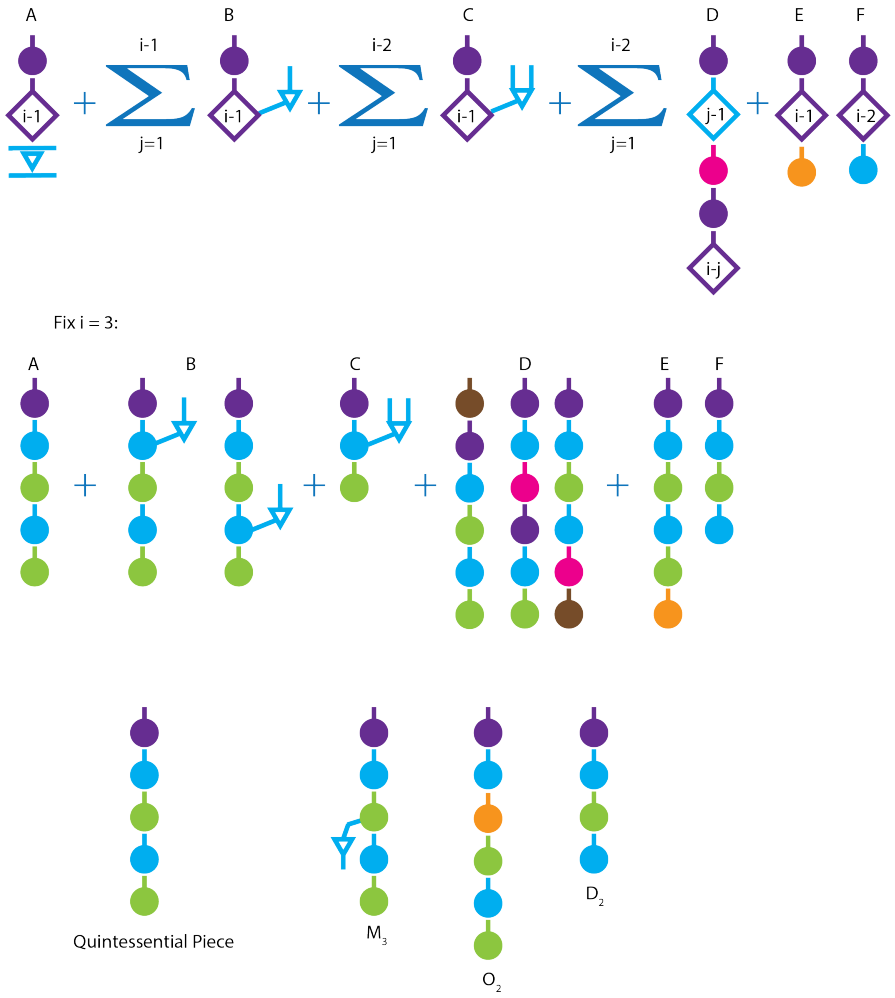

Figure 4.27: The labels used in the proof that ϕ^1 is a type DA homomorphism. We need to show that the top sum is equal to zero. The specific pieces for $i = 3$ are shown in the middle, and an example of each variation of the quintessential piece is shown at the bottom.

pieces result in $\sum_{k=1}^{2i-1} M_k$, the type B pieces result in $\sum_{k=1}^{i-1} M_{2k} + \sum_{k=1}^{2i-2} O_k$, the type C pieces result in $\sum_{k=1}^{i-2} D_k$, the type D pieces result in $O_1 + M_1 + \sum_{k=1}^{i-1} D_k + \sum_{k=1}^{i-1} M_{2k+1} + \sum_{k=2}^{2i-1} O_k$, and, finally, the type E and F pieces result in O_{2i-1} and D_{i-1} respectively. □

Now, to put the pieces together:

Theorem 7. *Given the conditions outlined earlier in the section (including the finiteness conditions of each lemma), the map ψ forms a strong deformation retraction of type DA structures from (M, δ^M) onto (N, δ^N) via the homotopy H^1.*

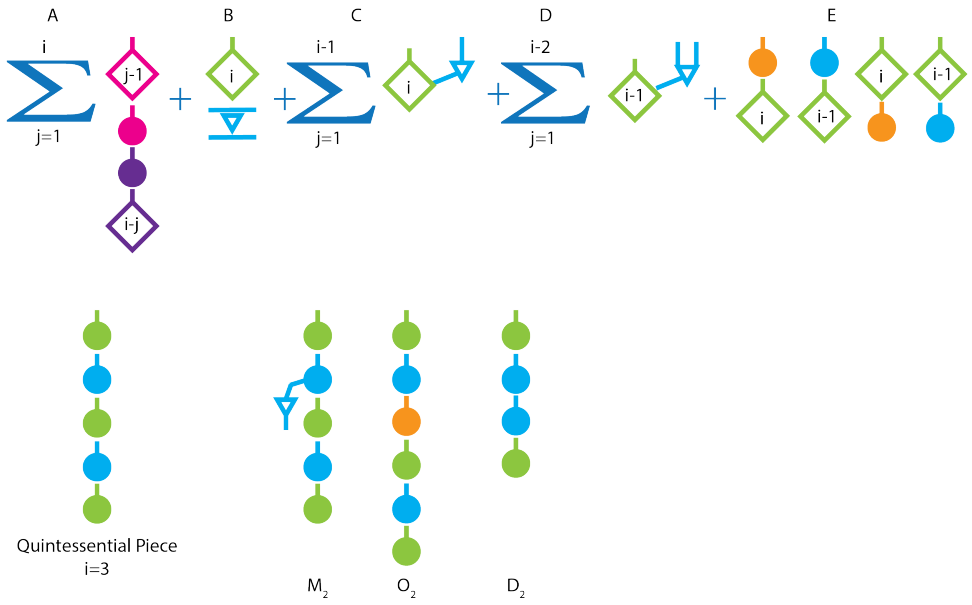

Figure 4.28: The labels used in the proof that $\phi^1 * \psi^1 = d(H^1)$. We need to show that the top sum is equal to zero. A represents $\phi^1 * \psi^1$ and B-E represent the terms of $d(H^1)$. An example of each variation of the quintessential piece is shown at the bottom.

Proof. We have already shown that ϕ^1 and ψ^1 are homomorphisms. So, all we need to show is that $\psi^1 * \phi^1 = \mathbb{I}^1$ and $\phi^1 * \psi^1 = d(H^1)$.

The first task is easy. For $i = 1$, we have $\psi * \phi = \mathbb{I}$, and, for $i > 2$, $\psi^1 * \phi^1 = 0$ because $H_D^2 = 0$, $H_D * \phi = 0$, and $\psi * H_D = 0$. So, we only need to show the second equation.

Again we follow the same technique as before. See figure 4.28 for the labeling. For $i \geq 3$, the pieces of type A result in $\sum_{k=1}^{i} D_k + \sum_{k=0}^{2i-1} O_k + \sum_{k=0}^{i-1} M_{2k+1}$, the pieces of type B result in $\sum_{k=1}^{2i-1} M_k$, the pieces of type C result in $\sum_{k=1}^{i-1} M_{2k} + \sum_{k=1}^{2i-2} O_k$, the pieces of type D result in $\sum_{k=2}^{i-1} D_k$, and, finally, the pieces of type E result in $D_1 + D_i + O_0 + O_{2i-1}$. The case of $i = 1$ and $i = 2$ can be checked directly.

Lastly, we need to show that $\psi^1 * H^1 = 0$, $H^1 * \phi^1 = 0$, and $H^1 * H^1 = 0$. These follow directly from the definition of composition and the facts that $\psi * H_D = \phi * H_D = H_D * H_D = 0$. □

4.2.3 Our Situation

Now that we have shown that we can successfully transfer the type DA structure from M to N, we would like to apply this work to our situation.

The first situation for us is transferring the structure from $M = CT(G)$ to $N = \tilde{I}$. This case is easy because we have an actual isomorphism of chain complexes. This means that $H = 0$. Therefore, all of the maps defined above are automatically finite. Thus, letting $\pi = e$, $i = \tilde{e}$, and $H = 0$, we arrive at a new type DA boundary map on $\tilde{I}$, where $\delta_1^N = (\mathrm{Id} \otimes e) \circ \delta_1^M \circ \tilde{e}$ and $\delta_2^N = (\mathrm{Id} \otimes e) \circ \delta_2^M \circ (\tilde{e} \otimes \mathrm{Id})$. It can easily be checked that the isomorphism does not interfere with the boundary map, and, thus, $\delta^O = \delta^N$, so we will move on the more interesting situation.

For the following discussion let $M = CT(G')$ and let $N = \tilde{I} \oplus \tilde{I}$. We know from the discussion before that the boundary map for M can be written as $\partial' = \begin{pmatrix} \partial_I^I & o \\ \partial_I^N & \partial_N^N \end{pmatrix}$. Let $\pi = \begin{pmatrix} \mathrm{Id}_I & 0 \\ 0 & H^I_{X_2} \end{pmatrix}$ and $i = \begin{pmatrix} \mathrm{Id}_I & 0 \\ H_{O_1,X_2}\partial_I^N & H^N_{O_1} \end{pmatrix}$.

Lemma 11. *The map π as defined above is a chain map.*

Proof. First, we need to show that $\pi\partial' = \partial^O\pi$, where $\partial^O = \begin{pmatrix} \partial_I^I & 0 \\ 0 & \partial_I^I \end{pmatrix}$. Now,

$$\pi\partial' = \begin{pmatrix} \mathrm{Id}_I & 0 \\ 0 & H^I_{X_2} \end{pmatrix} \begin{pmatrix} \partial_I^I & 0 \\ \partial_I^N & \partial_N^N \end{pmatrix} = \begin{pmatrix} \partial_I^I & 0 \\ H^I_{X_2}\partial_I^N & H^I_{X_2}\partial_N^N \end{pmatrix},$$

and

$$\partial^O\pi = \begin{pmatrix} \partial_I^I & 0 \\ 0 & \partial_I^I \end{pmatrix} \begin{pmatrix} \mathrm{Id}_I & 0 \\ 0 & H^I_{X_2} \end{pmatrix} = \begin{pmatrix} \partial_I^I & 0 \\ 0 & \partial_I^I H^I_{X_2} \end{pmatrix}.$$

The bottom right entries are equal because $H^I_{X_2}$ is a chain map, so we need to see that $H^I_{X_2}\partial_I^N = 0$. A rectangle in ∂_I^N must have c as its upper right corner. Call the point that c

gets moved to on the same α curve p. Then, p must be the upper right corner for any $H^I_{X_2}$ rectangle and the edge of the rectangle must be on the β curve containing c. Therefore, the $H^I_{X_2}$ rectangle must contain the O corresponding to X_2. □

Lemma 12. *The map i, as defined above is a chain map.*

Proof. Now,

$$\partial' i = \begin{pmatrix} \partial^I_I & 0 \\ \partial^N_I & \partial^N_N \end{pmatrix} \begin{pmatrix} \mathrm{Id}_I & 0 \\ H_{O_1,X_2}\partial^N_I & H^N_{O_1} \end{pmatrix} = \begin{pmatrix} \partial^I_I & 0 \\ \partial^N_I + \partial^N_N H_{O_1,X_2}\partial^N_I & \partial^N_N H^N_{O_1} \end{pmatrix},$$

and

$$i\partial^O = \begin{pmatrix} \mathrm{Id}_I & 0 \\ H_{O_1,X_2}\partial^N_I & H^N_{O_1} \end{pmatrix} \begin{pmatrix} \partial^I_I & 0 \\ 0 & \partial^I_I \end{pmatrix} = \begin{pmatrix} \partial^I_I & 0 \\ H_{O_1,X_2}\partial^N_I\partial^I_I & H^N_{O_1}\partial^I_I \end{pmatrix}.$$

Again, the bottom right entries are the same since $H^N_{O_1}$ is a chain map, so we just need $\partial^N_I + \partial^N_N H_{O_1,X_2}\partial^N_I = H_{O_1,X_2}\partial^N_I\partial^I_I$. Now,

$$\partial^N_I + \partial^N_N H_{O_1,X_2}\partial^N_I = (\mathrm{Id}_N + \partial^N_N H_{O_1,X_2})\partial^N_I + (H_{O_1,X_2}\partial^N_N + H^N_{O_1}H^I_{X_2})\partial^N_I = H_{O_1,X_2}\partial^N_I\partial^I_I$$

since $H^I_{X_2}\partial^N_I = 0$ as shown before. □

Now, define our homotopy to be $H = \begin{pmatrix} 0 & 0 \\ 0 & H_{O_1,X_2} \end{pmatrix}$. We will now show by a series of lemmas that π and i give us a strong deformation retraction.

Lemma 13. $H^2 = \pi \circ H = H \circ i = 0$.

Proof. First,

$$H^2 = \begin{pmatrix} 0 & 0 \\ 0 & H_{O_1,X_2} \end{pmatrix} \begin{pmatrix} 0 & 0 \\ 0 & H_{O_1,X_2} \end{pmatrix} = \begin{pmatrix} 0 & 0 \\ 0 & H_{O_1,X_2}H_{O_1,X_2} \end{pmatrix} = \begin{pmatrix} 0 & 0 \\ 0 & 0 \end{pmatrix}.$$

The proofs that $\pi \circ H$ and $H \circ i$ follow similarly from the facts that $H^2_{O_1,X_2} = 0$, $H^I_{X_2} H_{O_1,X_2} = 0$, and $H_{O_1,X_2} H^N_{O_1} = 0$. □

Theorem 8. *The maps π and i form a strong deformation retraction via the homotopy H.*

Proof. We have shown most of what we need in the lemmas above. All that remains to be seen is that $\pi \circ i = \mathrm{Id}$ and $i \circ \pi = \partial^M \circ H + H \circ \partial^M$. Now,

$$\pi \circ i = \begin{pmatrix} \mathrm{Id}_I & 0 \\ H^I_{X_2} H_{O_1,X_2} \partial^N_I & H^I_{X_2} H^N_{O_1} \end{pmatrix}.$$

Since $H^I_{X_2} \circ H^N_{O_1} = \mathrm{Id}$, all we need is that $H^I_{X_2} \circ H_{O_1,X_2} \circ \partial^N_I = 0$ which is true since $H^I_{X_2} H_{O_1,X_2} = 0$.

Next,

$$i \circ \pi = \begin{pmatrix} \mathrm{Id}_I & 0 \\ H_{O_1,X_2} \partial^N_I & H^N_{O_1} \end{pmatrix} = \begin{pmatrix} \mathrm{Id}_i & 0 \\ 0 & \mathrm{Id} \end{pmatrix} + \begin{pmatrix} 0 & 0 \\ 0 & H_{O_1,X_2} \partial^N_N + \partial^N_N H_{O_1,X_2} \end{pmatrix},$$

and

$$\partial^M H + H \partial^M = \begin{pmatrix} 0 & 0 \\ 0 & \partial^N_N H_{O_1,X_2} \end{pmatrix} + \begin{pmatrix} 0 & 0 \\ 0 & H_{O_1,X_2} \partial^N_N \end{pmatrix}.$$

So, $i \circ \pi = \mathrm{Id}^M_\partial H + H \partial^M$. □

So, we have the strong deformation of chain complexes that we want in order to utilize our algebra. We simply need to show that the resulting maps are all finite. These proofs will all rely on the fact that interposition of δ^L_M or δ^M_2 does not change the fact that $H^2_{O_1,X_2} = H^I_{X_2} \circ H_{O_1,X_2} = H_{O_1,X_2} \circ H^N_{O_1} = 0$. That is,

Proposition 4. *The following statements are all true:*

$$H_{O_1,X_2} \circ \delta^L_M \circ H_{O_1,X_2} = H^I_{X_2} \circ \delta^L_M \circ H_{O_1,X_2} = H_{O_1,X_2} \circ \delta^L_M \circ H^N_{O_1} = 0$$

and

$$H_{O_1,X_2} \circ \delta_2^M \circ H_{O_1,X_2} = H_{X_2}^I \circ \delta_2^M \circ H_{O_1,X_2} = H_{O_1,X_2} \circ \delta_2^M \circ H_{O_1}^N = 0.$$

Proof. There are a lot of statements to check here, but they all utilize the same reasoning, so we will show that $H_{O_1,X_2} \circ \delta_M^L \circ H_{O_1,X_2} = 0$ and leave the rest to the reader as an exercise. If the stabilization occurs in a type 3, 4, or 5 section, then the δ_M^L map will automatically not affect the H_{O_1,X_2} maps, so we only need to consider the case where the stabilization takes place in a type 2 section. Looking at figure 4.29 and recalling that p and q are the dots arising from the first rectangle and that r is the dot that combines with p to form the second rectangle, we again see that there are many cases depending on whether p, q, and r are each in section 1 or 2. Since all of the cases follow the same logic, we will content ourselves to analyzing the case where p and r are in section 1 and q is in section 2.

The left hand side shows the type of rectangle that would be necessary to move r past p. However, any such rectangle must itself contain p. The right picture shows the kind of rectangle that would be necessary to move p past r, thus avoiding the trouble. However, any such rectangle must contain r. Case 2 in both pictures is unaffected since q is assumed to be in section 2 and no edge rectangle can make a point change sections. However, even if q were also in section 1, we could not use an edge rectangle to avoid the troubles.

The argument that $H_{O_1,X_2}\delta_2^M H_{O_1,X_2}$ is similar enough that we will refrain from discussing it in depth. Just note that we only need to concern ourselves to the case where the stabilization is taking place in the type 3 section. Again any rectangle which would move a troublesome dot out of the way must contain the dot which it is trying to move past. □

Corollary 1. *The following statements are also true.*

$$H \circ \delta_M^L \circ H = \pi \circ \delta_M^L \circ H = H \circ \delta_M^L \circ i = 0$$

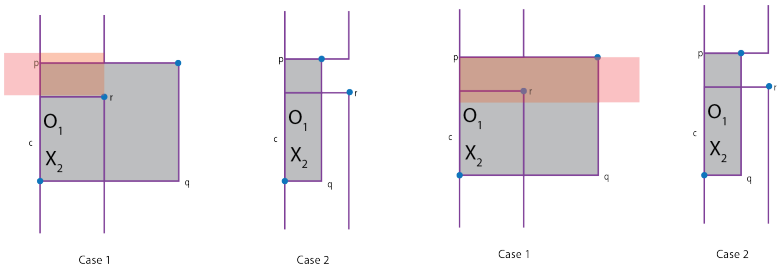

Figure 4.29: Figure used in the proof that $H_{O_1,X_2} \circ \delta_M^L \circ H_{O_1,X_2} = 0$. Both the right and left pictures show the case where p and r are in section 1 and q is in section 2. The points p and q are the positions of the dots that result from the first rectangle. The point r is used with p to form a second rectangle. The left hand side shows the type of rectangle that would be necessary to move r past p. However, any such rectangle must itself contain p. The right picture shows the kind of rectangle that would be necessary to move p past r, thus avoiding the trouble. However, any such rectangle must contain r. Case 2 in both pictures is unaffected since q is assumed to be in section 2 and no edge rectangle can make a point change sections. However, even if q were also in section 1, we could not use an edge rectangle to avoid the troubles.

and

$$H \circ \delta_2^M \circ H = \pi \circ \delta_2^M \circ H = H \circ \delta_2^M \circ i = 0.$$

Proof. This follows directly from the preceding proposition and the fact that since the stabilization is not allowed to occur in the type 1 section or the type 4 section, the maps δ_M^L and δ_2^M cannot take an element from $\tilde{N}$ to $\tilde{I}$ or vice versa. For instance, for $H \circ i$, relabel $(\tilde{I} \oplus \tilde{I})$ as $(\tilde{I}_1 \oplus \tilde{I}_2)$. If $y \in I_2$, then $H \circ i(y) = H_{O_1,X_2} \circ \delta_M^L \circ H_{O_1}^N(y) = 0$. If $y \in I_1$, then $H \circ i(y)$ is the map H applied to $(\delta_M^L(y) + \delta_M^L \circ H_{O_1,X_2} \circ \partial_I^N(y))$. Since $y \in I_1$, $\delta_M^L(y) \in I$, thus $0 \circ \delta_M^L(y) = 0$, and $H_{O_1,X_2} \circ \delta_M^L \circ H_{O_1,X_2} \circ \partial_I^N(y) = 0$, so the whole thing is zero. □

All right, now we would like to show that the maps δ_i^N, ϕ^1, ψ^1, and H^1 are all finite. Let's look at δ_i^N first. Now, δ_1^N is defined to be

$$(1 \otimes \partial^O) + (\mathrm{Id} \otimes \pi) \circ \delta_M^L \circ i + (\mu_2 \otimes \mathrm{Id}) \circ (\mathrm{Id} \otimes \mathrm{Id} \otimes \pi) \circ (\mathrm{Id} \otimes \delta_M^L) \circ (\mathrm{Id} \otimes H) \circ \delta_M^L \circ i + \cdots .$$

Thanks to the corollary above, the third term and above are all zero. Thus, the new type

DA structure is finite as well, and

$$\delta_1^N = (1 \otimes \partial^O) + (\mathrm{Id} \otimes \pi) \circ \delta_M^L \circ i.$$

The same corollary can then be applied again and again to show that ϕ^1, ψ^1, and H^1 are all finite as well.

The map δ_2^N also succumbs to the corollary becoming simply

$$(\mu_2 \otimes \mathrm{Id}) \circ (\mu_2 \otimes \mathrm{Id} \otimes \mathrm{Id}) \circ (\mathrm{Id} \otimes \mathrm{Id} \otimes \psi) \circ (\mathrm{Id} \otimes \delta_2^M) \circ \phi.$$

The maps δ_3^N and above all become zero.

So, now we have two different type DA structures on the module N, specially $(\tilde{I} \oplus \tilde{I}, \delta^O \oplus \delta^O)$ and $(\tilde{I} \oplus \tilde{I}, \delta^N)$. We would like to see that these are actually equal.

Theorem 9. *The sequence of maps $\delta_i^N = \delta_i^O$.*

Proof. We will relabel the module $(\tilde{I} \oplus \tilde{I})$ as $(\tilde{I}_1 \oplus \tilde{I}_2)$. Now, if $y \in I_2$, then $\delta_1^N(y) = (1 \otimes \partial^O)(y) + (\mathrm{Id} \otimes \pi) \circ \delta_M^L \circ i(y)$, while $\delta_1^O(y) = (1 \otimes \partial^O)(y) + \delta_O^L(y)$. Since the ∂^O part is the same in both maps, we need to see that $\delta_O^L(y) = (\mathrm{Id} \otimes \pi) \circ \delta_M^L \circ i(y)$. Since $y \in I_2$, $(\mathrm{Id} \otimes \pi) \circ \delta_M^L \circ i(y) = (\mathrm{Id} \otimes H_{X_2}^I) \circ \delta_M^L \circ H_{O_1}^N(y)$. So, we want to see that the algebra element that we get is the same, and that $H_{X_2}^I \circ H_{O_1}^N = \mathrm{Id}$ is unaffected by interposing δ_M^L.

To see that the algebra element is the same in either case, notice that a rectangle from $H_{O_1}^N$ doesn't actually change the α curve that a dot is on; it only moves it side to side. Furthermore, the rectangle that moves the dots is necessarily empty and, therefore, will not affect what kinds of rectangles that can be made with the idempotent piece that is spit out. The only thing that would potentially cause a problem is if the switched dots were actually now in each other's way, but this can't happen because the stabilization is never in section 1, and one of the dots therefore must not be in section 1.

This same reasoning applies not just to the algebra piece, but the map as a whole.

Referring back to figure 4.7, recall that since the X_2 rectangle had to use q as its top right corner and p as its bottom left corner, we were stuck only being able to use a thin annulus as a composition of rectangles. Now, we have the opportunity to bypass this problem by using δ_M^L to move p past the X or O that was the problem. However, any edge rectangle which would move p past the problem X or O must itself contain said X or O. Thus, no such move is possible.

We can, however, move p up or down along the thin annulus. This, however, is what we want as after we apply $H^I_{X_2}$, it is the same as applying δ^L_O since we are simply temporarily moving it across some empty space and then back again.

If, on the other hand, $y \in I_1$, then $(\mathrm{Id} \otimes \pi) \circ \delta^L_M \circ i(y) = \delta^L_M(y)$ since $H^I_{X_2} \circ \delta^L_M \circ H_{O_1,X_2} = 0$. Thus, this case is true trivially since the maps δ^L_M and δ^L_O are defined the same.

The arguments for why $(\delta^O_2 \oplus \delta^O_2) = \delta^N_2$ are exactly analogous, mutatis mutandis, to the preceding arguments. □

Now, since δ^L_O and $\overline{\delta^L_G}$ (the one which corresponded to $CT(G)$) are defined the same way, we have already proven the following theorem.

Theorem 10. *The type DA structure $(CT(G'), \delta'_i)$ is equivalent as a type DA structure to $((CT(G), \delta_i) \oplus (CT(G), \delta_i))$.*

4.3 Commutations

The next type of grid move that we will consider is called a commutation. Throughout this section we will again rely on inspiration from [5]. A commutation move is easy to understand. It is simply a move where we swap two adjacent rows or two adjacent columns in a grid diagram. In this section, we will focus on column commutations, but all of the same arguments may be made for row commutations by rotating the pictures around 90 degrees and adapting the maps accordingly.

Since the ends of our tangles are fixed we will not allow row commutations in the

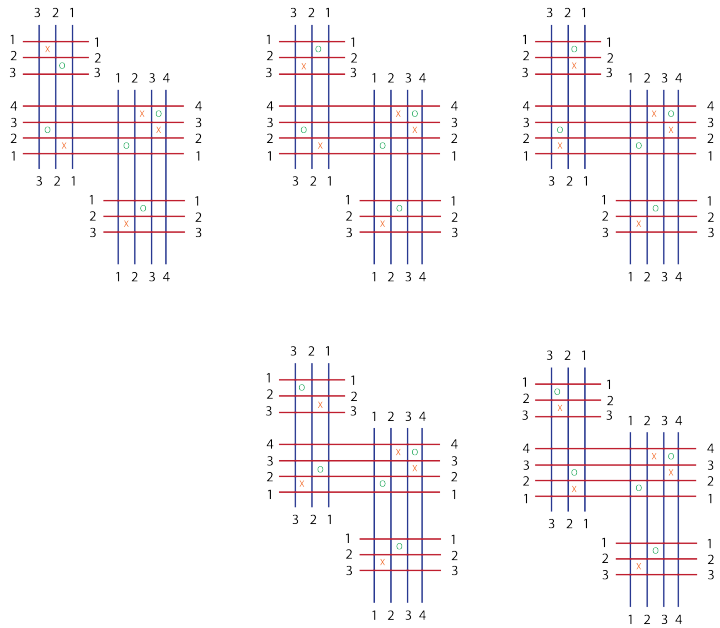

Figure 4.30: TOP LEFT: We cannot commute the two columns of sections 1 and 2 because neither columns' X's and O's are contained in the other. TOP MIDDLE: We can commute the two columns in sections 1 and 2 because the left column is contained in the right. In fact we may also consider the right column to be contained in the left column as well when wrapped around the grid. The result of the commutation is shown in the grid below it. TOP RIGHT: We can also commute the two columns in section 1 and 2 in this grid because they are "inside" each other when considered to be wrapped around the grid. The result of this commutation is shown in the grid below it. In general, when doing a commutation, the two strands involved either do not interact as in the right example or result in a Reidemeister 2 move as in the middle example. Changing the two columns in first example would result in a crossing change, and, thus, is not allowed.

type 1 or type 4 sections. Now, we cannot swap two columns or two rows arbitrarily without changing the tangle type, so we will limit commutations to swaps where one column's X's and O's are contained within the other column's X's and O's (bearing in mind that the top and bottom of grid segments are glued together). A commutation of this type results in no change to the tangle diagram (a planar diagram of the tangle, not the grid diagram) or in a Reidemeister 2 move. Neither changes the tangle type of the underlying tangle.

It will be easier to discuss the maps involved with commutation moves by combining the grid diagram before the commutation move with the grid diagram that

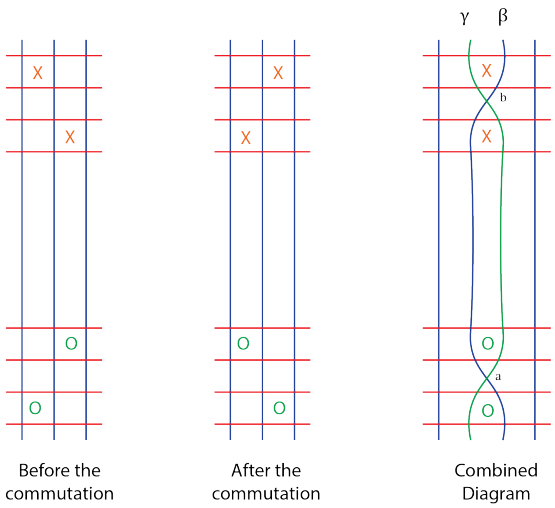

Figure 4.31: The grid diagram on the right is the result of combining the grid diagram on the left with the grid diagram in the middle. The grid diagram on the left occurs when we use the curve labeled β and ignore the γ curve. The diagram in the middle results when we used the curve labeled γ and ignore the curve labeled β.

results from the commutation into one combined diagram. See figure 4.31 for reference. We will label the β curve used in the diagram before the commutation as β and the β curve used in the diagram after the commutation as γ. There are two bigons which emerge with the β and γ curve as their edges. We will label one of the crossing points between the β and γ curve as a and one as b. Specifically, we will label as a the crossing which occurs at the southern tip of the bigon with the γ curve as its right side. Furthermore, although there is some latitude in deciding where these crossings occur, we will only insist that they do not cross on an α curve.

Although a commutation move will not result in a strong deformation retraction as the stabilization moves did, we will continue to use the same labeling as hopefully we are beginning to become familiar with it. We will call (M, ∂^M) the chain complex which corresponds to the grid diagram before the commutation move, (N, ∂^O) the chain complex which corresponds to the grid diagram after the commutation move, etc. We will then

define maps $\pi : M \to N$, $i : N \to M$, $H : M \to M$, and $L : N \to N$ such that

$$\pi \circ \partial^M = \partial^O \circ \pi \tag{4.20}$$

$$i \circ \partial^O = \partial^M \circ i \tag{4.21}$$

$$\pi \circ i = \mathrm{Id} + L \circ \partial^O + \partial^O \circ L \tag{4.22}$$

$$i \circ \pi = \mathrm{Id} + H \circ \partial^M + \partial^M \circ H \tag{4.23}$$

This will show that the two structures are equivalent as chain complexes. We will then show that we can extend these maps to an equivalence of the type D structures as well.

First, we define π and i. We will define π by looking at the grid diagram and counting pentagons which contain the point a. These will be similar to the rectangles defined for the boundary map in that their lower left corner and upper right corner must have a dot, and their interiors must be free dots, X's, and O's. This forces the pentagon to have one dot on the special β curve. When the pentagon is resolved, that dot is moved off of the beta curve and the other dot is moved to the γ curve. See figure 4.32 for examples of the pentagons counted in π. The pentagons do not have to be contained to one section of the grid diagram and may wrap around the grid diagram in just the same way that rectangles may.

For any two grid states $x \in M$ and $y \in N$, let $P(x, y)$ denote the set of all empty pentagons which carry x to y. Then π is defined as follows:

$$\pi(x) = \sum_{y \in S(N)} \sum_{p \in P(x,y)} y.$$

The map i is defined similarly except that its pentagons must have a vertex at the crossing b. This forces those pentagons to carry grid states in N to grid states in M.

Proposition 5. *The maps π and i as defined above are chain maps.*

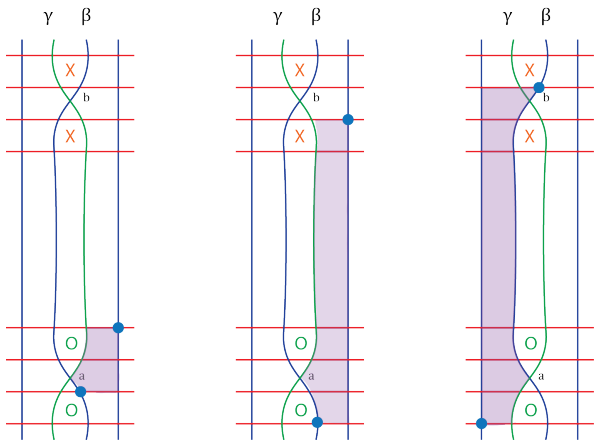

Figure 4.32: This figure shows three examples of pentagons which might be counted in the π map. Each pentagon has the point a as one of its vertices, has a dot at its upper right and lower left corners, and is otherwise free of dots, X's and O's. Notice that each of the pentagons has one dot on the special β curve and that a dot is moved to the γ curve when the pentagon is resolved.

Proof. We will show that π is a chain map and leave the proof that i is a chain map to the reader since they are exactly analogous. We need to show that

$$\pi \circ \partial^M + \partial^O \circ \pi = 0.$$

We will show that each combination of a pentagon and a rectangle occurs in two different ways and thus will always cancel in pairs. Referring to figures 4.33 and 4.34, the map $\pi \circ \partial^M + \partial^O \circ \pi$ counts combinations of rectangles and pentagons of the proper type. Such combinations are limited to four cases. The first case is where the combined structure of the pentagon and the rectangle contains four dots. Such a case does not share any corners and thus can be resolved in two different ways (the pentagon first or the rectangle first). Both ways result in the same output of grid states and thus cancel each other out. The second case is where the combined structure of the pentagon and the rectangle contains three dots. This can happen in several ways (again see 4.33). In each case, the combined structure can be divided into a pentagon and a rectangle in two different ways. Both ways result in the same output of dots and thus cancel each other out.

Finally, there is the situation where the combined structure of the pentagon and rectangle contains two dots. This can happen for two different reasons. The first (case 3) occurs when the combined structure wraps around the grid diagram horizontally. In this case the structure can again be divided in two different ways, each canceling with the other. Lastly, a combined structure with two dots can result when the combined structure wraps around a grid diagram vertically. Since each column not adjacent to the two bigons contains an X and an O, such a wrapping structure must necessarily involve only one of the empty columns directly beside the two bigons (and may potentially include part of the bigons). While such a structure cannot be divided in the usual way, whenever such a structure is possible on the left side, a corresponding structure is automatically possible on the right side and vice versa. In each case, the result of both structures is only to move the dot on the β curve to the corresponding spot on the γ curve (i.e. remaining on the same α curve). Such a structure is possible because it uses the exact same portion of the bigons which is necessarily empty of X's and O's since it was used on the other side as well. These two corresponding structures cancel with each other. □

Next, we will define our two homotopy maps $H : M \to M$ and $L : N \to N$. The map H counts hexagons that have both of the points a and b as vertices. In addition, each hexagon must have a dot in its lower left and upper right corners and its interior must be free of any other dots, X's or O's. One of the two corner dots must lie on the special β curve. Such a hexagon is possible on either the left or right side of the two bigons. See figure 4.35 for an example of each kind. A hexagon resolves by shifting its dots to the upper left and lower right corners of the hexagon just as rectangles and pentagons do. Denote the set of all empty hexagons from a grid state $x \in M$ to a grid state $y \in M$ by $H(x, y)$. Then, the map $H : M \to M$ is defined specifically to be:

$$H(x) = \sum_{y \in S(M)} \sum_{h \in H(x,y)} y.$$

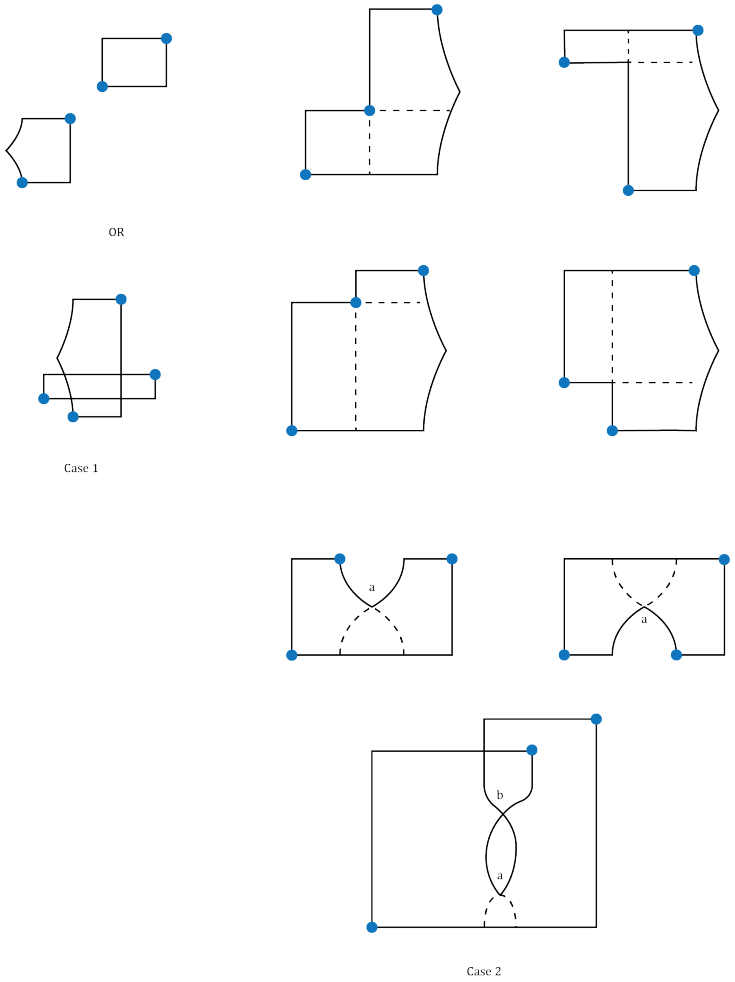

Figure 4.33: The first 2 cases in the proof that π is a chain map. Case 1 is where the combined structure of the pentagon and the rectangle has four starting dots, in which case we can do the rectangle first and then the pentagon or the pentagon first and then the rectangle. Case 2 is where the combined structure of the pentagon and the rectangle has 3 dots, in which case the structure can be divided in two different ways, each canceling with the other.

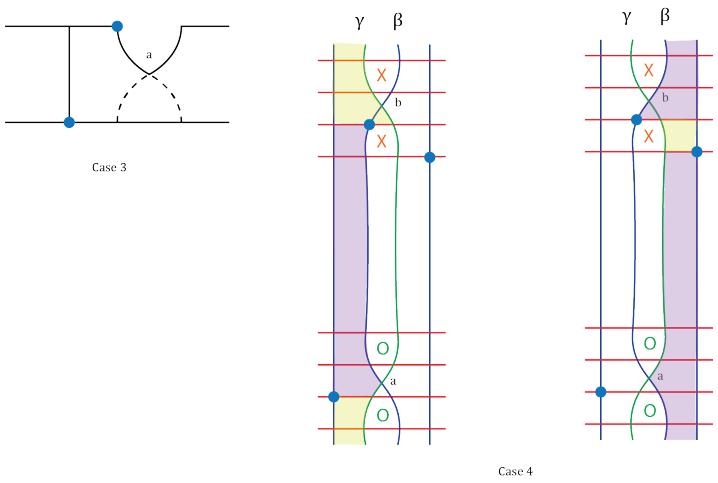

Figure 4.34: Shown are the third and fourth cases in the proof that π is a chain map. Both cases involve the combined structure having two dots. Case 3 occurs when the combined structure wraps around the grid diagram horizontally. Such a structure can be divided in two different ways, each canceling with the other. Case four involves the combined structure wrapping around the grid diagram vertically. Such a structure cannot be divided in two different ways. However, a corresponding structure can be found on the other side of the two bigons, and these will cancel with each other.

The map $L : N \to N$ will be defined analogously except that its hexagons must contain a dot on the special γ curve.

Theorem 11. *The equation*

$$i \circ \pi + \partial^M \circ H + H \circ \partial^M = Id \tag{4.24}$$

holds, and

$$\pi \circ i + \partial^O \circ L + L \circ \partial^O = Id. \tag{4.25}$$

Proof. This proof will follow along the same lines as the last one. Again, the proofs for the two equations are almost identical, so we will focus on the first one. The left side of the equation counts suitable combinations of two pentagons (one at a followed by one at b), a hexagon followed by a rectangle, and a rectangle followed by a hexagon respectively. We can combined the two shapes in each term into one combined structure. There are three

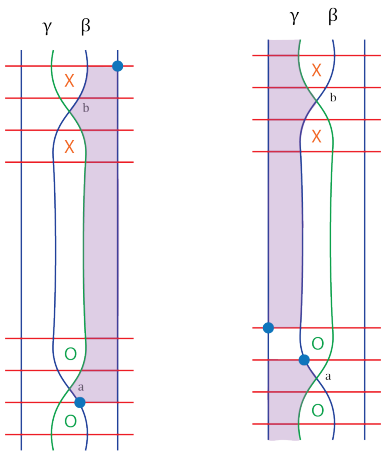

Figure 4.35: Shown are the two types of hexagons that occur in the H map. Each hexagon must have both of the points a and b as vertices and both must have a dot in their lower left and upper right corners. One of those dots must be on the special β curve. The map works just as rectangles and pentagons do by switching the dots to the upper left and lower right corners of the eligible hexagon. There is a corresponding map $L : N \to N$ which counts hexagons where one dot is on the γ curve.

cases (see figures 4.36 and 4.37 for reference). The first case involves a combined structure with four dots. This case can only occur with a hexagon and a rectangle, and either shape may be resolved first. Thus, there are two different ways to resolve the structure each resulting in the same output. So they cancel each other out. The second case involves combined structures which have three dots. These can result from any of the three combinations. Each of the combined structures is dividable in two different ways along the dotted lines in figure 4.36 resulting in two different ways to resolve the structure. Since each resolution results in the same output, the structures cancel with each other.

Finally, we look at the case where the combined structures contain two dots. These occur when the combined structure wraps around the grid diagram vertically and connects back up with itself (notice that a horizontal wrapping as in the previous proof is no longer possible since those resulted from pentagons combined with rectangles). Any such wrapping must only contain the columns directly to the left and right of the two bigons because any other column would contain and X, and O, and a dot along its length. Thus any eligible combined structure will be a "thin" annulus. Label the special β curve β_i and

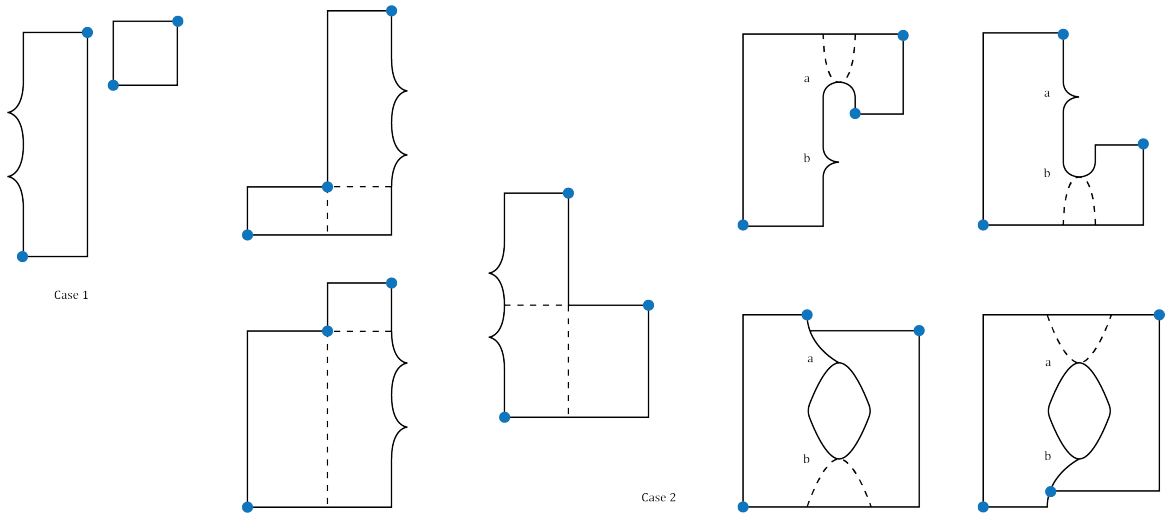

Figure 4.36: The first two cases in the proof that $i \circ \pi + \partial^M \circ H + H \circ \partial^M = \mathrm{Id}$. The first case is where the combined structure has four dots. In these, either the hexagon or the rectangle can be resolved first. Thus, they are resolvable in two different ways and cancel with each other. The second case involves the combined structure having three dots. In each case the structure is dividable along the dotted lines in two different ways and each yields the same output. Thus the two structures cancel with each other.

the β curves immediately to its left and right β_{i-1} and β_{i+1} respectively. Depending on the placement of the dots on these three curves, only one such thin structure is possible (either two pentagons, a rectangle followed by a hexagon, or a hexagon followed by a rectangle). Since the columns immediately next to the two bigons are necessarily empty, this structure is always possible and results in the identity. □

Next, we would like to extend this equivalence to the type D structures. We shall do this by extending our chain maps π and i to type D homomorphisms ψ and ϕ respectively and extending our homotopies H and L to type D maps H_D and L_D respectively. It would be nice to proceed algebraically as we did in the case for stabilizations, and indeed there is a way to extend the type D structure from M to N. Unfortunately, however, since $\pi \circ i$ is no longer the identity, the transferred structure is not necessarily (and almost never is) equal to the original type D structure on N. However, they are still equivalent as we will show. We will, therefore, have to proceed more directly.

Define π^L in the same way that δ^L is defined, but instead of counting rectangles

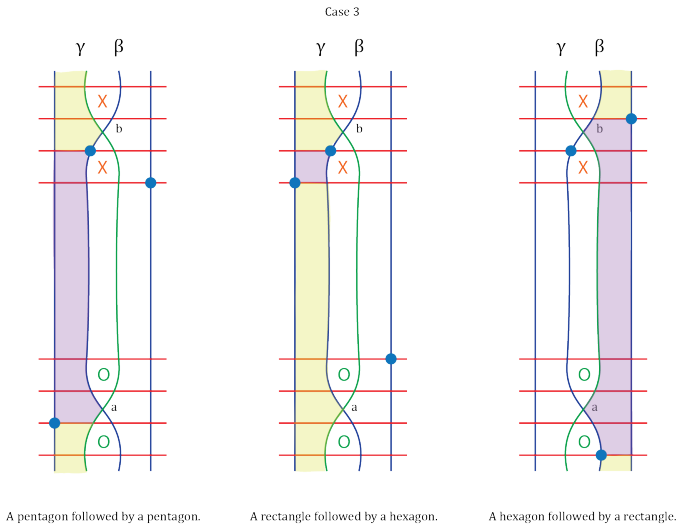

Figure 4.37: Depending on the placement of the dots on β_{i-1}, β_i, and β_{i+1}, one (and only one) of the following three cases will be possible, leading to the identity.

which go off of the α edge of the diagram in the type 1 piece, count pentagons which go off the edge in the type 1 piece. These pentagons must specifically be pentagons which include the special point a at one of their vertices. Define i^L similarly except it will count pentagons with the special point b at one of their vertices. Otherwise, the maps works exactly the same way as the δ^L map.

Specifically, for π^L, start by gluing a properly labeled shadow piece to the left edge of the type 1 piece of the combined grid complex. Provide the shadow piece with X's and O's along the idempotent diagonal such that each row created by the newly formed long α curves has exactly one X and one O. Then give the shadow dots along its idempotent diagonal on any α curve which does not have a dot in the type 1 piece of the original combined grid complex. Now, form suitable pentagons (i.e. pentagons whose interior is empty of X's, O's, and dots) where one corner dot is in the original combined grid complex and one is in the algebra shadow piece. Resolve each pentagon individually as a term in the output of π^L (meaning to switch the dots from the upper right corner and lower left corner to the upper left corner and lower right corner). For each term detach the altered algebra piece and tensor it together with the altered chain complex.

Next, define $\psi : CT(M) \to A(-\partial^L(\mathcal{T})) \otimes CT(N)$ by

$$\psi(x) = (1 \otimes \pi(x)) + \pi^L(x),$$

where, $(1 \otimes \pi)(x) = 1 \otimes \pi(x)$.

We will define maps i^L and H^L in a similar manner. The map i^L will count pentagons exactly as π^L does, except the pentagons will have the special point b as one of the vertices. Finally, the map H^L and L^L will count hexagons which go off of the edge in the same manner. Just as with δ^L, the hexagons and pentagons can only go off of the α edge in the type 1 piece (either to the left or the right).Define the map
$\phi : CT(M) \to A \otimes CT(N)$ by

$$\phi(x) = (1 \otimes i)(x) + i^L(x),$$

the map $H_D : CT(M) \to A \otimes CT(M)$ by

$$H_D(x) = (1 \otimes H)(x) + H^L(x),$$

and the map $L_D : CT(N) \to A \otimes CT(N)$ by

$$L_D(x) = (1 \otimes L)(x) + L^L(x).$$

Now we will lay the groundwork for the type D equivalence.

Lemma 14. *The maps ψ and ϕ as defined above are type D homomorphisms.*

Proof. Since the proofs are basically identical, we will prove that ψ is a type D homomorphism, and leave the proof that ϕ is a type D homomorphism to the reader.

Recall that to be a type D homomorphism, we need

$$(\mu_1 \otimes \mathrm{Id}) \circ \psi + (\mu_2 \otimes \mathrm{Id}) \circ (\mathrm{Id} \otimes \psi) \circ \delta_M + (\mu_2 \otimes \mathrm{Id}) \circ (\mathrm{Id} \otimes \delta_N) \circ \psi = 0.$$

The proof is very similar to the chain complex case. If we expand out the equation above, we see that we can have any combination of pentagon and rectangle, and that one or both of the rectangle and pentagon may venture into the algebra piece. This analysis is valid because remember for simple algebra elements (i.e. ones where only one of the dots is off of the idempotent diagonal), the sole purpose of μ_2 is to ask whether or not a change could have been made, and if so, to make the change. Since all of our maps only spit out elements where one dot is moved off of the diagonal (or even better where no dots are moved off of the diagonal), we can simply analyze shapes in the same way we did in the chain complex case.

Referring to figure 4.38, we see various shapes representing combinations of pentagons and rectangles. The purple line in each case represents a potential boundary between the algebra piece and the type 1 piece of the original combined grid complex. For the four dot combinations, no matter where we put the line, we can still resolve either shape first. Where the line is now, the top example would be a term of $(\mu_2 \otimes \mathrm{Id}) \circ (\mathrm{Id} \otimes \pi) \circ \delta^L$ or $(\mu_2 \otimes \mathrm{Id}) \circ (\mathrm{Id} \otimes \delta^L) \circ \pi$. Notice it might seem that if we move the purple line completely in between the rectangle and that pentagon that we might be in trouble. However, no such combination is possible because the algebra generator is an idempotent. Since every possible combination can be realized in two different ways, they cancel each other out.

For the case where the combined shape has three dots, we play the same game, except now we need to notice that no matter where we put the purple line, we can still use the dotted lines to give us two different manifestations. For instance, in the top left example, if we cut along the vertical dotted line, we get a term from

$(\mu_2 \otimes \mathrm{Id}) \circ (\mathrm{Id} \otimes \pi) \circ \delta^L$ and if we cut along the horizontal dotted line, we get a term from $(\mu_2 \otimes \mathrm{Id}) \circ (\mathrm{Id} \otimes \delta^L) \circ \pi$. Again, not all combinations of shapes and purple lines are possible given the dot structure of the idempotent algebra piece. For instance, the first example in the second row of case 2 is not possible where the purple line is, but if we move the purple line, we will get an acceptable combination. Again, since every possible combination can be realized in two different ways, they cancel each other out.

When the combined structure of the pentagon and rectangle has two dots, the argument is exactly the same as in the chain complex case. The case of horizontal annulus (minus a small triangle) shown on the left in figure 4.39 is actually not possible given the dot structure of the idempotent algebra generator. The vertical annulus case is unaffected as since it wraps around the β edge, it cannot go off of the α edge. Thus, the terms cancel in pairs as before. □

Next, we will show the type D equivalence.

Theorem 12. *The maps ψ and ϕ defined above provide a type D homotopy equivalence between the structure (M, δ_M) and (N, δ_O).*

Proof. Once again, the proof follows along the same lines as the chain complex case with some minor adjustments. Since we have already shown that ψ and ϕ are type D homomorphisms, we need to show that

$$\phi * \psi + (\mu_1 \otimes \mathrm{Id}) \circ H_D + (\mu_2 \otimes \mathrm{Id}) \circ (\mathrm{Id} \otimes H_D) \circ \delta_M + (\mu_2 \otimes \mathrm{Id}) \circ (\mathrm{Id} \otimes \delta_M) \circ H_D = \mathbb{I},$$

and that

$$\psi * \phi + (\mu_1 \otimes \mathrm{Id}) \circ L_D + (\mu_2 \otimes \mathrm{Id}) \circ (\mathrm{Id} \otimes L_D) \circ \delta_N + (\mu_2 \otimes \mathrm{Id}) \circ (\mathrm{Id} \otimes \delta_N) \circ L_D = \mathbb{I}.$$

Since the arguments are almost identical, we will do the top equation and leave the other to the reader. The terms on the left side of the equation represent suitable combinations of

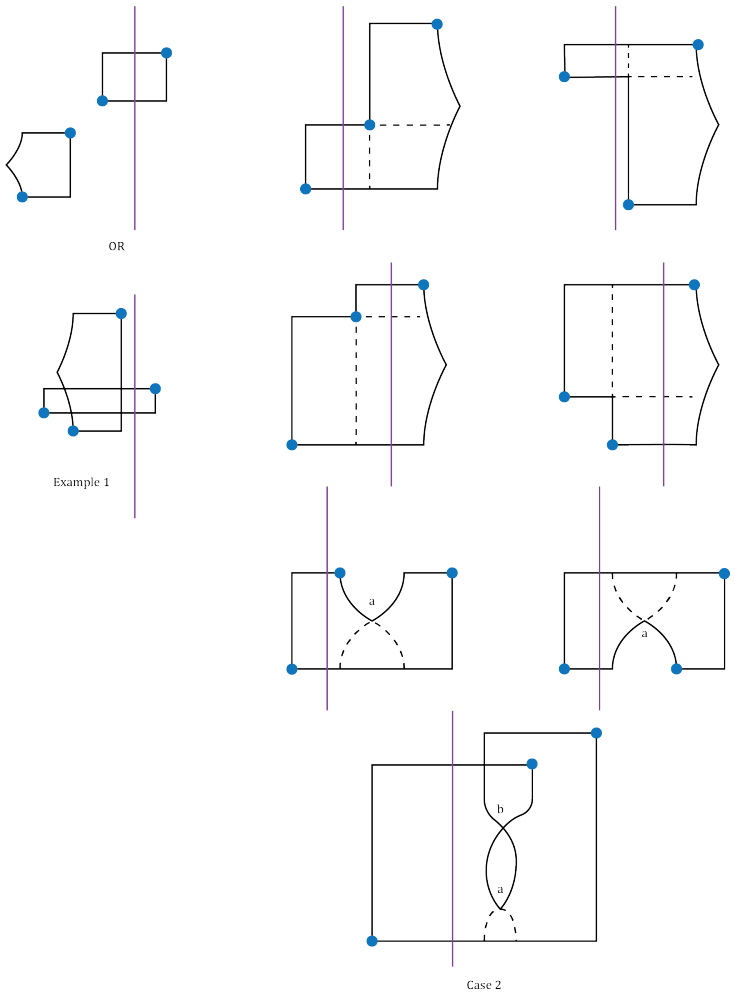

Figure 4.38: The different types of combined shapes with three or four shared dots in the proof that ψ is a type D homomorphism. Each combined shaped represents a rectangle composed with a pentagon or vice versa. The purple line indicates the boundary between the type 1 piece of the original combined grid complex and the algebra piece. Notice that the points a and b must always occur in the original combined grid complex. The proof lies in understanding that no matter where you put the purple line, if the shape is possible, then it is still dividable according to the dotted lines into two different manifestations each with the same output.

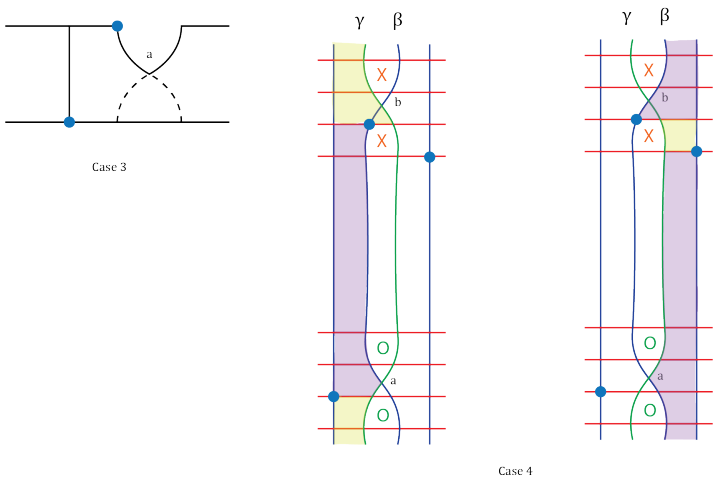

Figure 4.39: These two cases work the same as in the chain complex case. The left example is not possible given the idempotent structure of the algebra piece. The argument for the second case is unaffected as the combined structure is thin and, thus, cannot go off the edge.

hexagons with rectangles and pentagons with pentagons where either or both of the shapes may now go off the grid. There are again three cases depending on whether the combined structure of the rectangle and hexagon or pentagon and pentagon have four, three, or two dots.

Referring to figure 4.40, we again use a purple line to indicate where the boundary between the original combined grid complex and the algebra piece is. The proof lies in seeing that any combination of structure and purple line still allows us to resolve the structure in two ways (with the exception of case 3 which will serve as our identity), and, thus, cancels. Looking at figure 4.40, we see that in the case where the combined structure has two dots, we may resolve either shape first, and so they cancel in pairs. Remember that although there is no way to resolve the rectangle first if it is completely in the algebra piece, no such arrangement is possible since the algebra piece in question is an idempotent.

In the case where the combined structure has three dots, if the combination is possible with a given purple line, then the same dotted line can be used to divide the shape two different ways. For example, in figure 4.40, the example with the first purple line in case 2 if cut vertically represents a term of $(\mu_2 \otimes \mathrm{Id}) \circ (\mathrm{Id} \otimes \delta_M^L) \circ (1 \otimes H)$, and if cut

horizontally represents a term of $(\mu_2 \otimes \mathrm{Id}) \circ (\mathrm{Id} \otimes (1 \otimes H)) \circ \delta^L_M$. Of particular interest is the case in the bottom left of the figure 4.40, where the combined shape purple line combination, when divided horizontally, yields a term of $(\mu_2 \otimes \mathrm{Id}) \circ (\mathrm{Id} \otimes i^L) \circ \pi^L$, and when divided vertically, yields a term of $(\mu_1 \otimes \mathrm{Id}) \circ H_D$. □

4.3.1 Switches

There are a couple of special cases of commutations which we will handle separately. The first is called a switch move. This is where we swap two adjacent columns (or rows) but two or more of the X's and O's involved in the switching share the same α row (or β column). See figure 4.41 for reference. This type of move will either result in no significant changes to the planar diagram or a Reidemeister 1 move, neither of which changes the tangle type.

A switch move is handled exactly the way we handle any regular commutation move, except now we are forced to the put the swapping point in the row which shares the X's and O's. Simply draw the diagram as shown in the figure and all of the same argumentation from before works equally well.

We draw attention to the switch move for two reasons. First, in the knot Floer homology context, this move plays a special role in the analysis of Legendrian knots, and so we would like to keep the same nomenclature here. Perhaps more importantly though, we will use this move to ease our workload about stabilization moves. Recall from section 4.2 that we only proved invariance for two stabilization moves, $X : SW$ and $O : SW$. We will now rectify this situation.

Proposition 6. *Any stabilization move can be reached from either an $X : SW$ stabilization or an $O : SW$ stabilization by a series of switch moves.*

Proof. This fact should be pretty apparent, but figure 4.42 shows an example of how to get from an $X : SW$ stabilization move to an $X : NE$ stabilization move. □

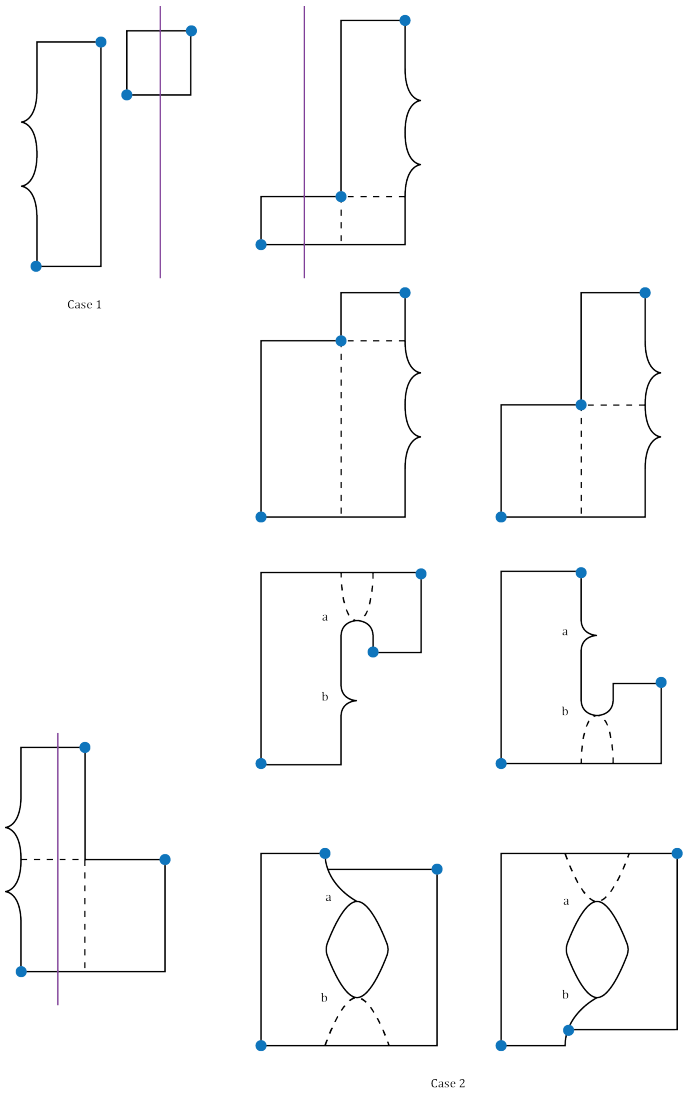

Figure 4.40: Shown are the cases in the proof that ϕ is a type D homotopy equivalence where the combined structure has either two or three dots. A purple line is used to indicate the boundary between the original combined complex and the algebra piece. The key is to realize that no matter where you put the line, if the structure is possible, then it is still resolvable in two different ways.

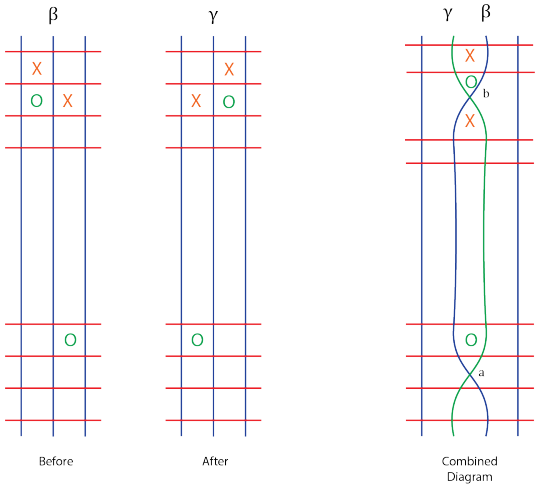

Figure 4.41: This figure shows the combined diagram for a switch move. The left image shows the diagram before the switch. The middle image shows the diagram after the switch. The right diagram is the combined diagram. We simply create a combined diagram as with any commutation move and put the X's and O's in question in the same row of the diagram.

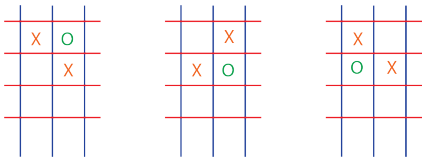

Figure 4.42: An example of how one can produce an X:NE stabilization move from an X:SW stabilization move and some switch moves (shown going from left to right in the figure). Any stabilization move can be reached from either an X:SW or an O:SW stabilization move by a series of switch moves.

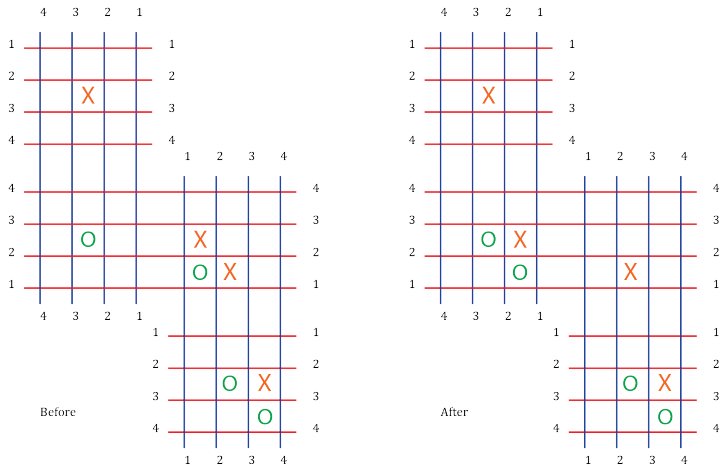

Figure 4.43: An example of a stretch "commutation" move. In this example, an X-O pair is being moved from the third section to the second section.

4.3.2 Stretches

The second special case for a commutation move involves "commuting" an X-O pair from one section of the diagram to another section of the diagram. An example is given in figure 4.43. The figure shows an X-O pair being moved from the third section to the second section. Again, we don't allow any moves that would change the end points of our tangle (e.g. stretching an X-O pair into the type 1 or type 4 section). We require that the column (or row) being moved into be empty. This can be accomplished by an addition move if necessary (and this case is why we required the end α and β curves to be empty if possible).

Once again, we simply need to alter the combined diagram to fit the circumstances and all of our previous work will hold up. We will discuss a column stretch move, but once again, all of this discussion holds for rows as well if we rotate all of the arguments by 90 degrees. We will create the combined diagram for a stretch move by letting the bigon containing the X-O pair occur in the α region between the sections in question (see figure 4.44). While this case seems complicated at first, it actually serves to limit the types of combined shapes that can be formed, and any shape which can be formed can be divided in exactly the same way as it was for a normal commutation.

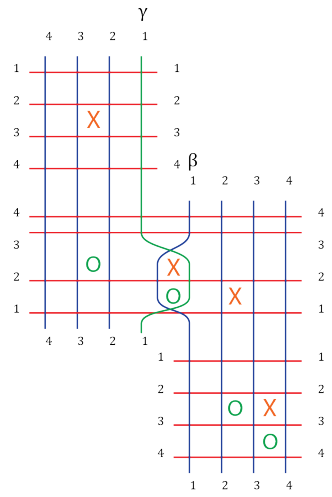

Figure 4.44: An example of a combined diagram for a column stretch move. The bigon containing the X-O pair occurs in the α space between the sections in question.

CHAPTER 5

TANGLE MOVES

We shall now describe how to accomplish all of the tangle moves in figure 1.11 by means of the grid moves laid out in the previous sections. In all of the moves demonstrated below, there may be other straight strands above and/or below the strand diagram pictured which will not be affected by the move. There may also be other sections glued to the beginning or end of the tangle which would not be affected by the grid moves along the way. Furthermore, the strand diagrams are drawn in purple instead of the usual orange and green because the orientation of the tangle does not affect the move, i.e. the X's and O's may be interchanged in any allowed combination and the tangle move still works. Any reference to "reorganization" in the description of the moves means moving X's and O's through blank columns or rows. Note in each case that none of the intermediate grid moves affect the ends of the tangle.

5.1 R1

The first tangle move we will investigate is an R1 move. The beginning and ending states of the move are shown below in figures 5.1 and 5.2. This move is quite complicated. The path of grid moves which accomplish the R1 move is shown in figure 5.3. Step 1 is an addition, a shrink move, and some reorganization. Step 2 is an O:NE destabilization. Step 3 is a commutation move on columns 2 and 3 of sections 3 and 4. Step 4 is a combination

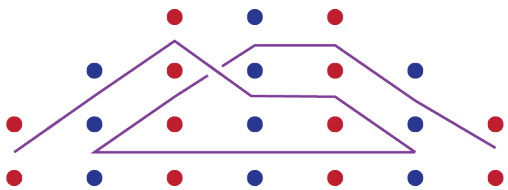

Figure 5.1: The beginning state of the R1 tangle move.

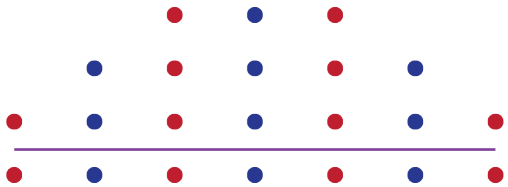

Figure 5.2: The ending state of the R1 tangle move.

of an addition move, a shrink (stretch) move, and some reorganization. Step 5 is an X:SE destabilization. Step 6 is a commutation move on columns 1 and 2 in sections 5 and 6. Step 7 is a combination of a shrink move and some reorganization. Step 8 is an X:SE destabilization along with some reorganization. Step 9 is an O:SE destabilization. Finally, Step 10 is a subtraction move and some reorganization. A strand diagram of the type show in figure 5.4 may also be straightened by a similar sequence of moves. Thus, they may also be converted from one to the other as well.

5.2 R2

The second tangle move we will tackle is an R2 move. The beginning and ending states of the move are shown below in figures 5.5 and 5.6. Unsurprisingly, this tangle move can be accomplished by means of commutation moves alone. Figure 5.7 shows the sequence of grid moves. The first move is a commutation move on the rows in sections 2 and 3, and the second move is a commutation move on the columns in sections 1 and 2. A strand diagram of the type show in figure 5.8 may also be straightened by a similar sequence of commutation moves. Thus, they may also be converted from one to the other as well.

5.3 R3

The R3 move is shown in figures 5.9 and 5.10. The sequence of grid moves connecting the two strand diagrams is shown in figure 5.11. Move 1 is a commutation move on rows 2 and 3 in sections 2 and 3. Move 2 is a commutation move on columns 2 and 3 in sections 1 and 2. Move 3 is a commutation move on columns 1 and 2 in sections 1 and 2. Move 4 is a commutation move on columns 2 and 3 in sections 3 and 4. Move 5 is a commutation move on rows 1 and 2 in sections 2 and 3. Move 6 is a commutation move on

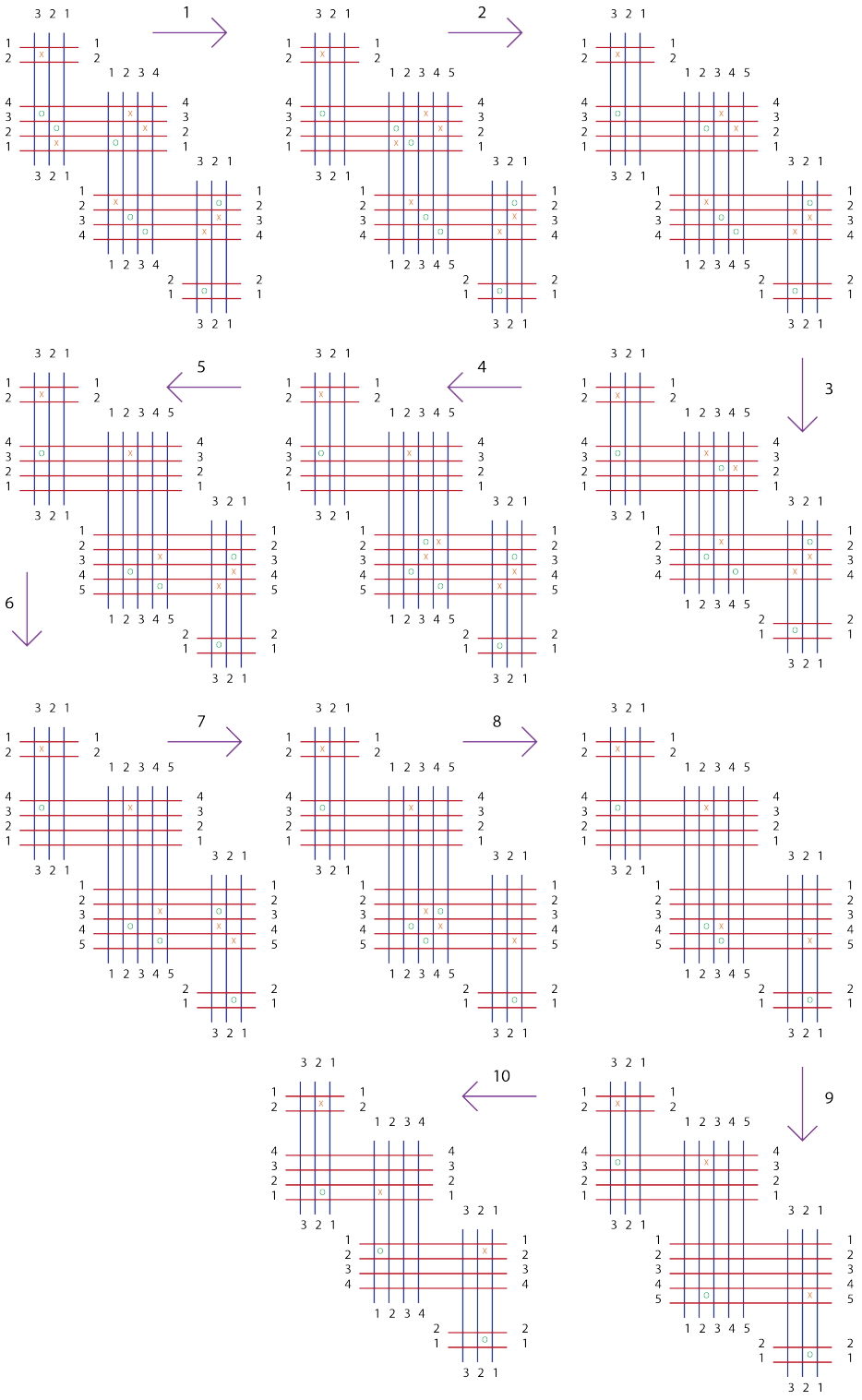

Figure 5.3: This sequence of grid moves accomplishes an R1 tangle move.

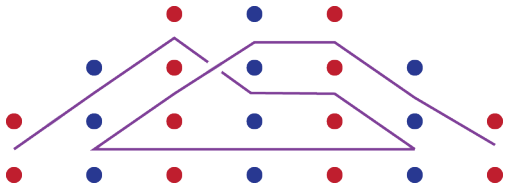

Figure 5.4: The other possible beginning state of an R1 move.

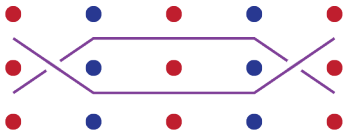

Figure 5.5: The beginning state of the R2 tangle move.

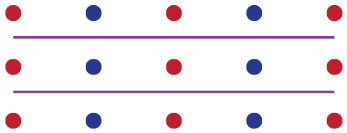

Figure 5.6: The ending state of the R2 tangle move.

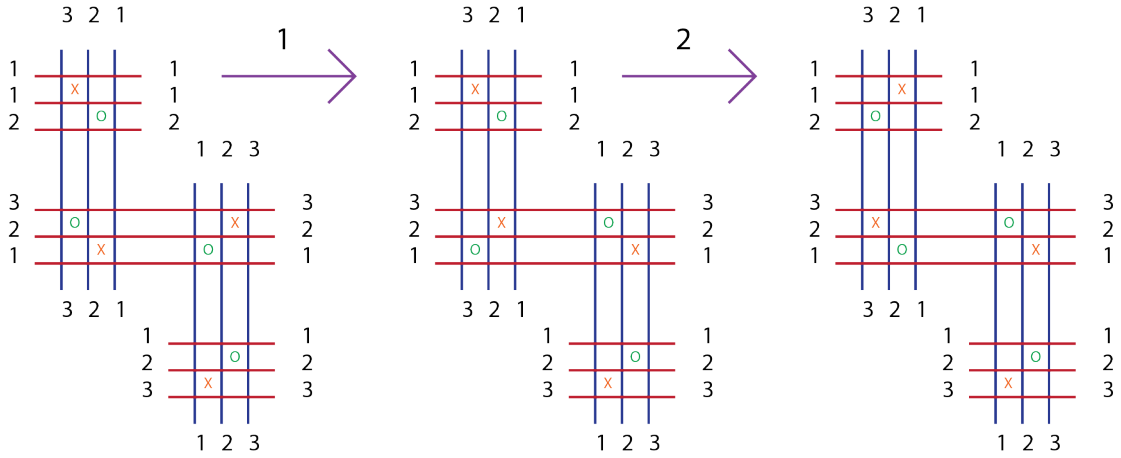

Figure 5.7: This sequence grid moves accomplishes an R2 tangle move.

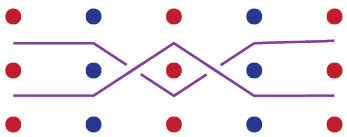

Figure 5.8: The other possible beginning state of an R2 move.

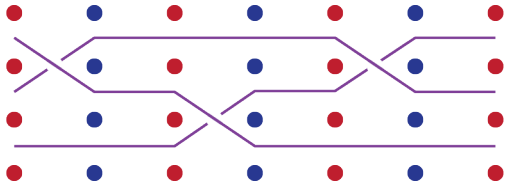

Figure 5.9: The starting tangle diagram for an R3 move.

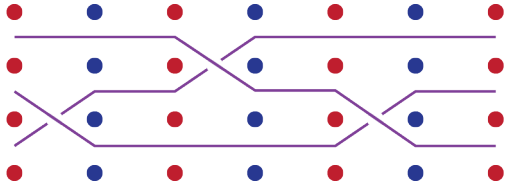

Figure 5.10: The ending tangle diagram for an R3 move.

rows 2 and 3 in sections 4 and 5. Move 7 is a commutation move on rows 1 and 2 in sections 4 and 5. Move 8 is a commutation move on columns 1 and 2 in sections 3 and 4.

5.4 S Moves

The next tangle move we will handle is an S move. The beginning and ending states of the move are shown below in figures 5.12 and 5.13. This tangle move is more complicated but can be realized by a sequence of commutation moves, destabilizations, and shrink moves, along with some reorganization. Figure 5.14 shows the sequence of grid moves. The first move is a commutation move on columns 1 and 2 in sections 3 and 4. The second move is a combination of an addition and a shrink move. Move 3 is an X:NW destabilization move. Move 4 is just reorganization. Lastly, move 5 is a combination of an X:SW destabilization move, a subtraction move, and some reorganization. A strand diagram of the type show in figure 5.15 may also be straightened by a similar sequence of moves. Thus, the two S shapes may also be converted from one to the other as well.

5.5 Cap Moves

5.5.1 Cap 1 Moves

The first cap move is shown in figures 5.16 and 5.17. The sequence of grid moves connecting the two strand diagrams is shown in figure 5.18. Move 1 is a commutation

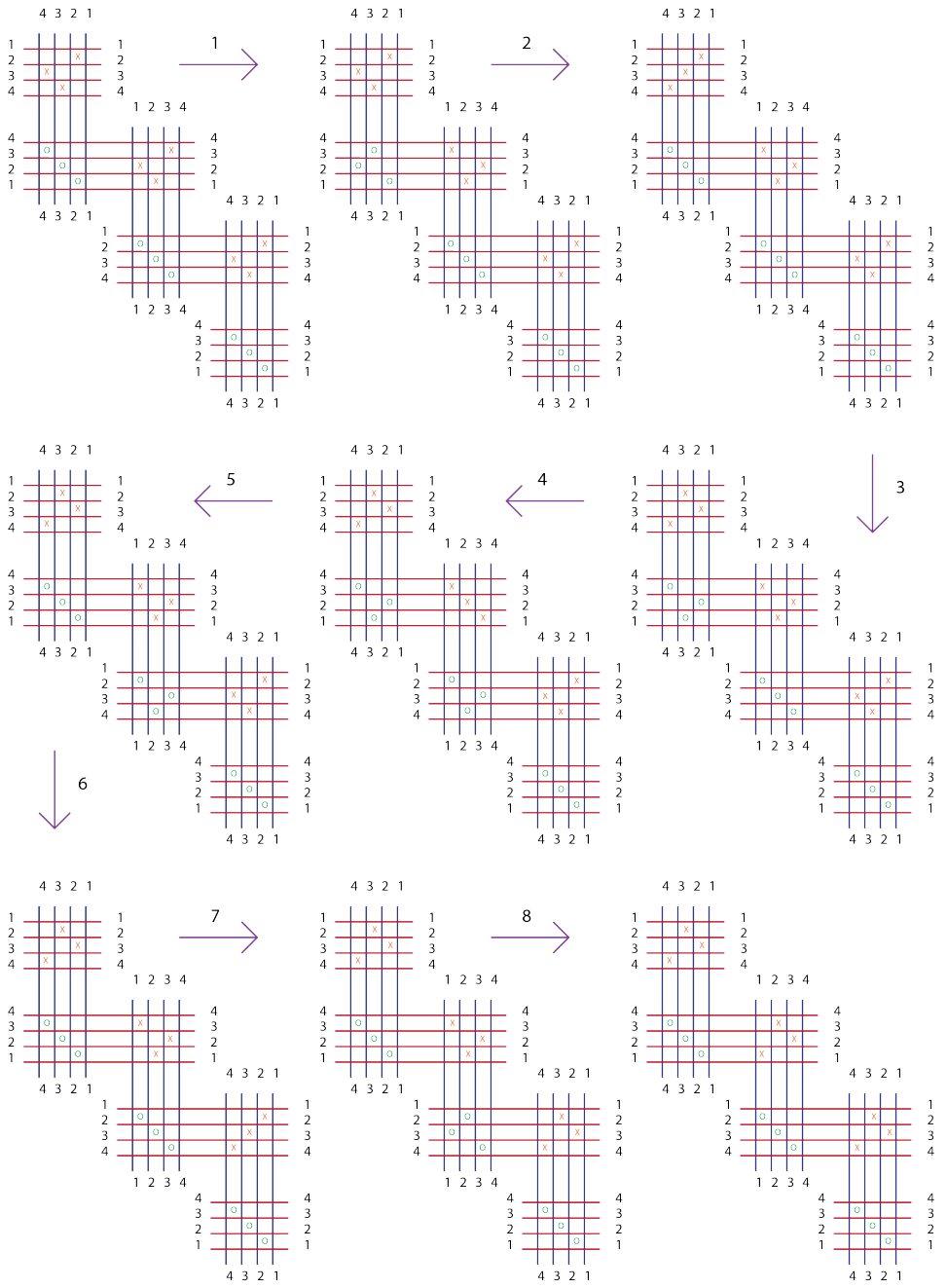

Figure 5.11: The sequence of grid moves that accomplish an R3 tangle move.

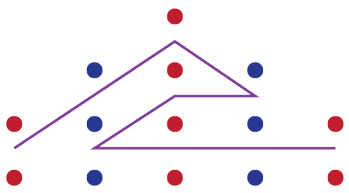

Figure 5.12: The beginning state of the S tangle move.

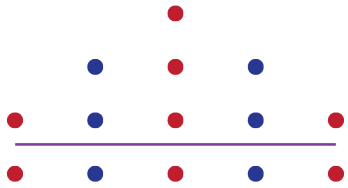

Figure 5.13: The ending state of the S tangle move.

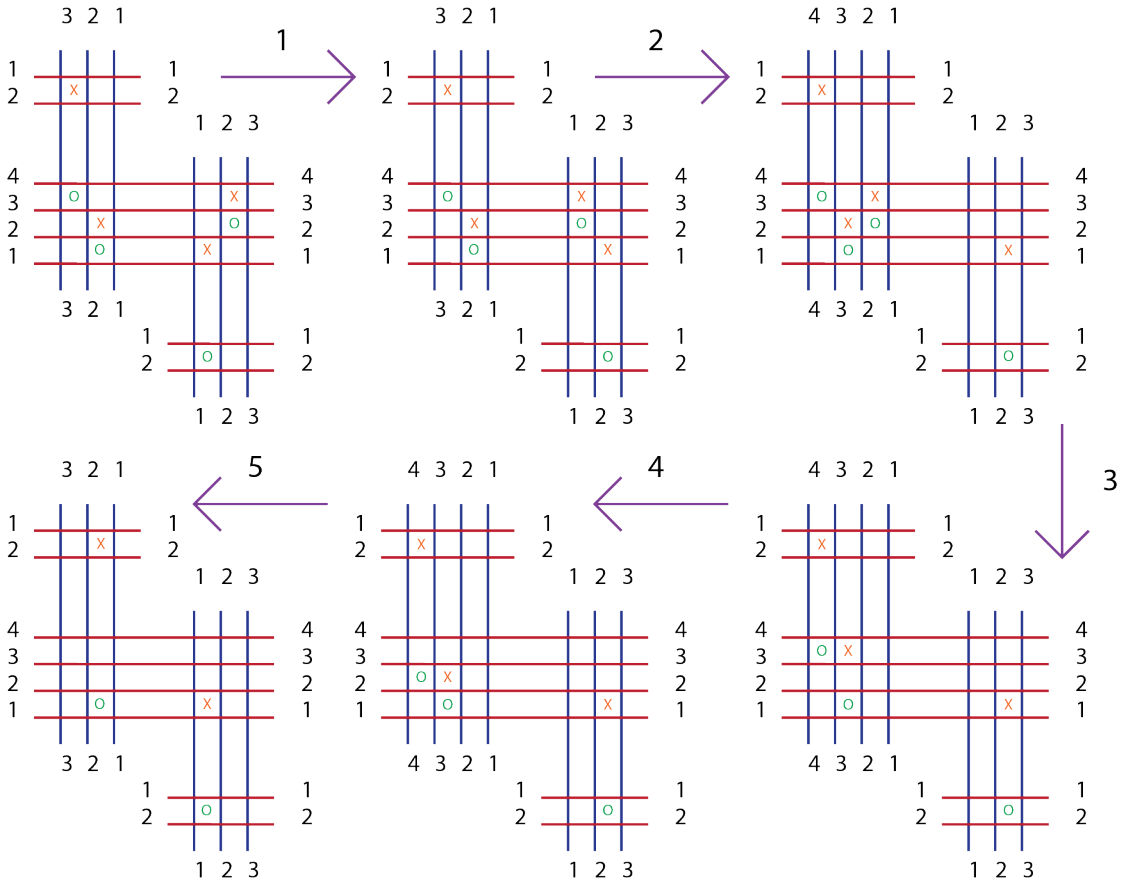

Figure 5.14: The sequence of grid moves that constitute an S tangle move.

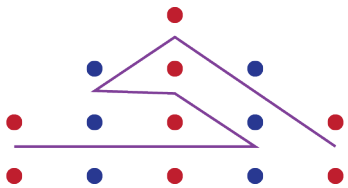

Figure 5.15: The other possible beginning state of an S move.

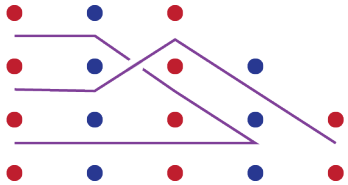

Figure 5.16: The starting tangle diagram for a Cap 1 move.

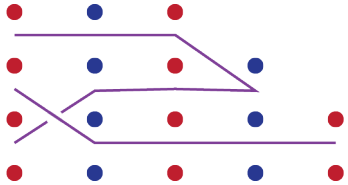

Figure 5.17: The ending tangle diagram for a Cap 1 move.

move on the first and second beta columns in the third and fourth sections. Move 2 is a commutation move on the first and second columns in the first and second sections. Move 3 is a commutation move on the second and third rows in the second and third sections. Finally, move 4 is a commutation move on the first and second rows in the second and third sections.

5.5.2 Cap 2 Moves

The second cap move is shown in figures 5.19 and 5.20. The sequence of grid moves connecting the two strand diagrams is shown in figure 5.21. Move 1 is a commutation move on the second and third rows in sections 2 and 3. Move 2 is a commutation move on the second and third columns in sections 1 and 2. Move 3 is a commutation move on the first and second rows of sections 2 and 3. Finally, move 4 is a commutation move on the first and second columns of sections 3 and 4.

5.6 Cup Moves

5.6.1 Cup 1 Moves

The first cup move is shown in figures 5.22 and 5.23. The sequence of grid moves connecting the two strand diagrams is shown in figure 5.24. Move 1 is a commutation move on the first and second rows in sections 2 and 3. Move 2 is a commutation move on

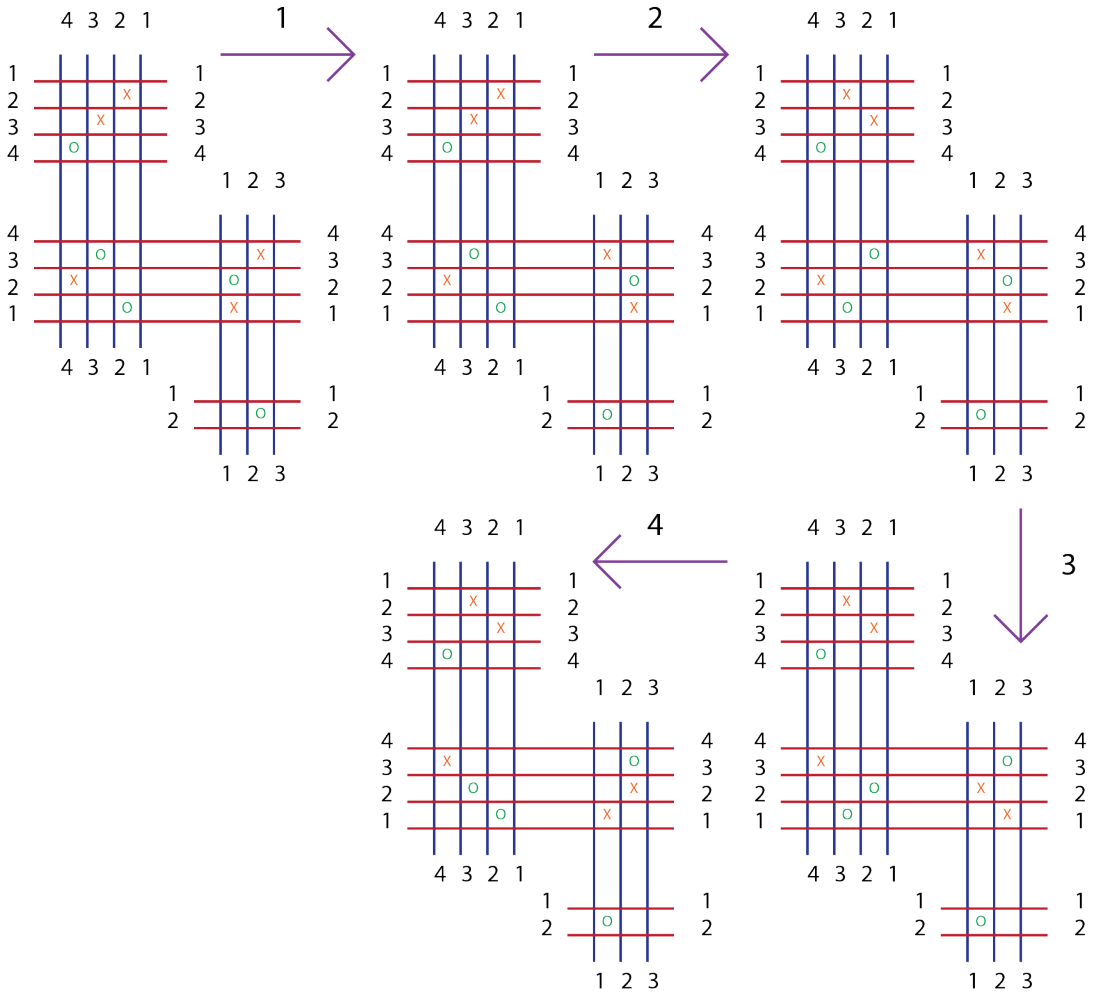

Figure 5.18: The sequence of grid moves that accomplish a Cap 1 tangle move.

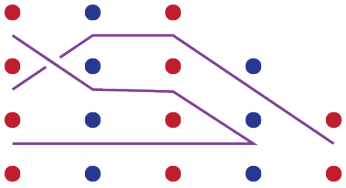

Figure 5.19: The starting tangle diagram for a Cap 2 move.

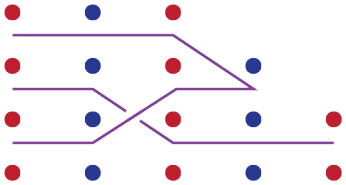

Figure 5.20: The ending tangle diagram for a Cap 2 move.

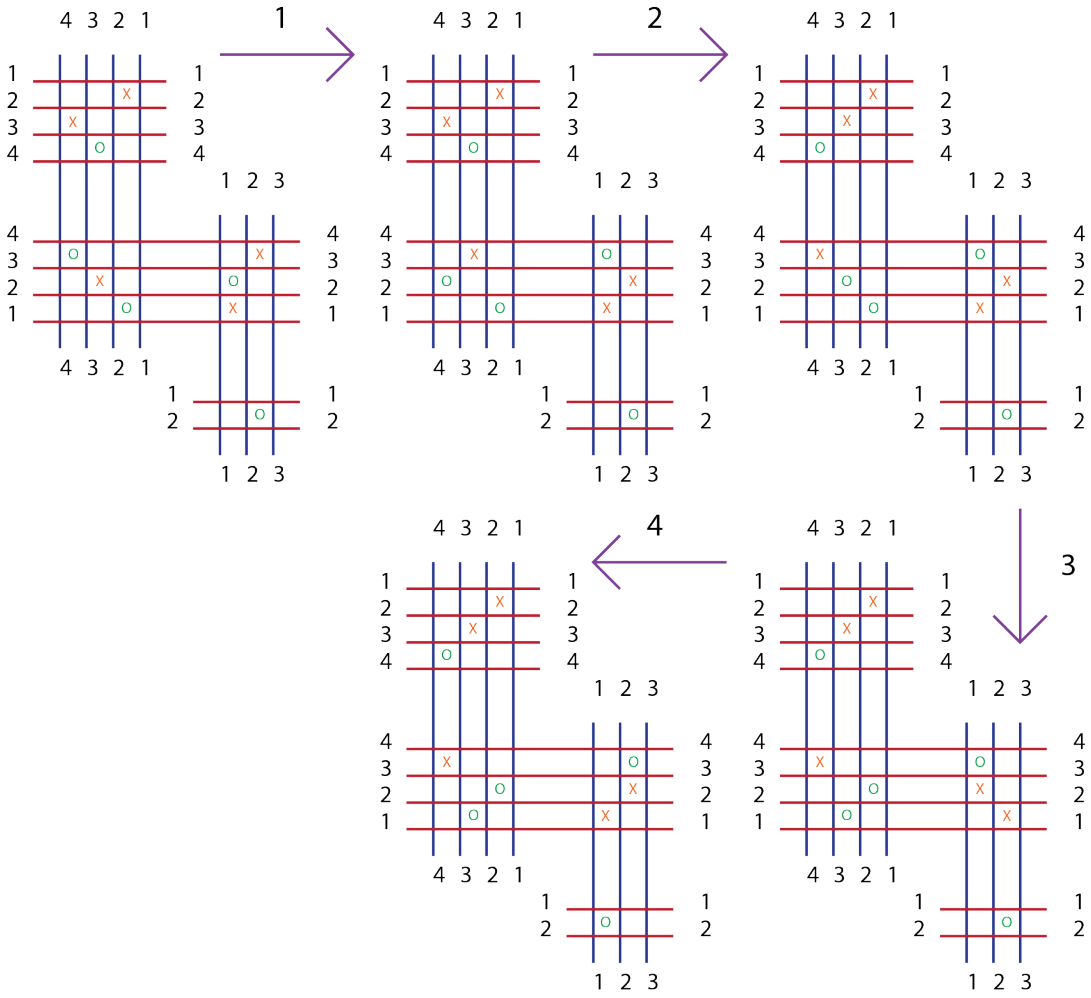

Figure 5.21: The sequence of grid moves that accomplish a Cap 2 tangle move.

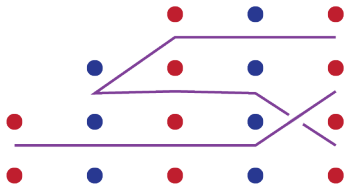

Figure 5.22: The starting tangle diagram for a Cup 1 move.

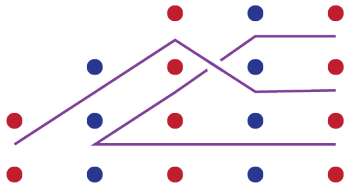

Figure 5.23: The ending tangle diagram for a Cup 1 move.

the second and third rows in sections 2 and 3. Move 3 is a commutation move on the first and second columns in sections 1 and 2. Finally, move 4 is a commutation move on the first and second columns in sections 3 and 4.

5.6.2 Cup 2 Moves

The second cup move is shown in figures 5.25 and 5.26. The sequence of grid moves connecting the two strand diagrams is shown in figure 5.27. Move 1 is a commutation move on the first and second columns in sections 1 and 2. Move 2 is a commutation move on the first and second rows of sections 2 and 3. Move 3 is a commutation move on the second and third columns of the third and fourth sections. Finally, move 4 is a commutation move on the second and third rows of sections 2 and 3.

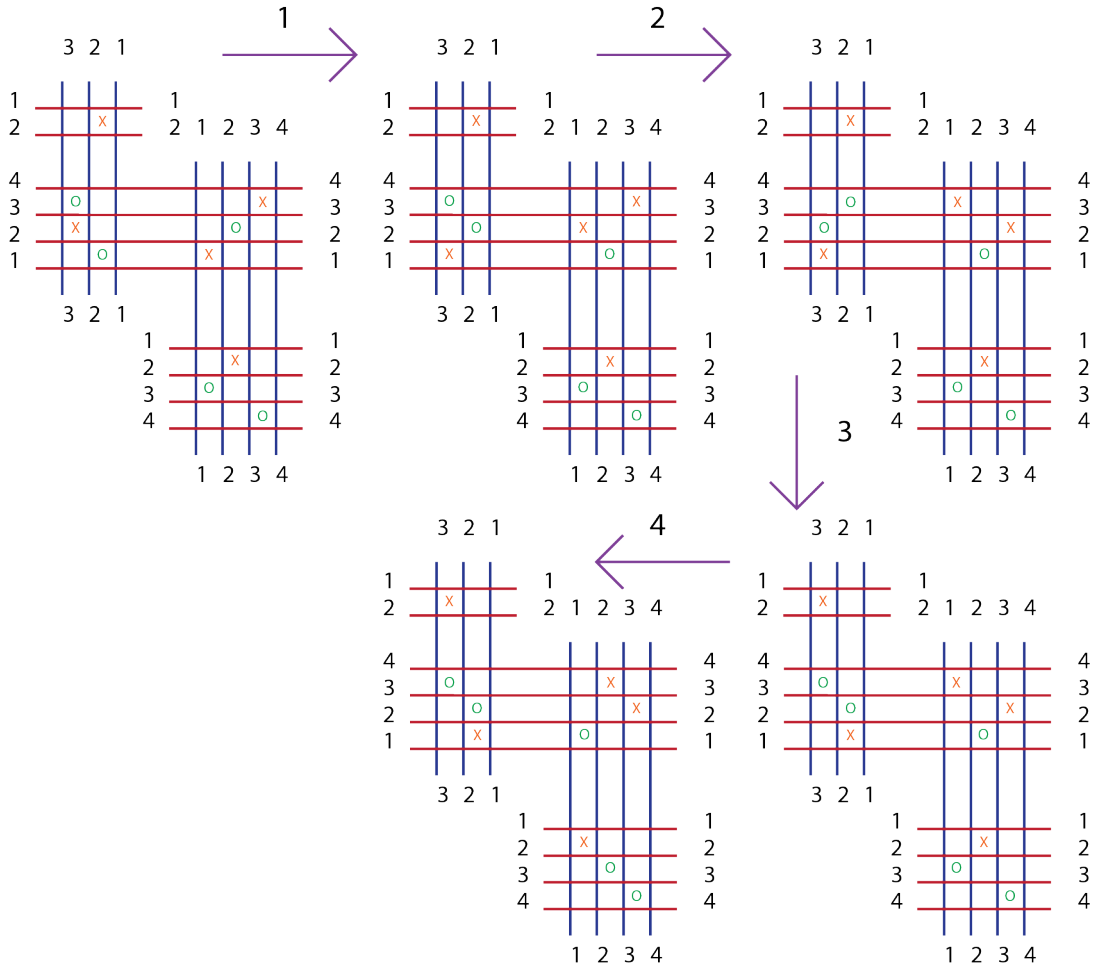

Figure 5.24: The sequence of grid moves that accomplish a Cup 1 tangle move.

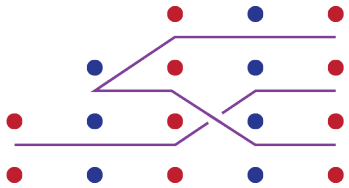

Figure 5.25: The starting tangle diagram for a Cup 2 move.

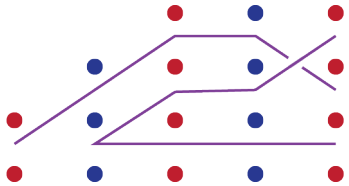

Figure 5.26: The ending tangle diagram for a Cup 2 move.

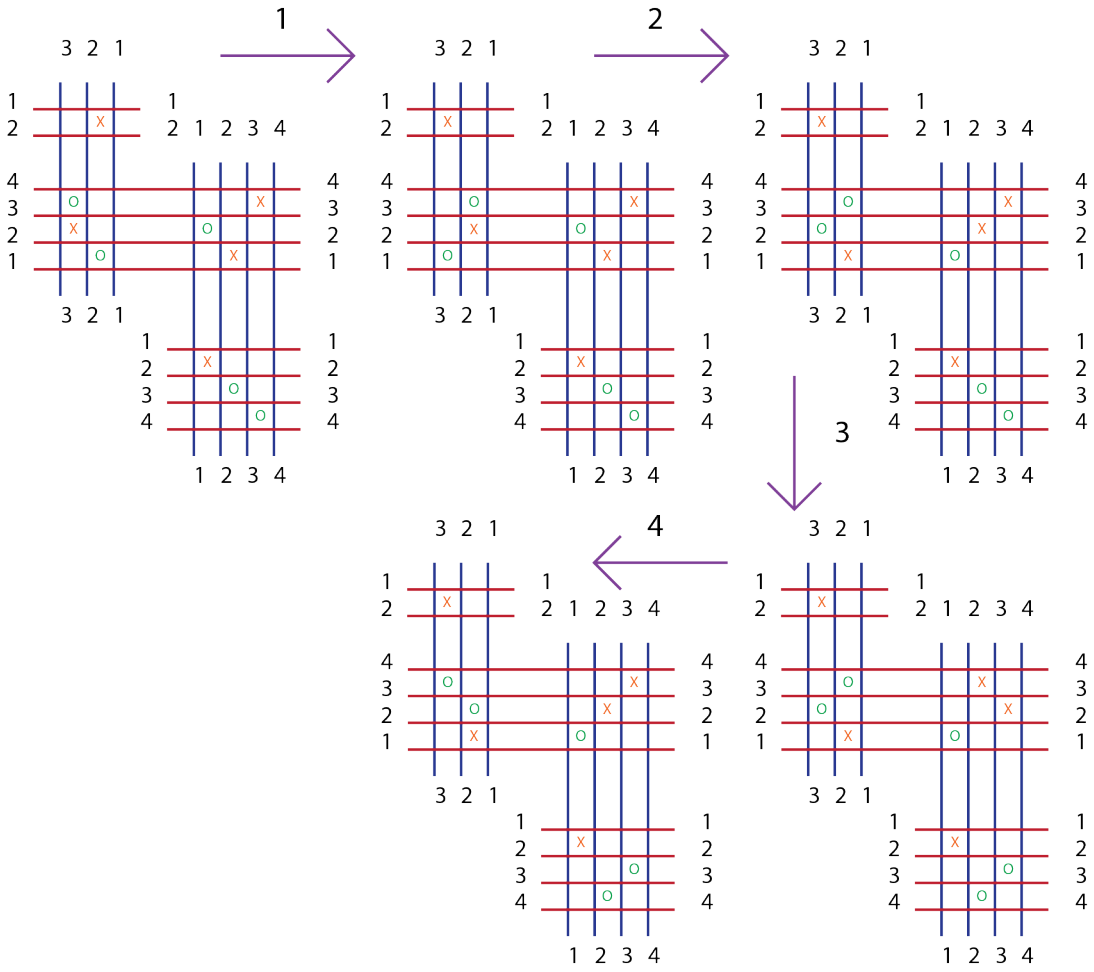

Figure 5.27: The sequence of grid moves that accomplish a Cup 2 tangle move.

CHAPTER 6

SPECIAL CASES

Just as with grid moves, there are a couple of special cases with tangle moves as well.

6.1 Slide Moves

The first special move is called a slide move. It results when we wish to slide a whole segment of a tangle past another section. Both sections may be complicated or may be trivial (i.e. consist of straight strands). See figure 6.1 for a diagram of such a move. In the figure, the box labeled T and the box labeled S may represent complicated sections of a tangle or trivial sections. The important thing is that section T and section S do not interact. The tangle may have other things happening to the left or right of what is shown in the diagram.

This type of move simply uses the tools that we have built up so far to slide the box along the tangle one piece at a time. A complicated tangle section may be slid along the diagram one piece at a time. In figure 6.2 we see an example of sliding a cup and a crossing along the grid diagram. In step 1, we make some room for ourselves using

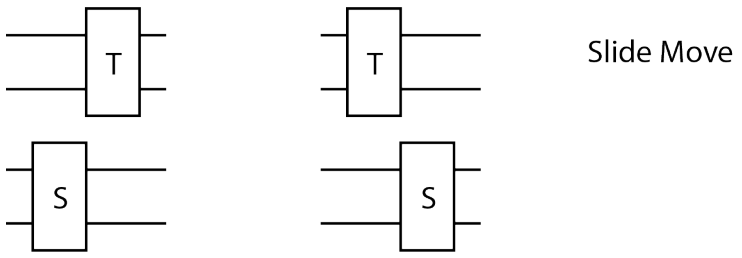

Figure 6.1: This figure shows a slide move. The box labeled T and the box labeled S may represent complicated sections of a tangle or trivial sections. The important thing is that the section T and S do not interact. The tangle may have other things happening to the left or right of what is show in the diagram.

additions and subtractions. Then, in steps 2 through 4, we slide the cup along the grid diagram piece by piece using stabilizations followed by stretch moves. In steps 5 and 6, we use a pair of commutations to slide a single crossing along the grid diagram.

In this example we are somewhere in the middle of the grid diagram (as cups are not allowed in the first section and we are not allowed to alter the ends of the tangle) and other things remain unchanged in other sections of the grid complex (with the exception of the additions and subtractions in step 1 which can automatically be matched in the section glued to it). Also note that we could have had other complex pieces of the tangle above and below in the strand diagram. This would not have affected our ability to slide the pieces as we never required anything from the other α and β rows and columns in the sections of the grid as we progressed. Thus, we just as easily could have slid the complicated piece of the tangle past another (separated) complicated piece of the tangle.

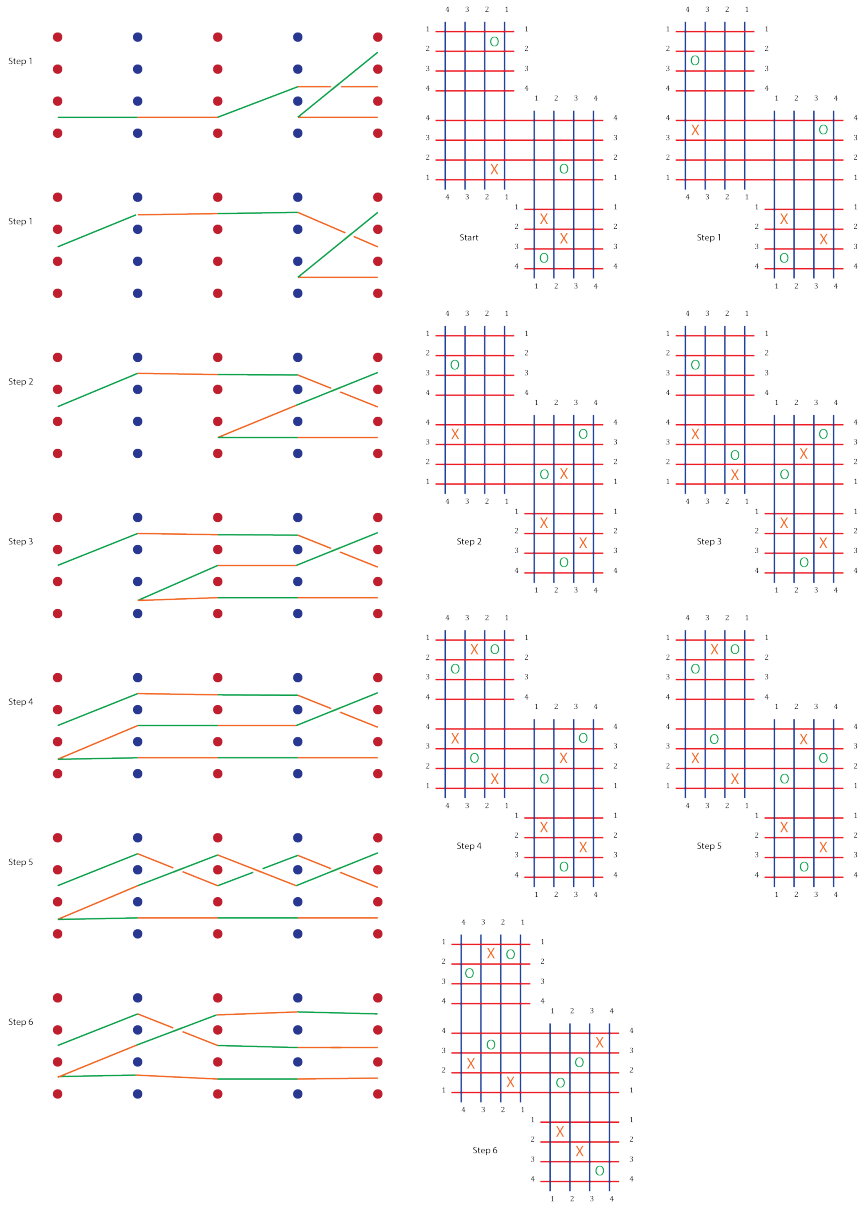

Figure 6.2: This figure shows an example of how the grid moves allow us to slide the individual pieces of a complex tangle along the grid diagram one at a time. In step 1, we make some room for ourselves using additions and subtractions. Then, in steps 2 through 4, we slide the cup along the grid diagram piece by piece using stabilizations followed by stretch moves. In steps 5 and 6, we use a pair of commutations to slide a single crossing along the grid diagram.

CHAPTER 7

CONCLUSION

To sum up, we have been able to take the construction put forward by Petkova and Vértesi and show that many of the arguments that apply to grid diagrams for knots can be applied to grid diagrams for tangles. In particular, we showed that the stabilization and commutation arguments used in combinatorial knot Floer homology can be applied mutatis mutandis to combinatorial tangle Floer homology, giving us an equivalence of chain complexes (either exactly in the case of commutations or up to the size of the grid in stabilizations). We then added a new move, the stretch move, and showed that the same arguments which work for commutations work for this move as well.

We then extended these arguments to the context of A_∞-structures. We developed for our stabilization arguments a new type of algebraic notation and used this notation to demonstrate and simplify useful algebraic results. These results were then applied to produce type D and type DA equivalences between grid complexes and their stabilized counterparts.

For commutation moves we proceeded more directly, constructing the needed type D homomorphisms and homotopies as needed and then showing that these give us a type D equivalence between tangle grid diagrams and their commuted counterparts. We also showed that these arguments can also be applied to our new stretch move.

Finally, we showed that these grid moves are sufficient to accomplish the planar tangle moves required to establish equivalence of the tangles themselves (with the exception of one move). It is the author's opinion that the last move can be conquered using algebraic infrastructure similar to that brought to bear on the stabilization problem.

While much has been accomplished, there is more work to be done in this area of

research. First, the type D equivalence for commutation moves can be extended to a type DA equivalence. Second, I would like to incorporate the bigrading normally used in tangle Floer homology into my work. Lastly, the arguments laid out in this paper are only applicable to (m, n)-tangles where m and n are nonzero. There is a way to incorporate $(m, 0)$, $(0, n)$, and $(0, 0)$ tangles into this construction. This is accomplished by gluing the α curves in the type 1 and/or type 4 sections of the grid diagram to themselves. Any such glued section would then allow rectangles, pentagons, etc. to wrap horizontally around the grid in those sections, and results in a type A structure, a type D structure, or a true chain complex.

Furthermore, there are more versions of knot Floer homology which are stronger invariants of the knot, e.g. the "hat" version and the "minus" version. The minus version is the strongest invariant of these and it seems capable of being generalized to the tangle picture as well. The main obstacle is that the proofs of invariance for stabilizations in the minus theory involve quasi-isomorphisms instead of homotopy equivalences and the A_∞ theory would have to be adjusted appropriately.

REFERENCES

[1] Peter Ozsváth and Zoltán Szabó. Holomorphic disks and knot invariants. *Advances in Mathematics*, 186(1):58–116, 2003.

[2] J. Rasmussen. Floer homology and knot complements. 2003.

[3] Ciprian Manolescu, Peter Ozsváth, and Sucharit Sarkar. A combinatorial description of knot Floer homology. *Annals of Mathematics*, 169:633–660, 2009.

[4] Ciprian Manolescu, Peter Ozsváth, Zoltán Szabó, and Dylan Thurston. On combinatorial link Floer homology. *Geom. Topol.*, 11:2339–2412, 2007.

[5] Peter S. Ozsváth, András I. Stipsicz, and Zoltán Szabó. *Grid Homology for Knots and Links*, volume 208. American Mathematical Society, 2015.

[6] Robert Lipshitz, Peter Ozsváth, and Dylan P. Thurston. Slicing planar grid diagrams: A gentle introduction to bordered heegaard Floer homology. *Proceedings of the 15th Gökova Geometry-Topology Conference*, pages 91–119, 2008.

[7] Robert Lipshitz, Peter S. Ozsváth, and Dylan P. Thurston. Bimodules in bordered heegaard Floer homology. *Geometry and Topology*, 19:525–724, 2015.

[8] Bernhard Keller. Introduction to A-infinity algebras and modules. *Homology Homotopy Appl.*, 3:1–35, 2001.

[9] Peter Ozsváth and Zoltán Szabó. Kauffman states, bordered algebras, and a bigraded knot invariant. *Advances in Mathematics*, 328:1088–1198, 2018.

[10] Ina Petkova and Vera Vértesi. Combinatorial tangle Floer homology. *Geometry and Topology*, 20:3219–3332, 2016.

[11] Ina Petkova and Vera Vértesi. An introduction to tangle Floer homology. *Proceedings of the Gökova Geometry and Topology Conference*, 2016.

[12] Alexander P. Ellis, Ina Petkova, and Vera Vértesi. Quantum $gl(1|1)$ and tangle Floer homology. *Unpublished*, 2015.

[13] Martin Markl. Transferring A_∞ (strongly homotopy associative) structures. *Proceedings of the 25th Winter School Geometry and Physics*, pages 139–151, 2006.

[14] Martin Markl. Ideal perturbation lemma. *Communications in Algebra*, 29:5209–5232, 2001.

[15] Ciprian Manolescu. An introduction to knot Floer homology. *Unpublished*, 2016.

[16] Kenji Lefèvre-Hasegawa. Sur les A_∞-catégories. *Unpublished Ph.D. Thesis*, 2003.

[17] Lawrence P. Roberts. A type D structure in Khovanov homology. *Advances in Mathematics*, 293:81–145, 2016.

[18] Lawrence P. Roberts. A type A structure in Khovanov homology. *Algebraic Geometry and Topology*, 16(6):3653–3719, 2016.

[19] Maxim Kontsevich and Yan Soibelman. Homological mirror symmetry and torus fibrations. 2001.

[20] V.K.A.M. Gugenheim and J.D. Stasheff. On perturbations and A_∞-structures. 1986.

[21] J. Chuang and A. Lazarev. On the perturbation algebra. *Journal of Algebra*, 519, 2017.

[22] J. Huebschmann. On the construction of A_∞-structures. 2008.

[23] Robert Lipshitz, Peter S. Ozsváth, and Dylan P. Thurston. Bordered heegaard Floer homology. *Memoirs of the American Mathematical Society*, 254, 2018.